The Gum Nebula as a probe of Galactic Structure

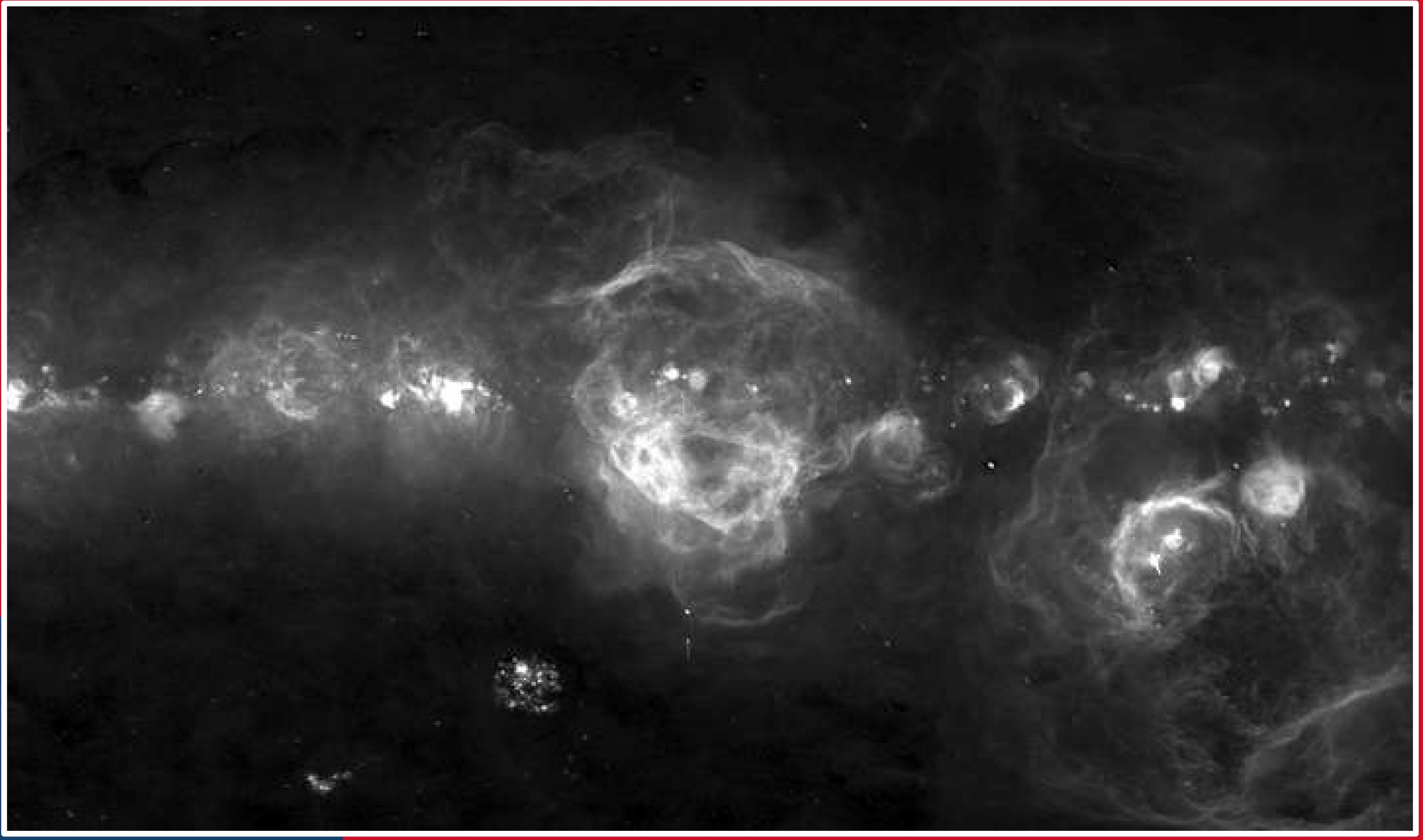

Cormac Purcell, The Sydney Institute for Astronomy

The Gum Nebula as a probe of Galactic Structure

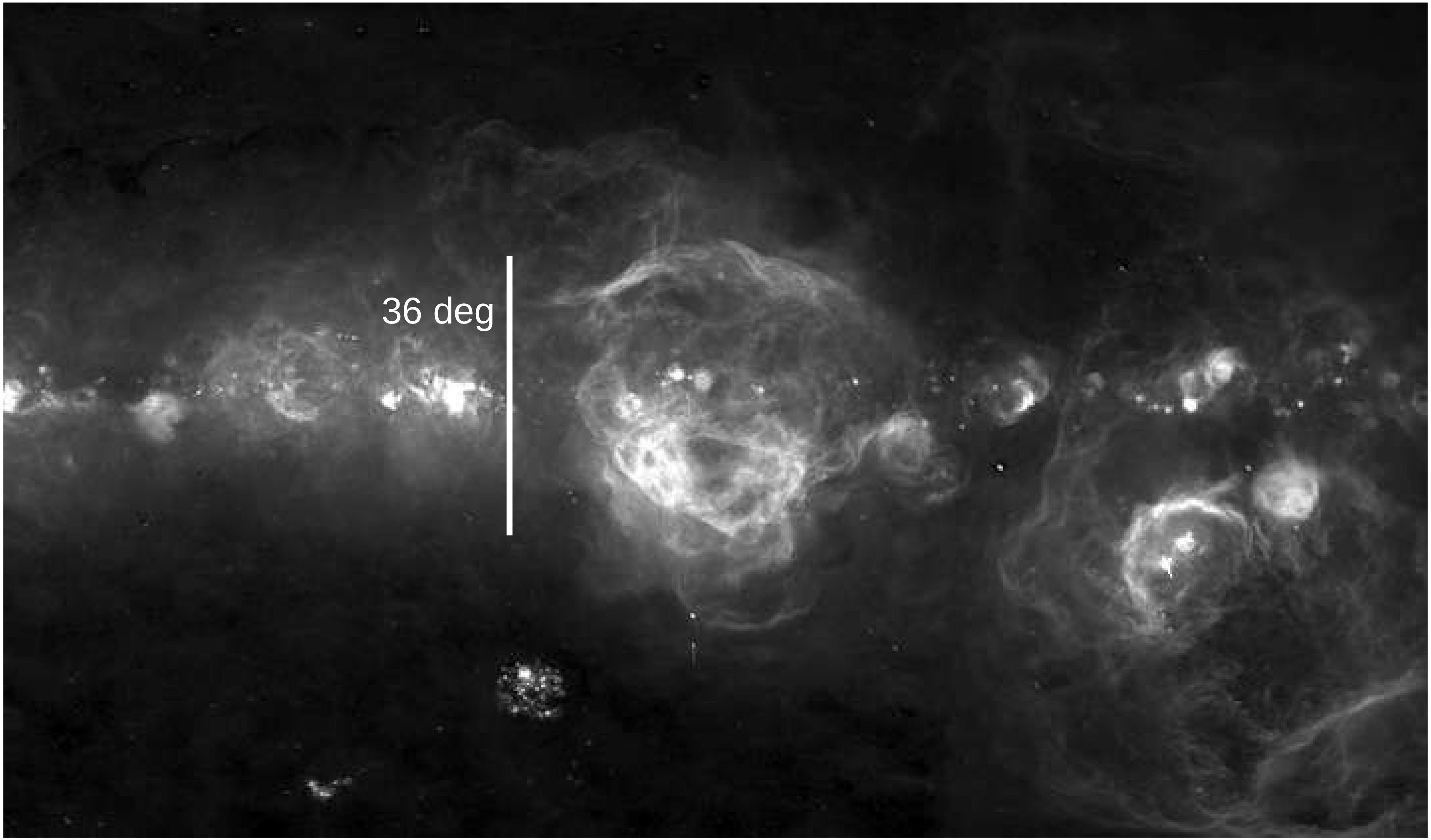

Cormac Purcell, The Sydney Institute for Astronomy

Motivation – Galactic B-fields

- Magnetic fields affect all phases of ISM
- Accelerate cosmic rays via diffusive shock acceleration (Bell 1978)

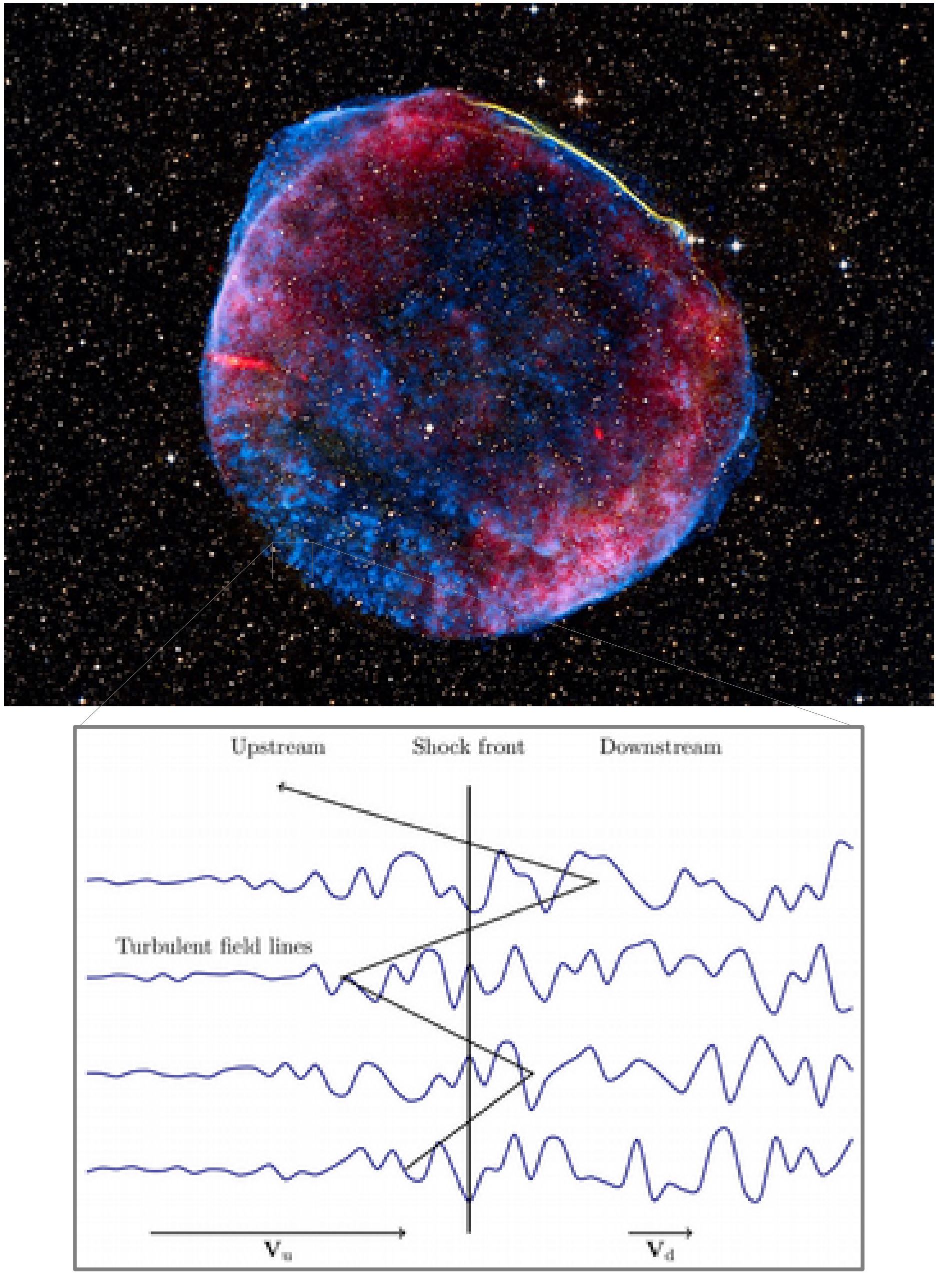

http://sprg.ssl.berkeley.edu/~pulupa/illustrations/

Motivation – Galactic B-fields

- Magnetic fields affect all phases of ISM
- Accelerate cosmic rays via diffusive shock acceleration (Bell 1978)
- Magnetic pressure balances out gravity on Galactic and molecular-cloud scales, affecting gas flow in spiral arms and collapse within star-forming clouds.

Collapsing magnetised cloud core

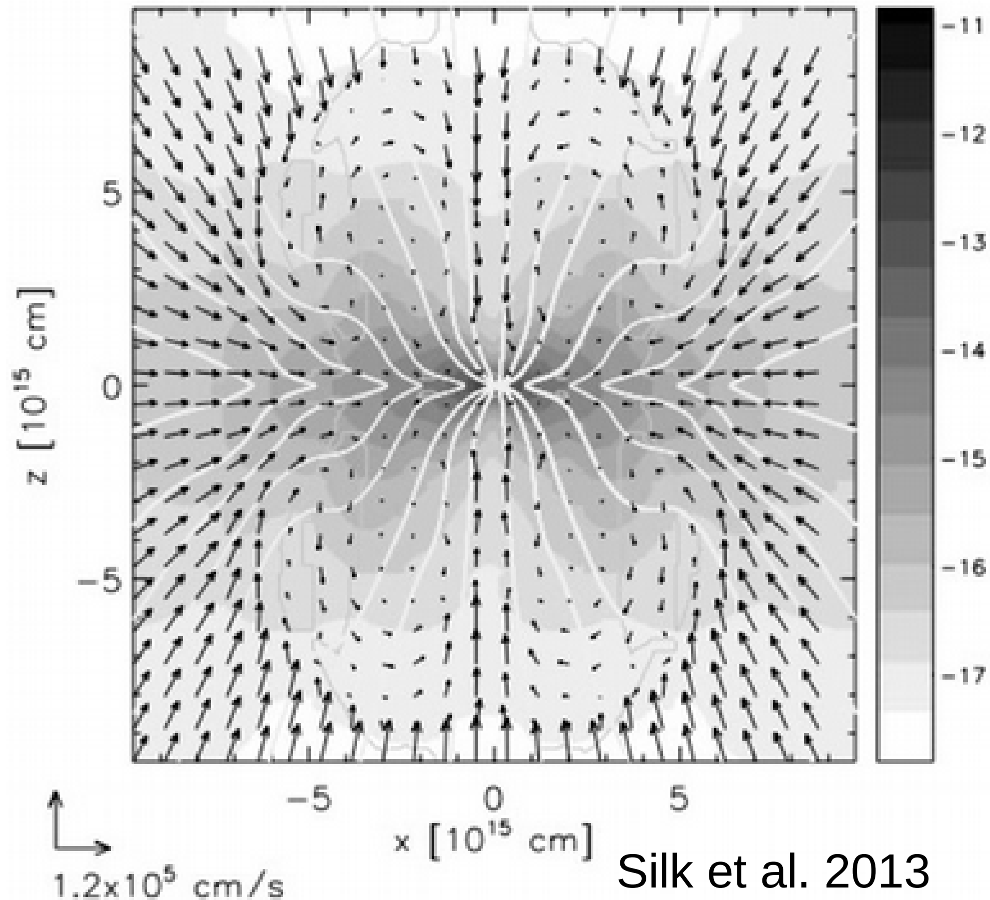

Silk et al. 2013

Motivation – Galactic B-fields

- Magnetic fields affect all phases of ISM
- Accelerate cosmic rays via diffusive shock acceleration (Bell 1978)
- Magnetic pressure balances out gravity on Galactic and molecular-cloud scales, affecting gas flow in spiral arms and collapse within star-forming clouds.
- Many structures within the Galaxy can only be explained by invoking magnetic fields:
  - Non-thermal filaments in the Galactic Centre

Motivation – Galactic B-fields

- Magnetic fields affect all phases of ISM
- Accelerate cosmic rays via diffusive shock acceleration (Bell 1978)
- Magnetic pressure balances out gravity on Galactic and molecular-cloud scales, affecting gas flow in spiral arms and collapse within star-forming clouds.
- Many structures within the Galaxy can only be explained by invoking magnetic fields:
    - Non-thermal filaments in the Galactic Centre
    - Broad-line absorption filaments towards the Brick molecular cloud.

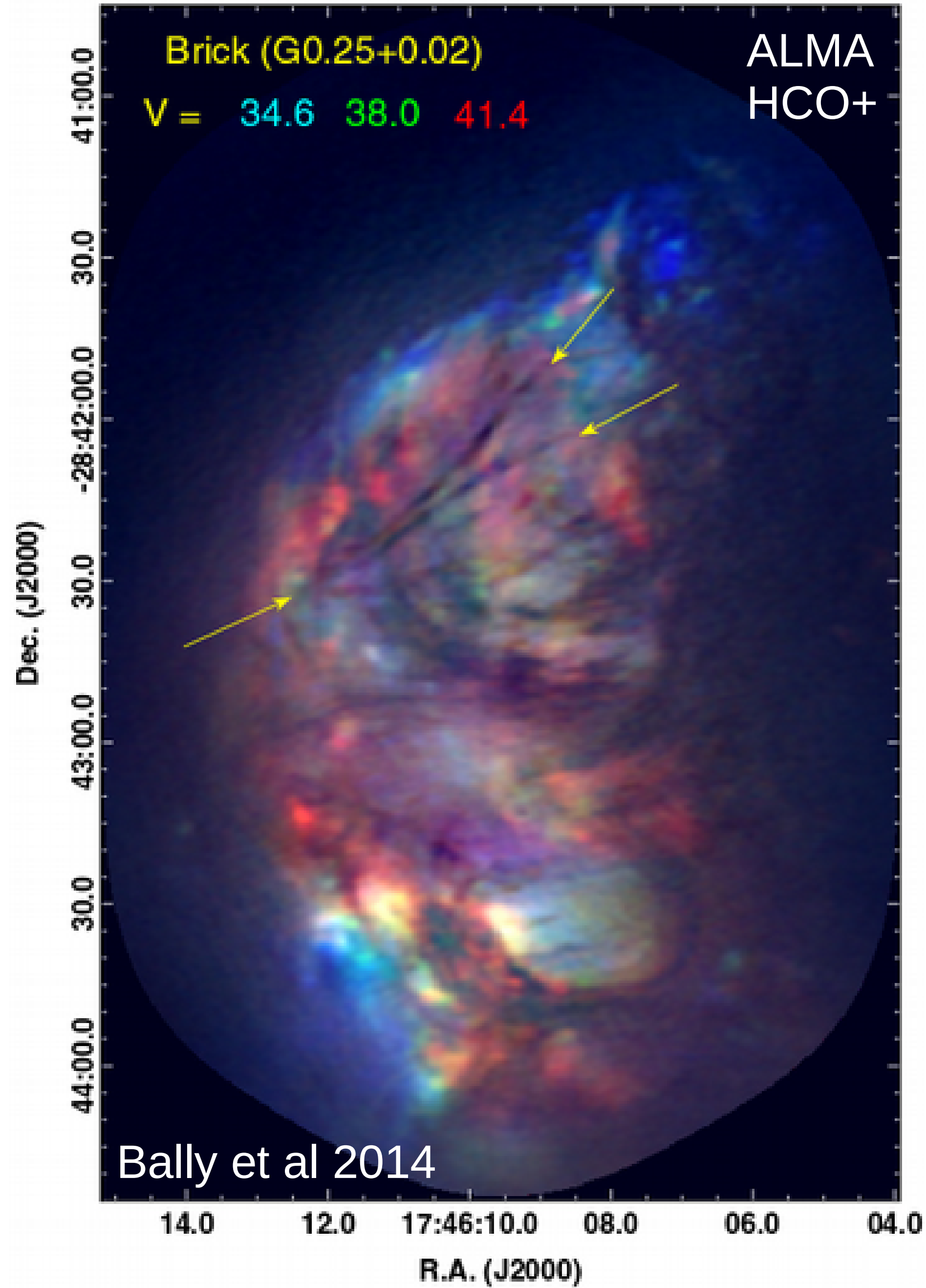

Motivation – Galactic B-fields

- Magnetic fields affect all phases of ISM
- Accelerate cosmic rays via diffusive shock acceleration (Bell 1978)
- Magnetic pressure balances out gravity on Galactic and molecular-cloud scales, affecting gas flow in spiral arms and collapse within star-forming clouds.
- Many structures within the Galaxy can only be explained by invoking magnetic fields:
  - Non-thermal filaments in the Galactic Centre
  - Broad-line absorption filaments towards the Brick molecular cloud.

Pillai et al 2015

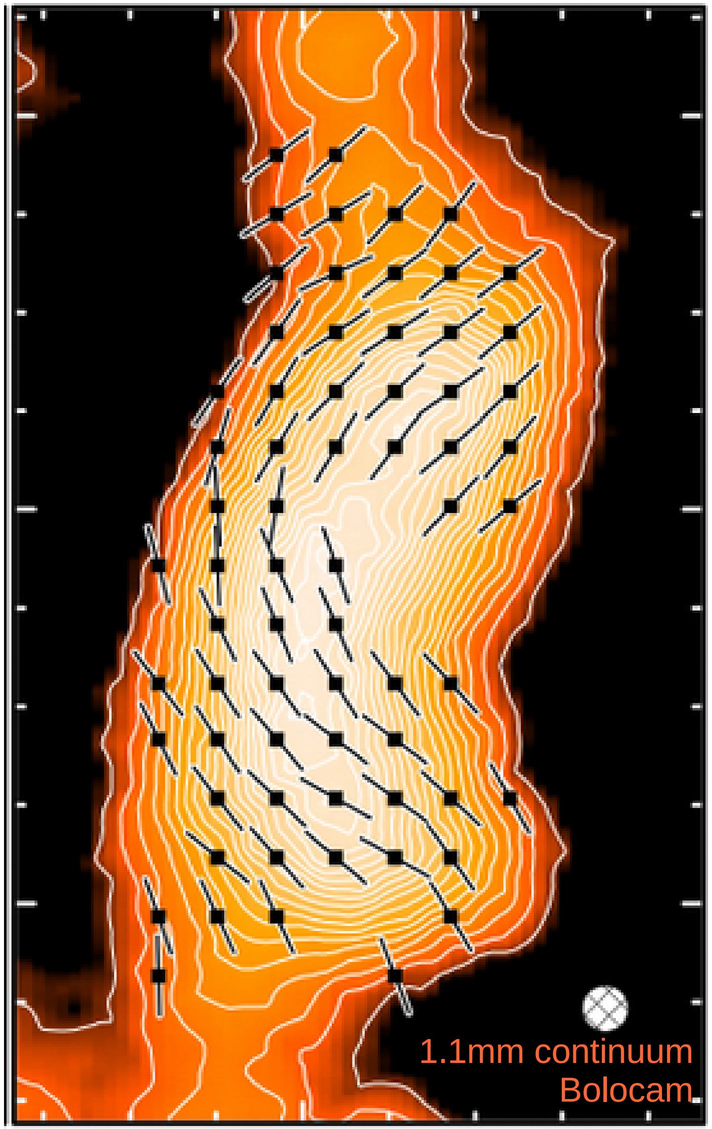

Motivation – Galactic B-fields

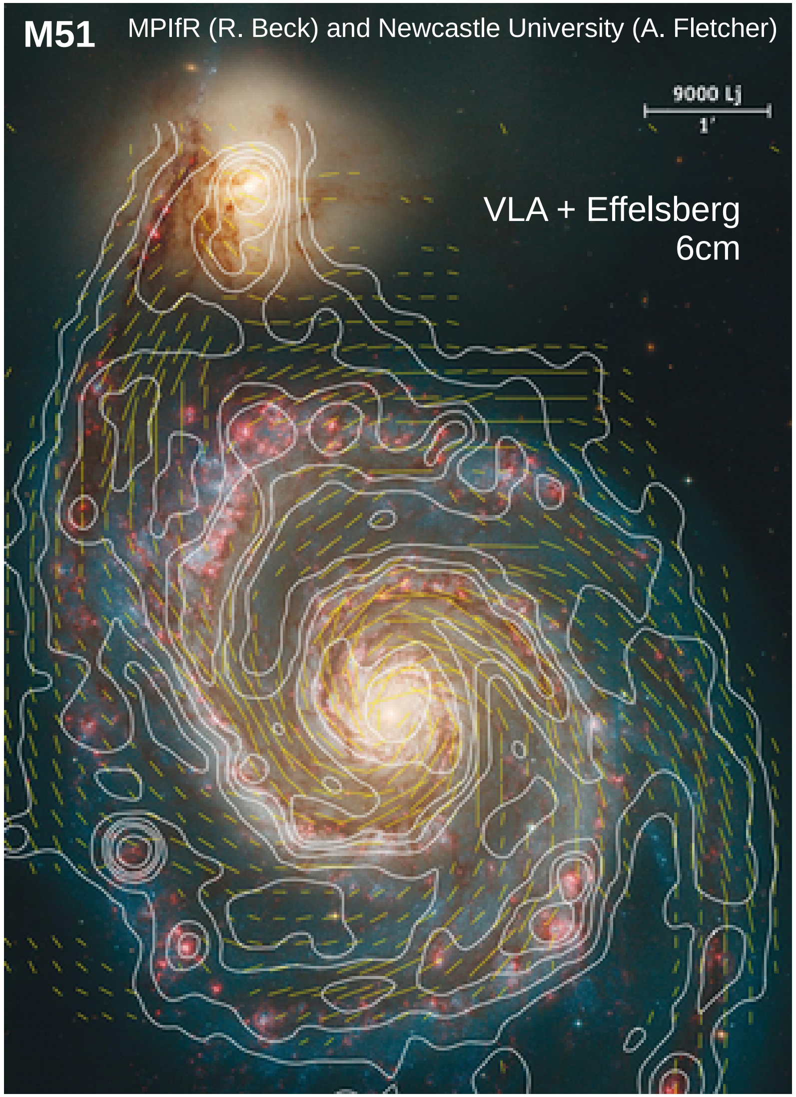

Fletcher et al. 2011

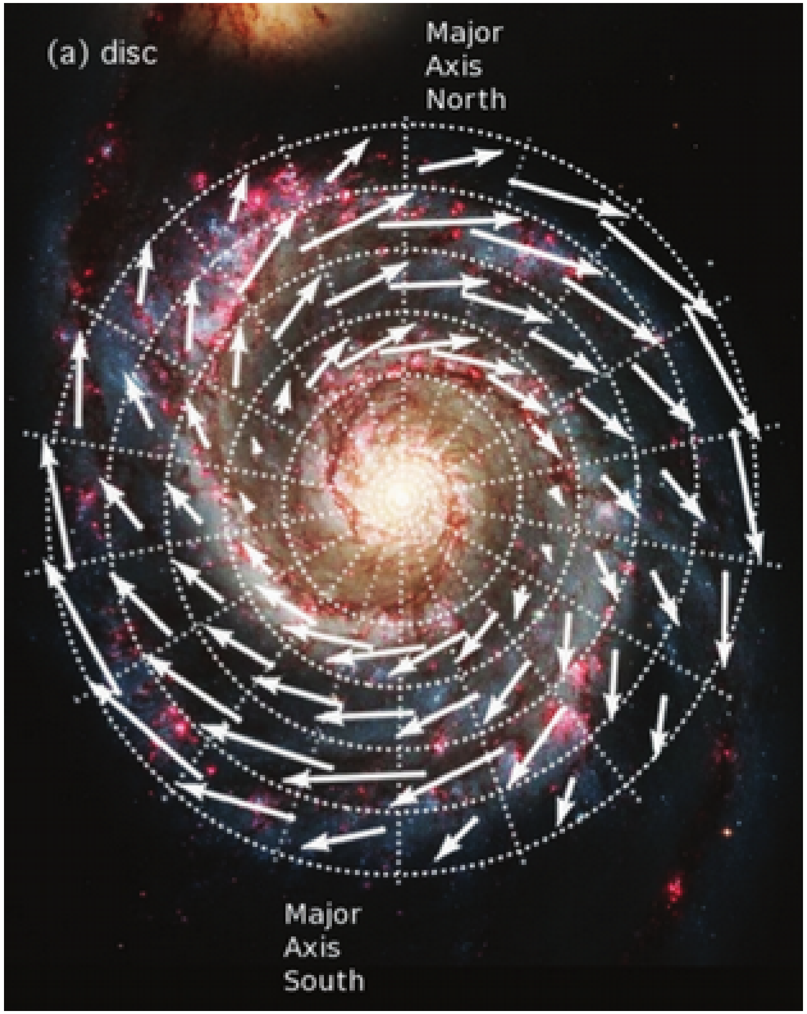

Motivation – Galactic B-fields

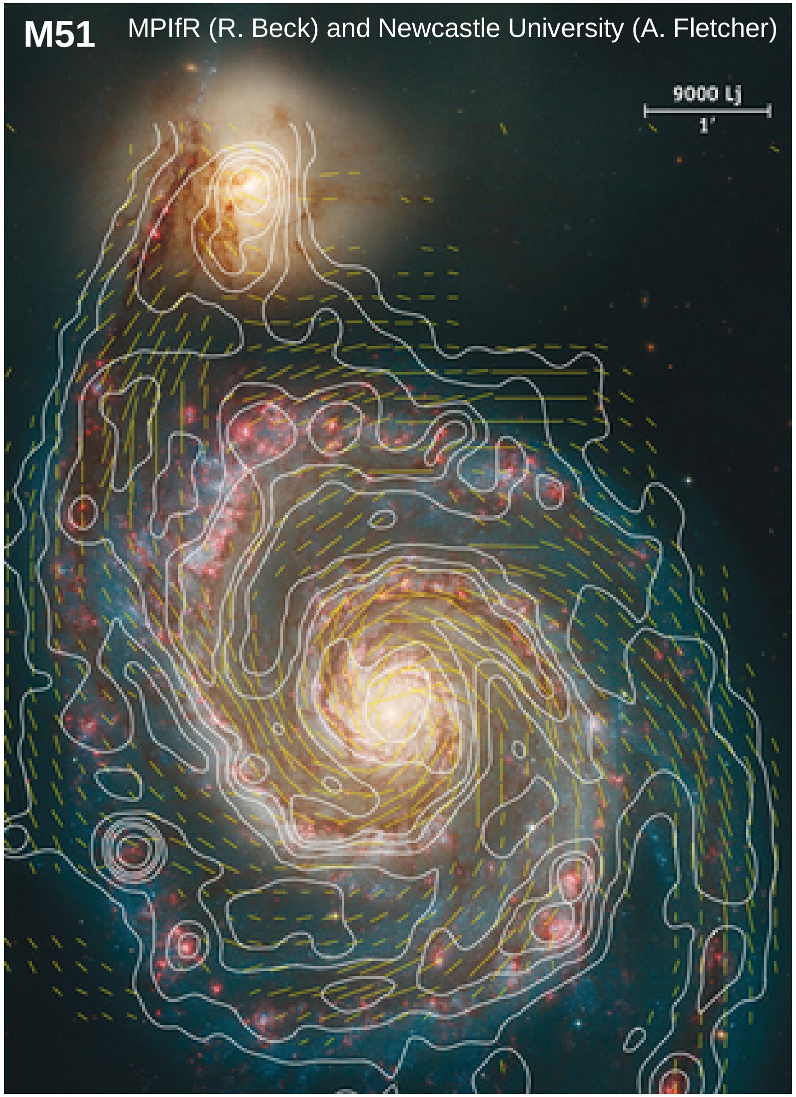

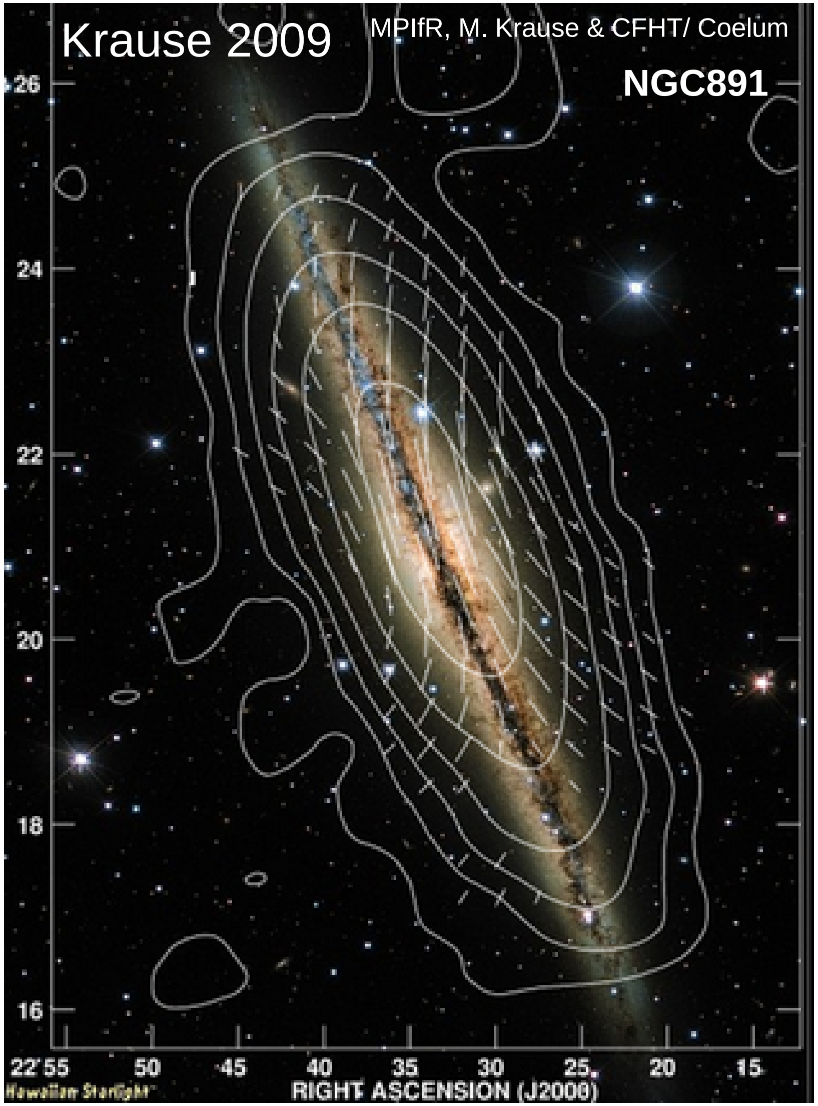

Motivation – Galactic B-fields

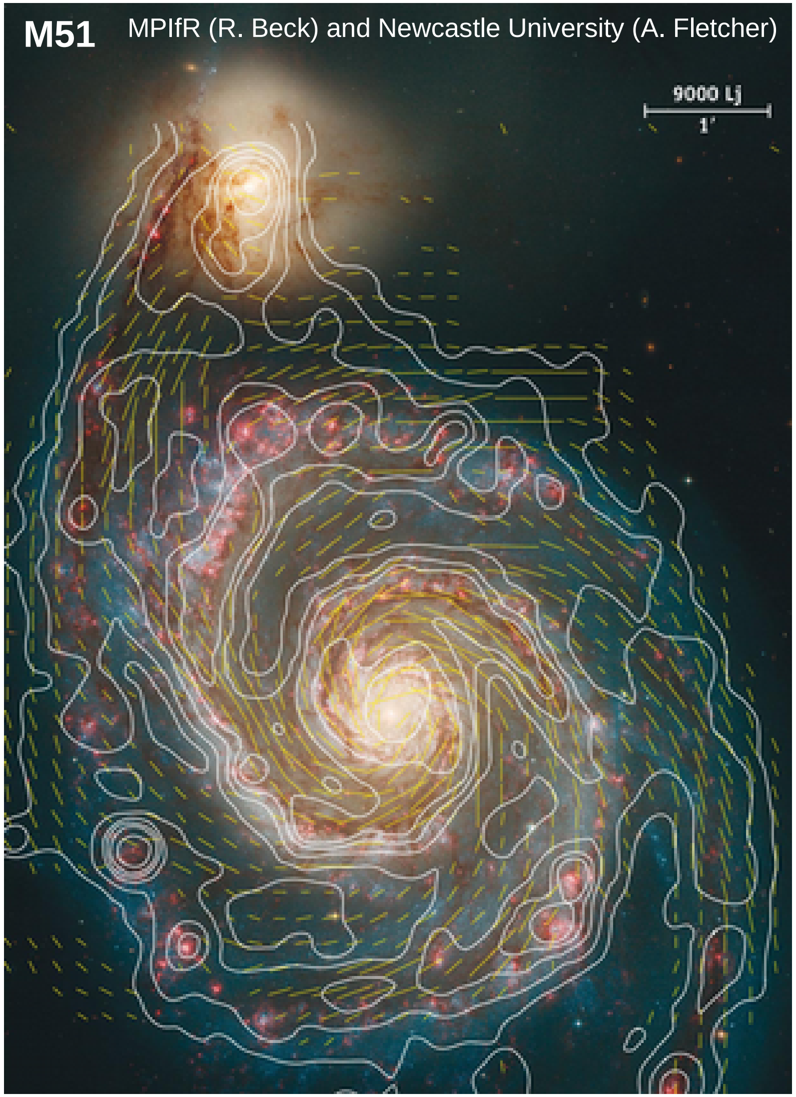

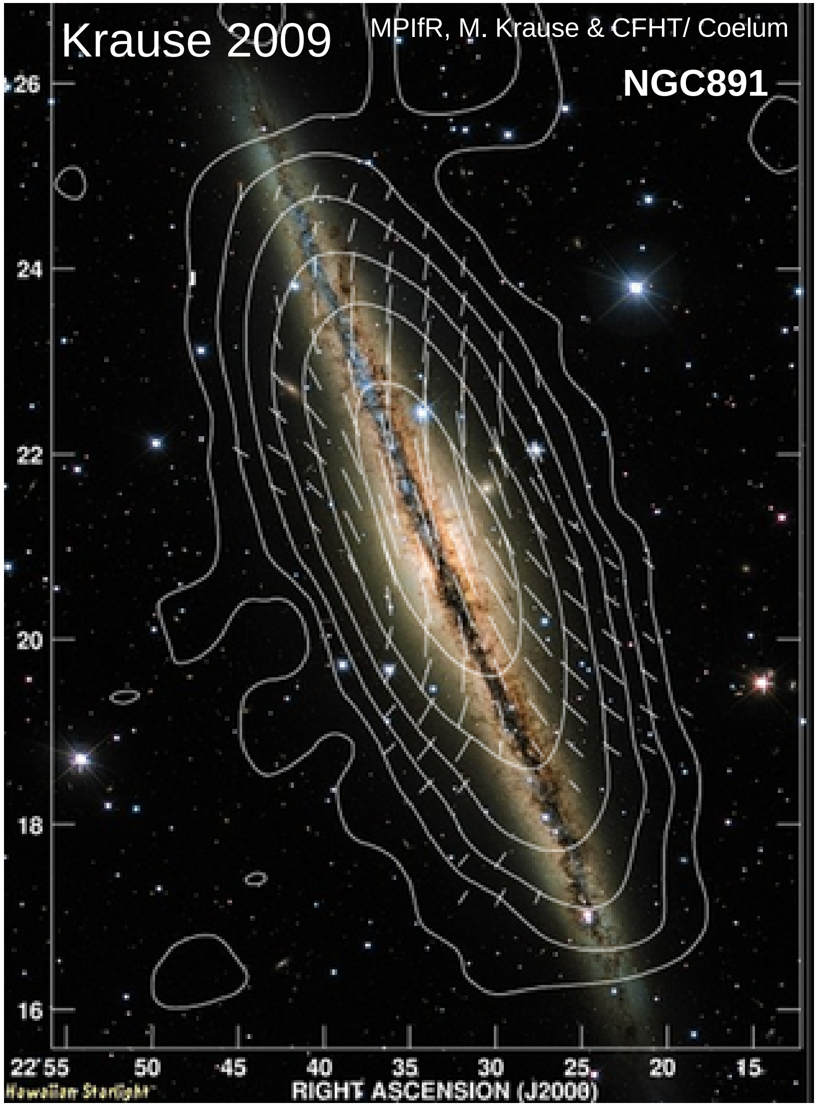

- Know more about the magnetic fields in external galaxies than our own Milky Way

Motivation – Galactic B-fields

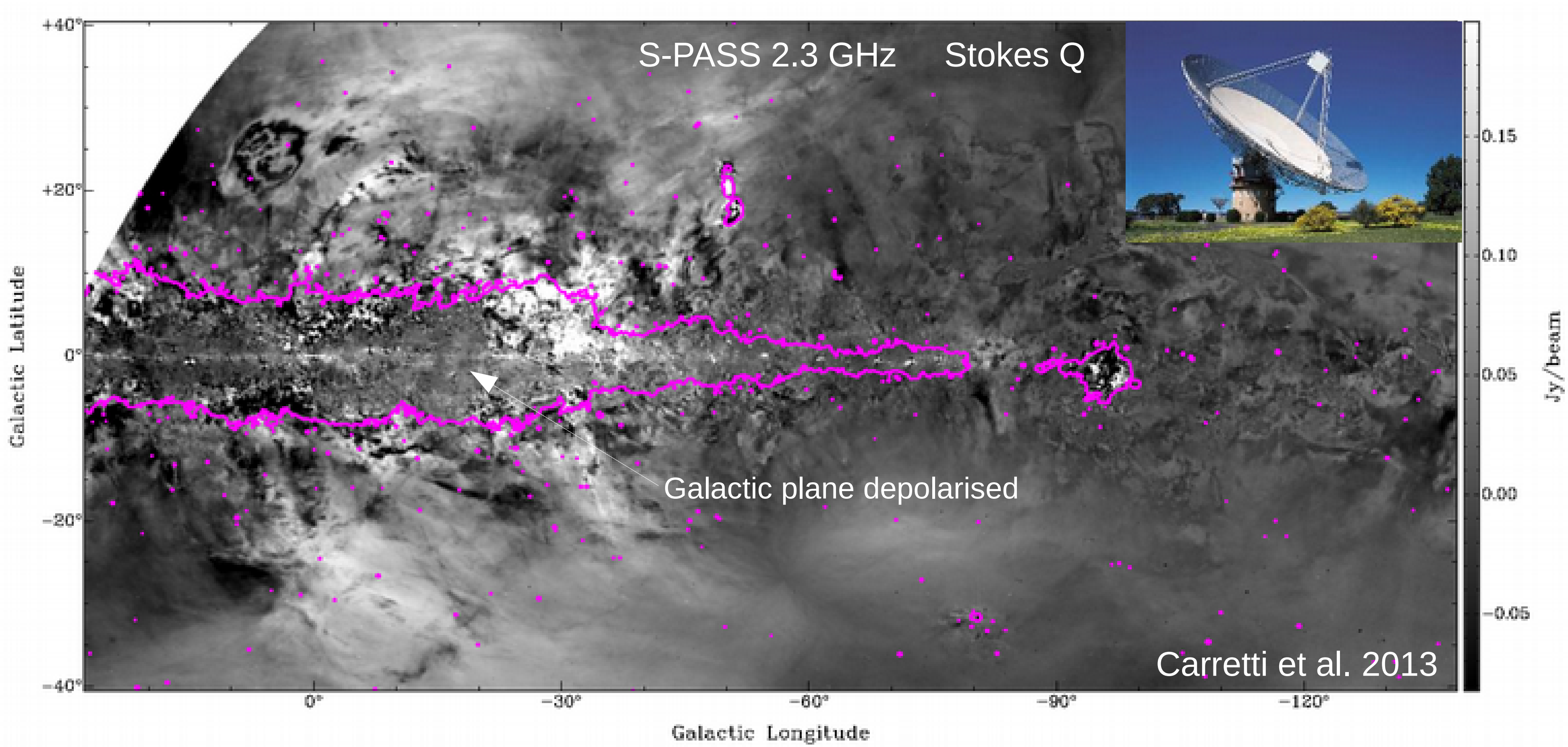

- Problem is that we are embedded in our Galaxy: suffer from obscuration, confusion and depolarisation.
- We have to infer the magnetic field by modelling observations – requires large datasets.

Motivation – Galactic B-fields

- Several ways to determine magnetic field orientation and strength in the ISM:

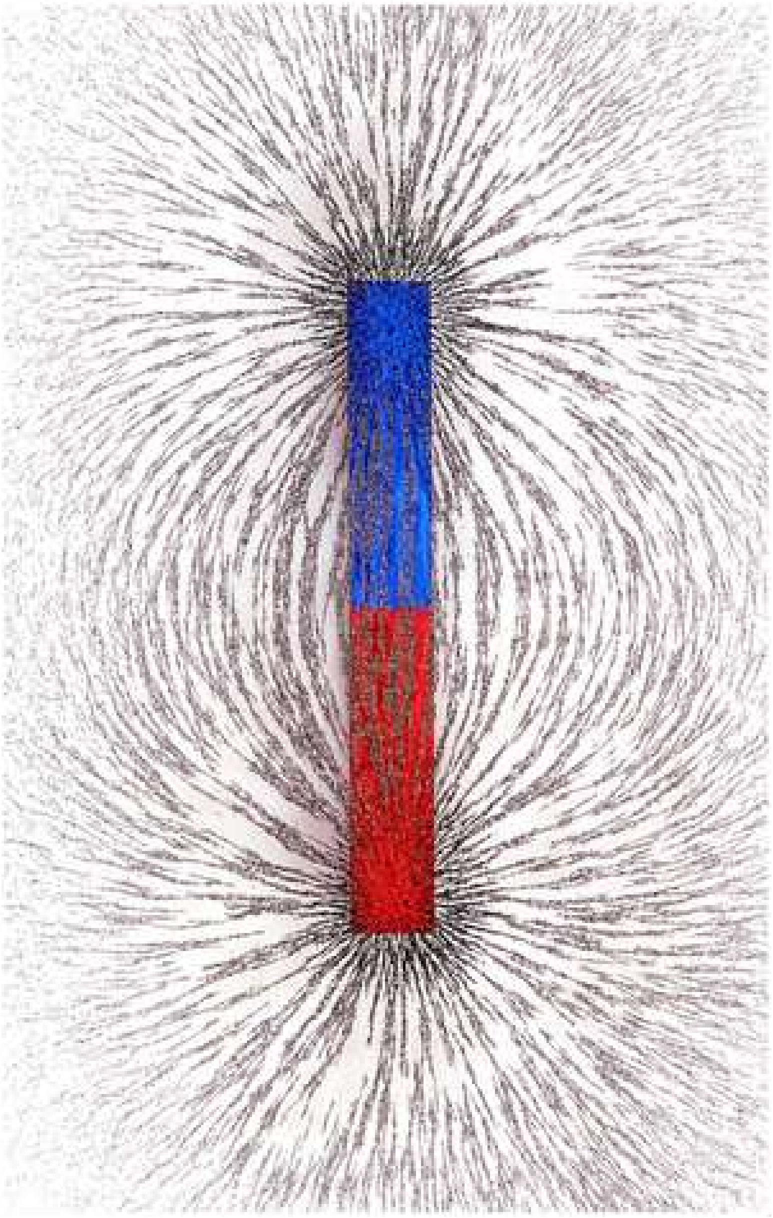

Motivation – Galactic B-fields

- Several ways to determine magnetic field orientation and strength in the ISM:
- Optical and IR polarisation from dust-grains aligned along the field lines, e.g., Heiles et al. 2000

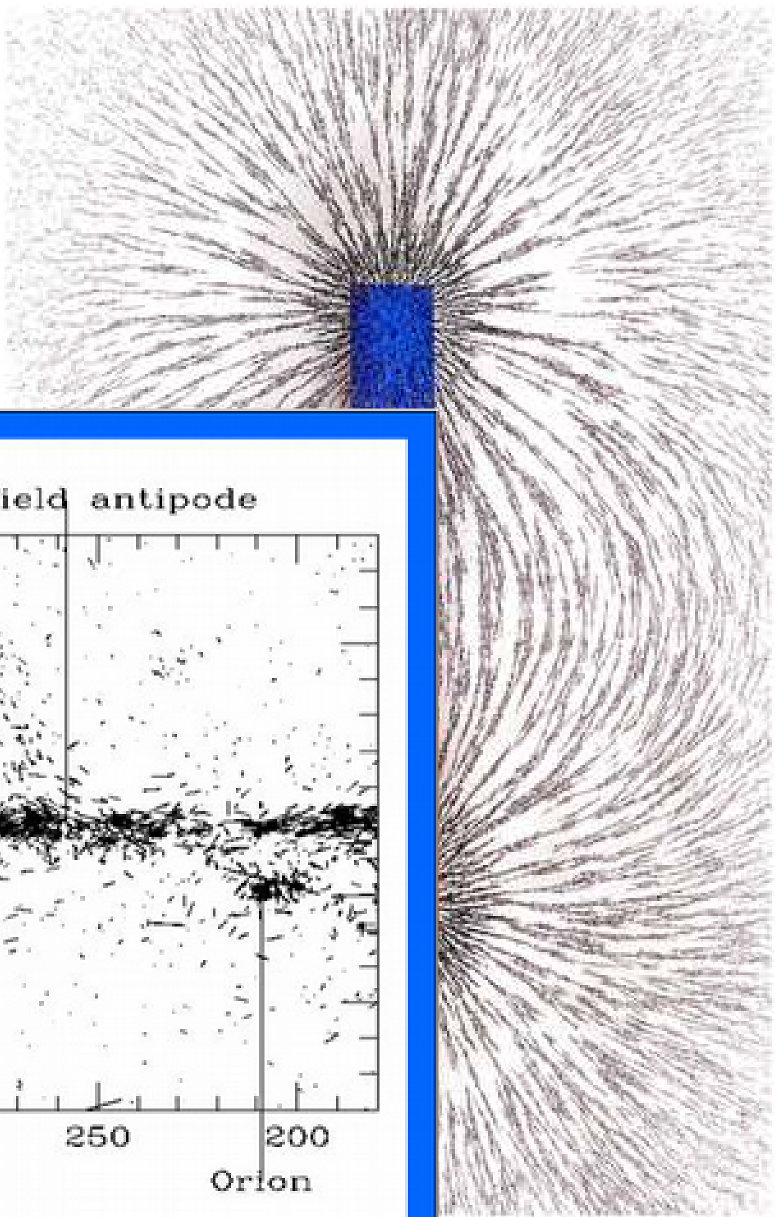

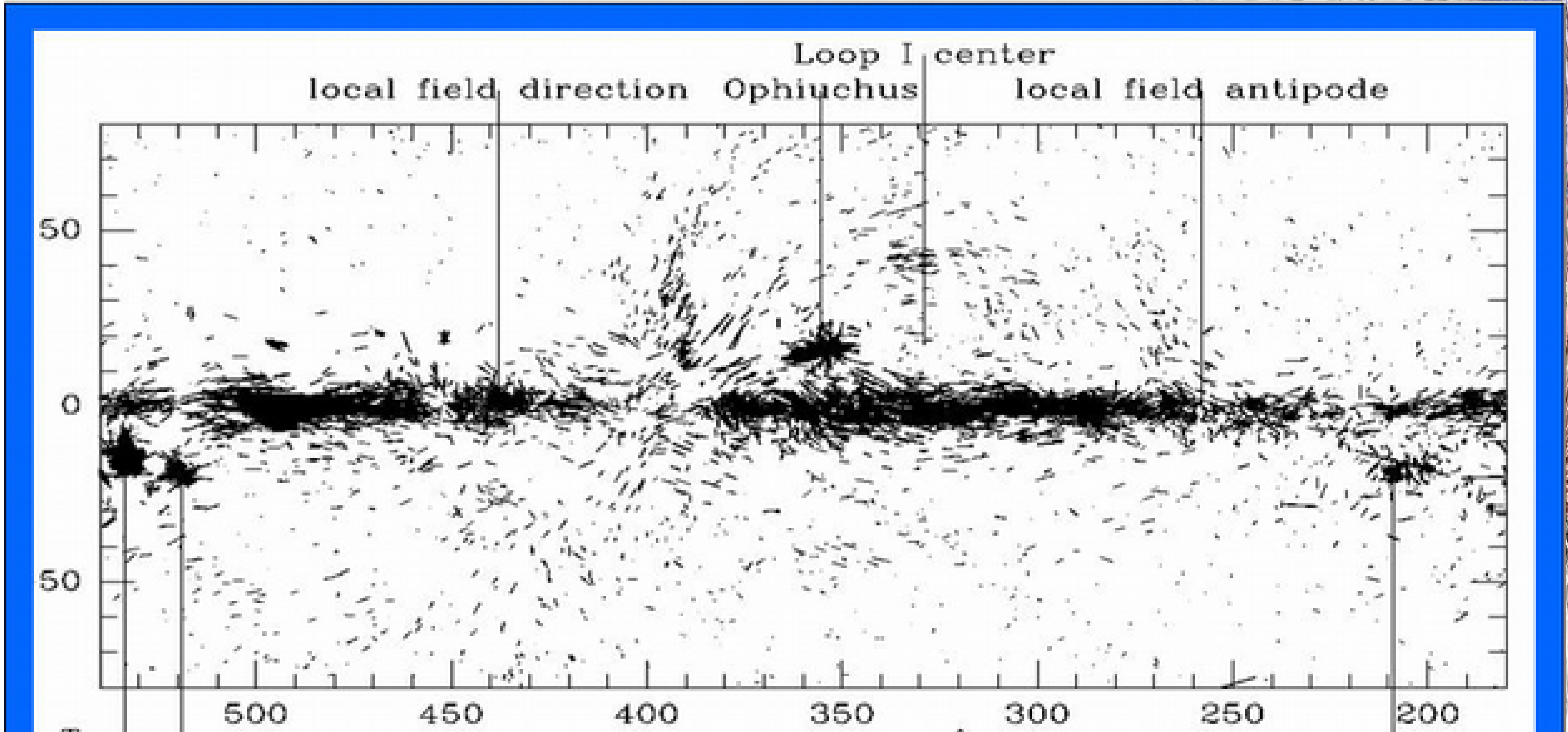

Heiles et al. 2000

Motivation – Galactic B-fields

- Several ways to determine magnetic field orientation and strength in the ISM:
- Optical and IR polarisation from dust-grains aligned along the field lines, e.g., Heiles et al. 2000
- Zeeman splitting of masers
  - MAGMO: OH maser survey (Green et al. 2012)

Figure: James Green

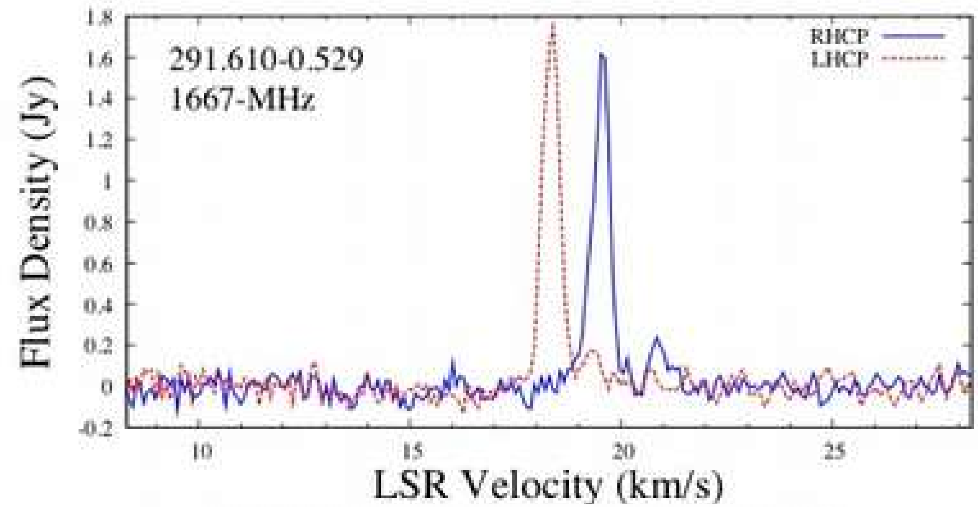

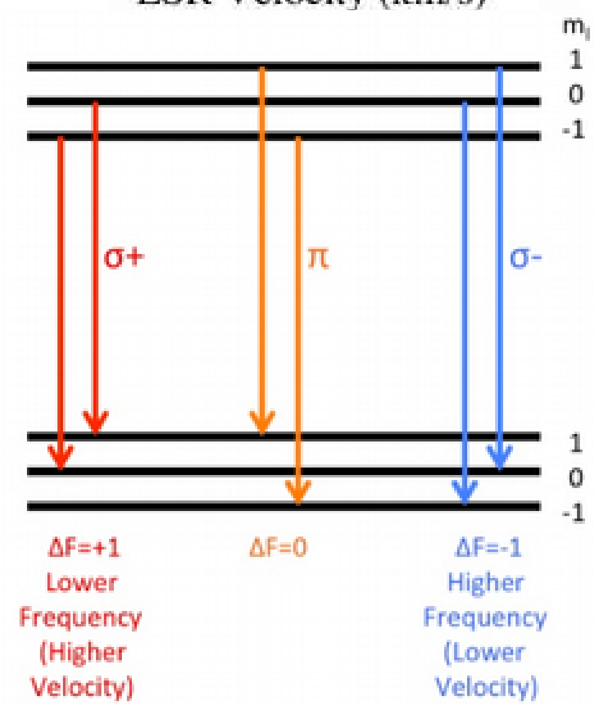

Motivation – Galactic B-fields

- Several ways to determine magnetic field orientation and strength in the ISM:
- Optical and IR polarisation from dust-grains aligned along the field lines, e.g., Heiles et al. 2000
- Zeeman splitting of masers
  - MAGMO: OH maser survey (Green et al. 2012)
- Synchrotron emission, e.g.,
  - Haslam 408 MHz map,
  - Reich et al 1.4 GHz map

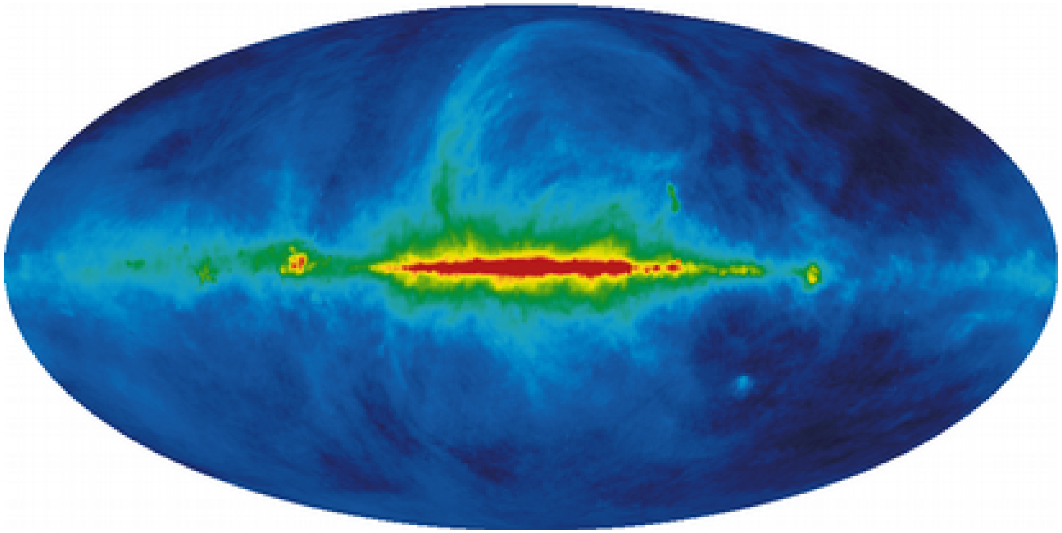

Haslam et al. 1982

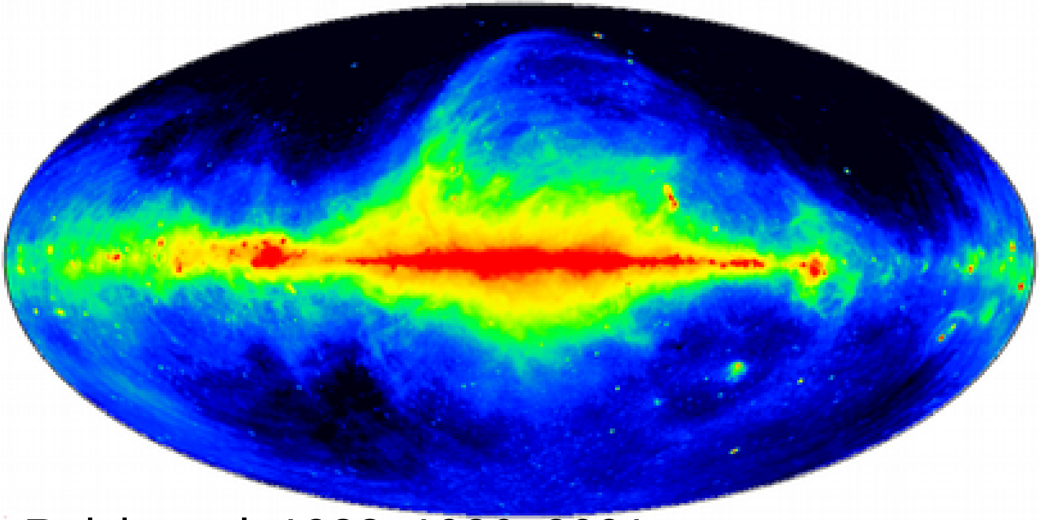

Reich et al. 1982, 1986, 2001

Motivation – Galactic B-fields

- Several ways to determine magnetic field orientation and strength in the ISM:
- Optical and IR polarisation from dust-grains aligned along the field lines, e.g., Heiles et al. 2000
- Zeeman splitting of masers
  - MAGMO: OH maser survey (Green et al. 2012)
- Synchrotron emission, e.g.,
  - Haslam 408 MHz map,
  - Reich et al 1.4 GHz map
- Faraday rotation of polarised background sources
  - Taylor et al. 2009

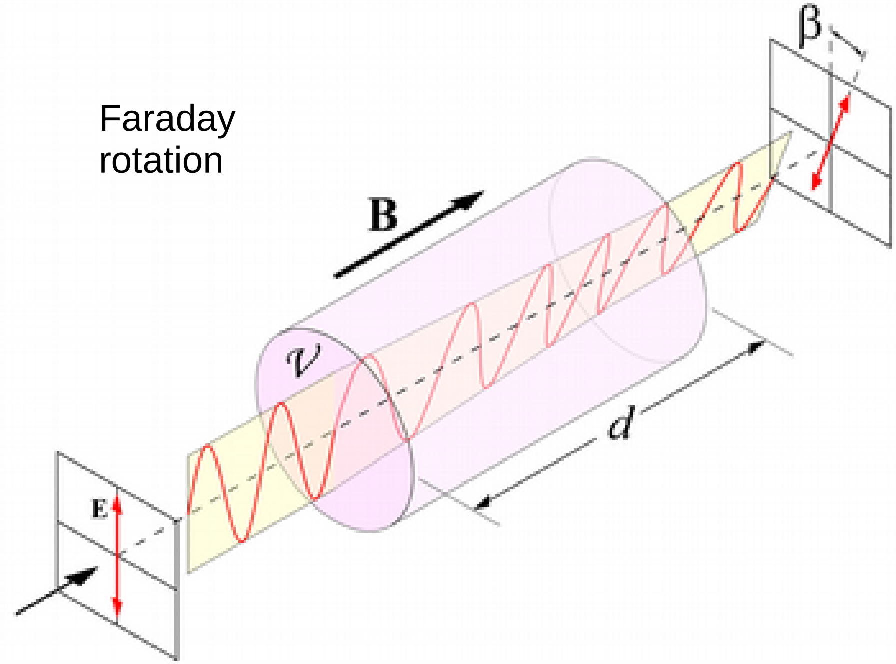

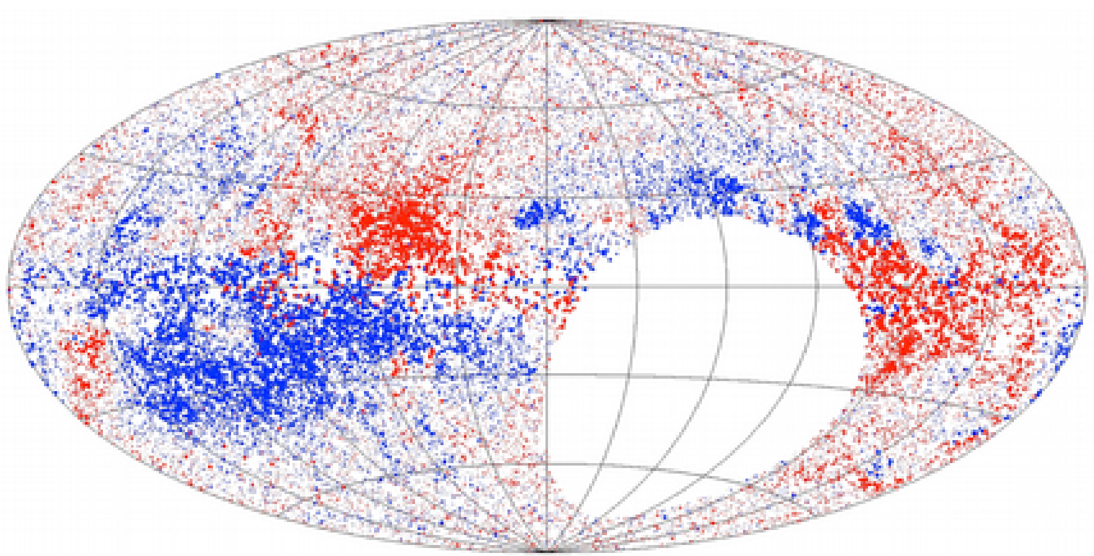

Measuring B-fields: Faraday Rotation

- Faraday rotation:

  Requires ionised gas threaded by a magnetic field

  Frequency dependent change in the polarisation angle

- Properties of rotating gas described by the Rotation Measure:

$$\Delta\theta = \mathrm{RM}\,\lambda^2 \quad \mathrm{rad},$$

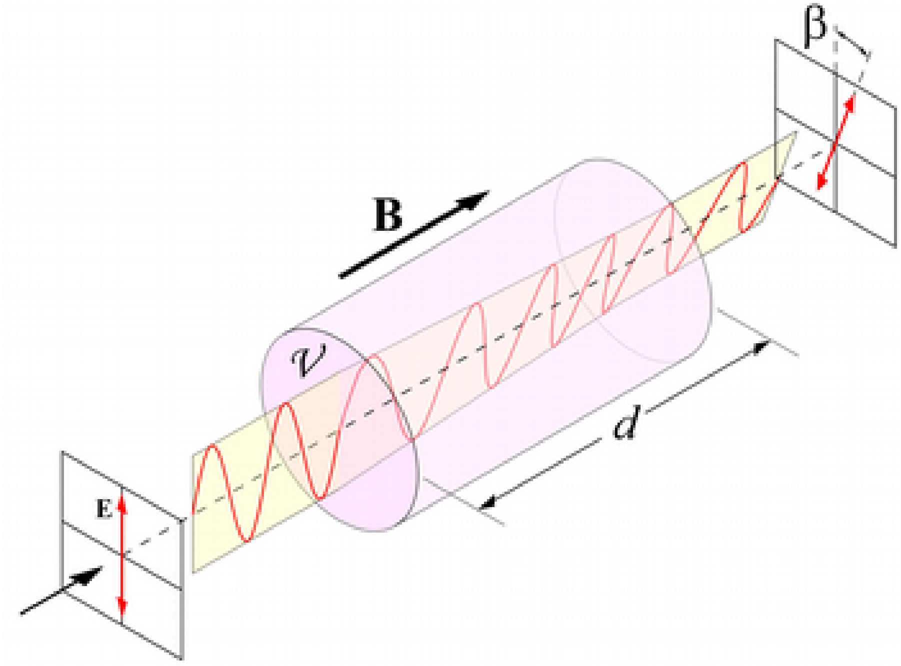

Measuring B-fields: Faraday Rotation

- Faraday rotation:

  Requires ionised gas threaded by a magnetic field

  Frequency dependent change in the polarisation angle

- Properties of rotating gas described by the Rotation Measure:

$$\Delta\theta = \mathrm{RM}\,\lambda^2 \quad \mathrm{rad},$$

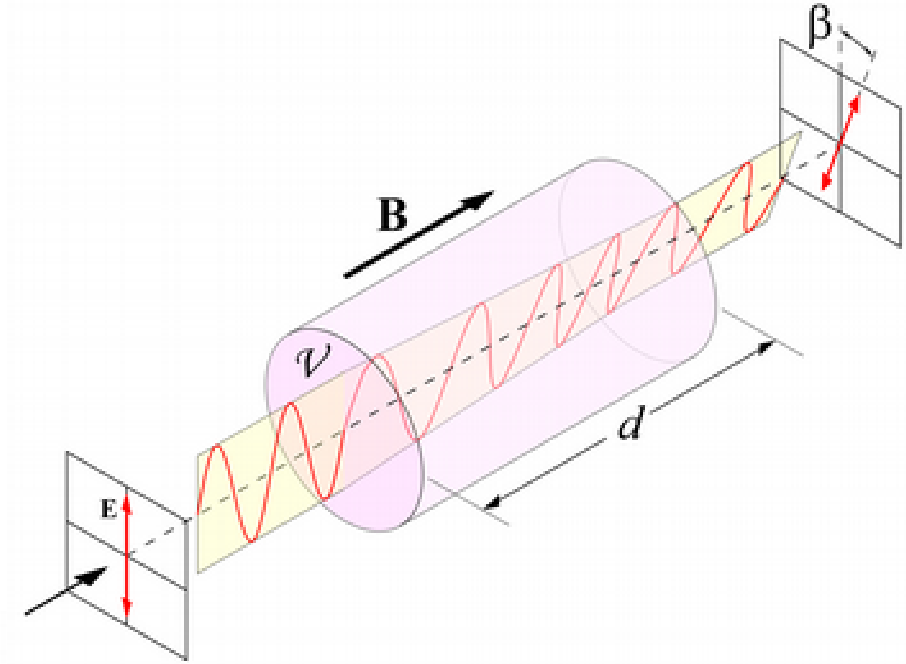

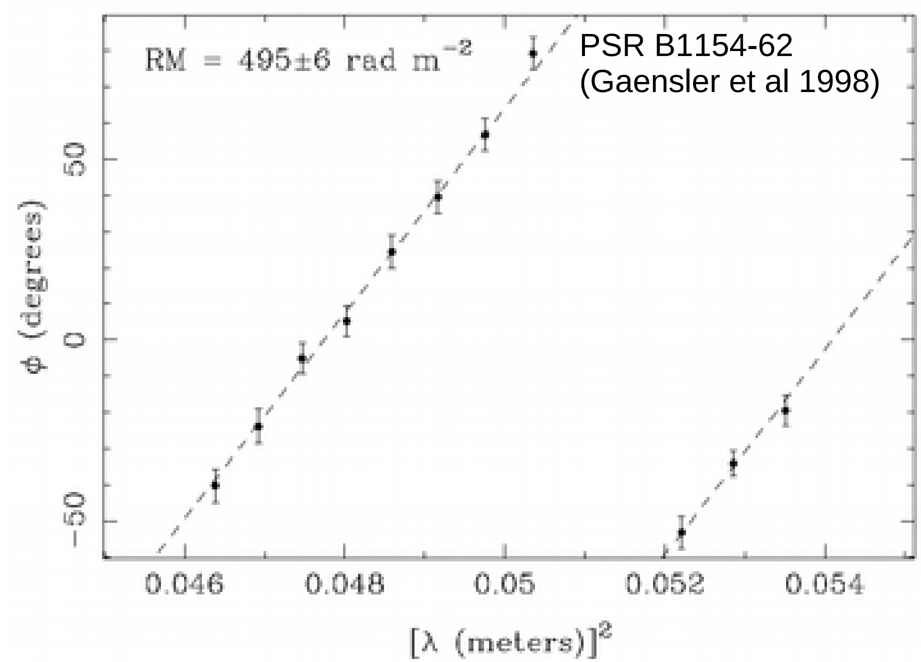

Measuring B-fields: Faraday Rotation

- Faraday rotation:

  Requires ionised gas threaded by a magnetic field

  Frequency dependent change in the polarisation angle

- Properties of rotating gas described by the Rotation Measure:

$$\Delta\theta = \mathrm{RM}\,\lambda^2 \quad \mathrm{rad},$$

$$\mathrm{RM} = 0.81 \int_{obs}^{src} n_e\, B_{||}\, dl \quad \mathrm{rad\,m^{-2}}.$$

  If electron-density is known, can calculate the line-of-sight B-field and vice-versa

  (assuming the path-length is known)

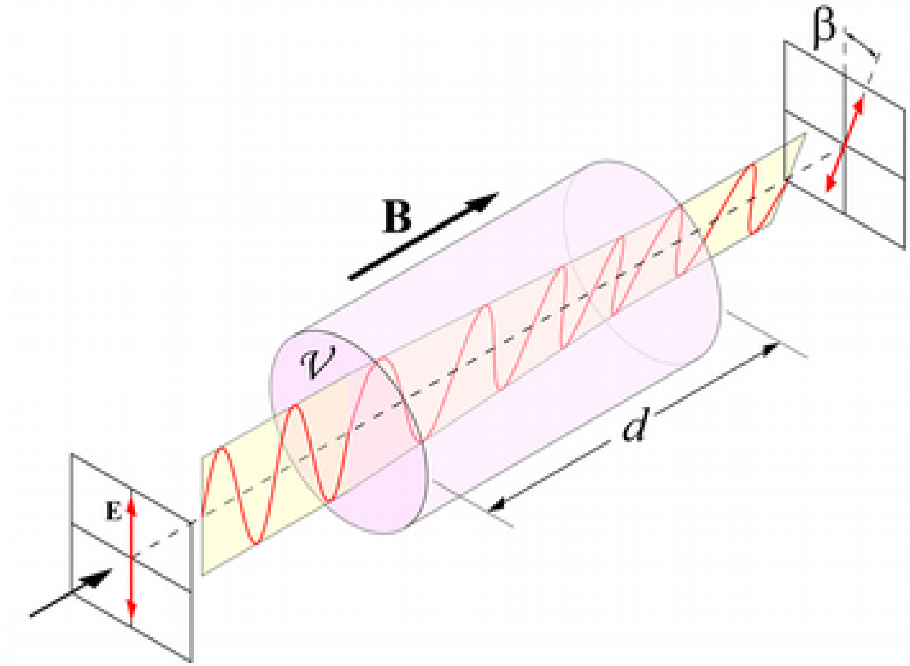

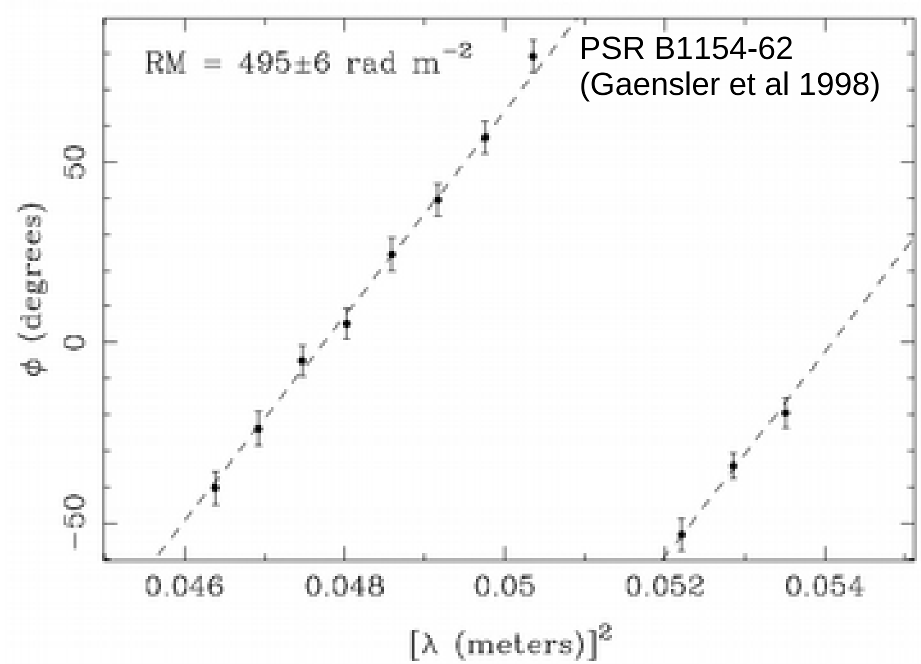

Measuring B-fields: Faraday Rotation

NVSS all-sky RM map

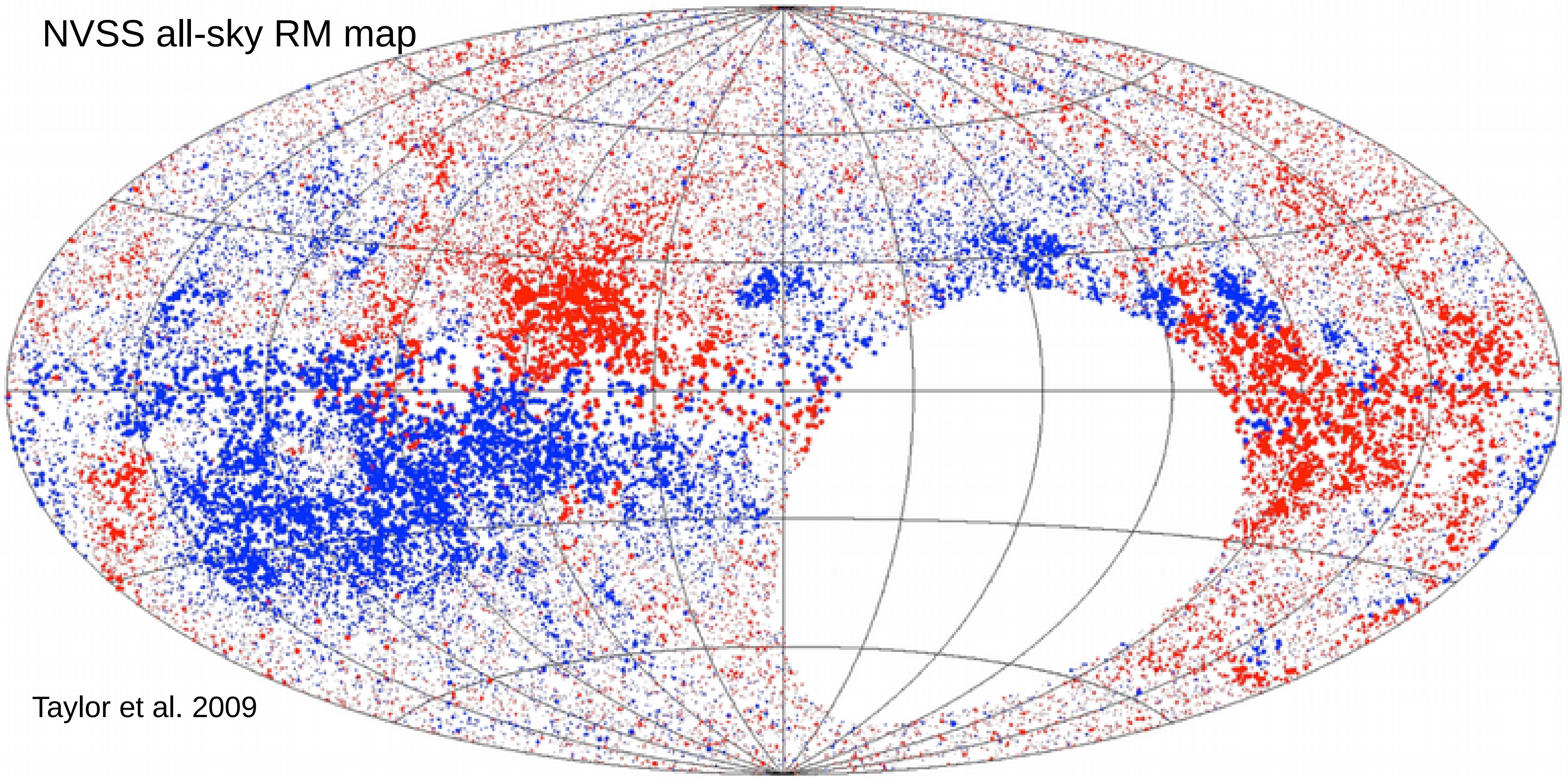

Taylor et al. 2009

Measuring B-fields: Faraday Rotation

NVSS all-sky RM map
+ additions

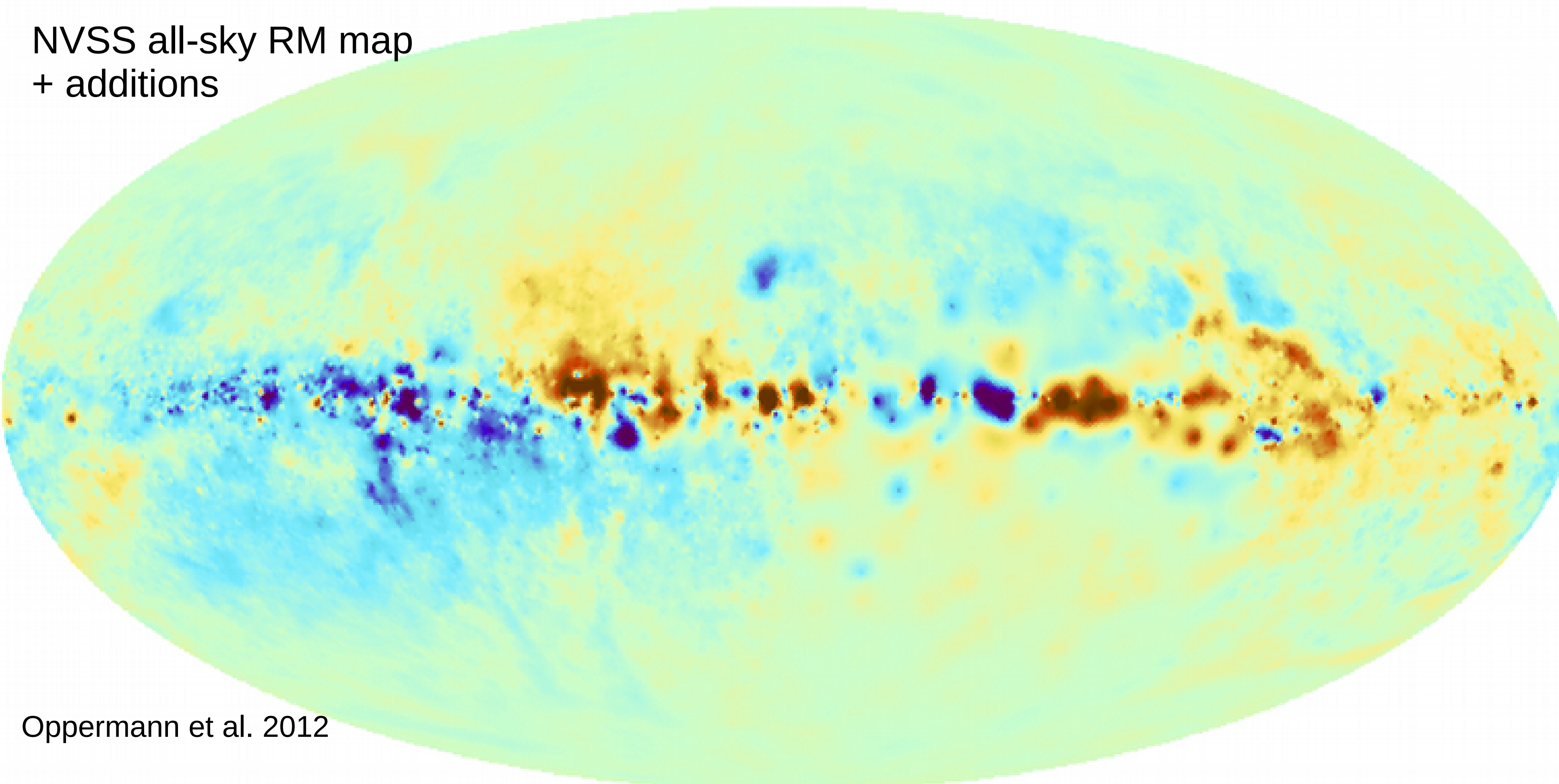

Oppermann et al. 2012

Measuring B-fields: Faraday Rotation

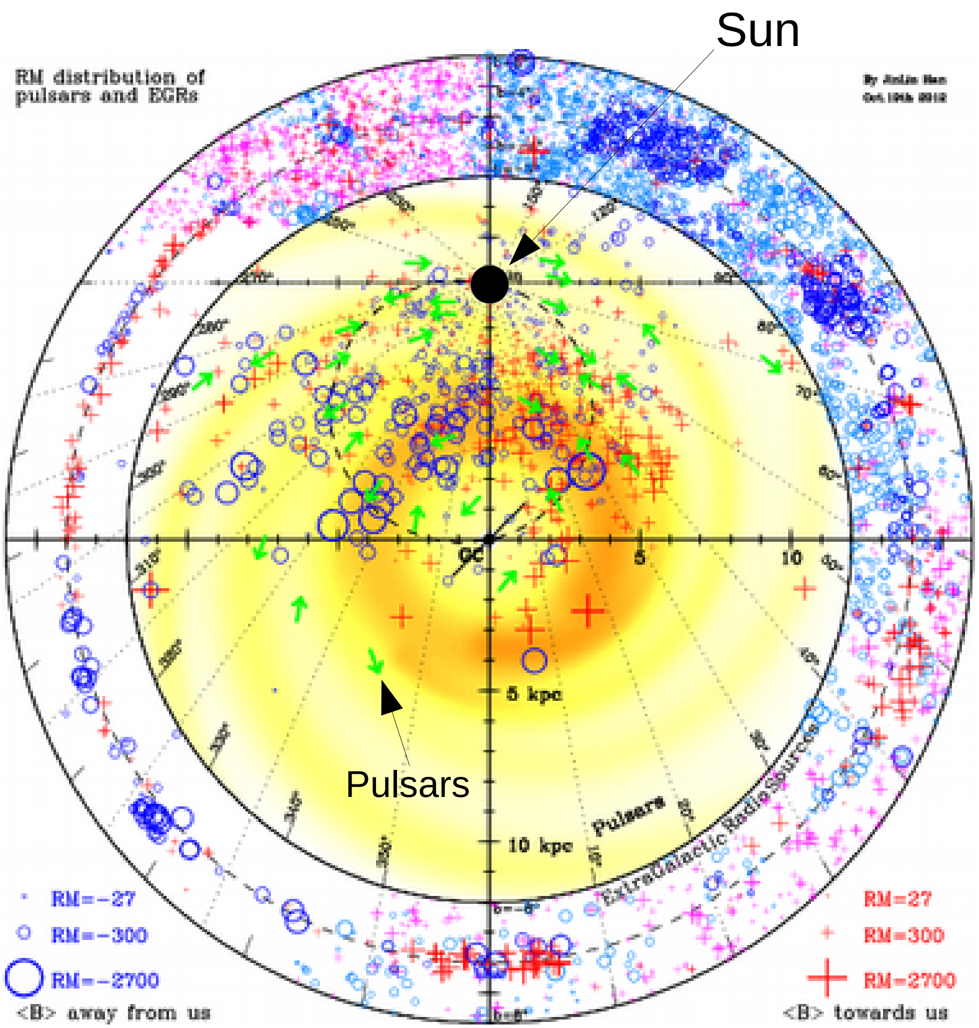

JinLin Han, 2013

Measuring B-fields: Faraday Rotation

Sun

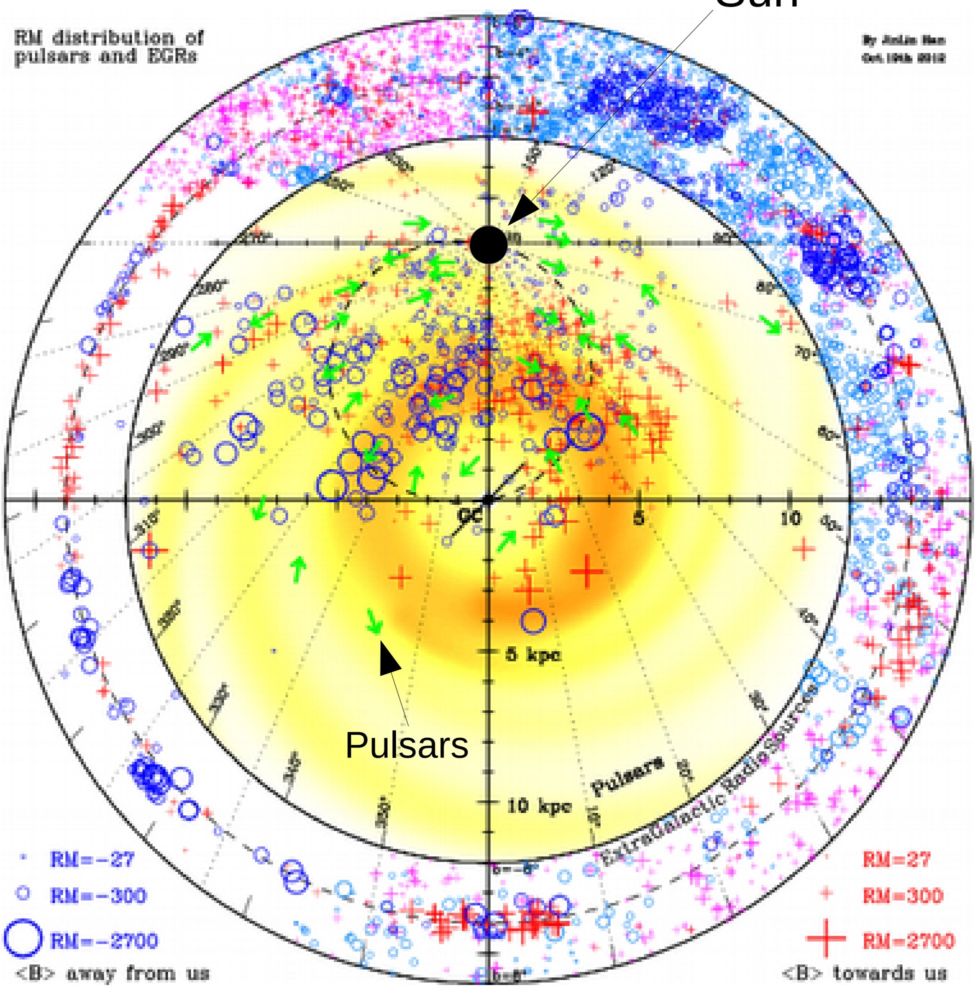

JinLin Han, 2013

Two most recent models of the Galactic B-field:

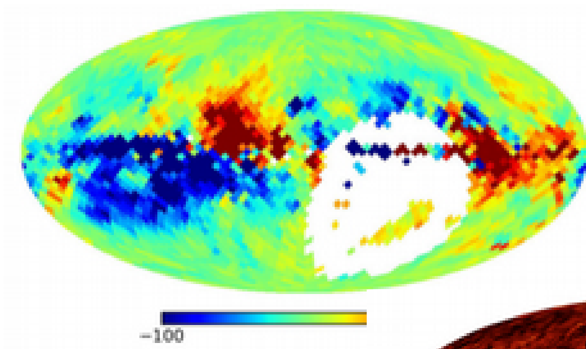

Binned RM data

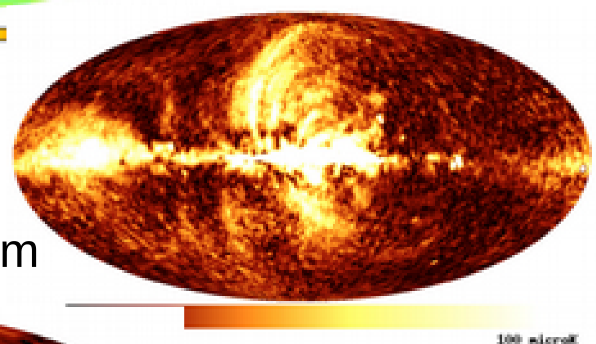

Polarised radio-continuum

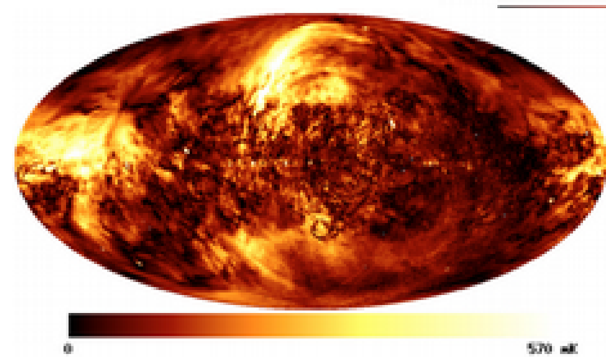

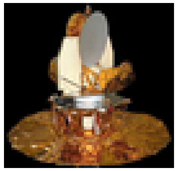

WMAP

Sun et al. 2008 Jansson & Farrar 2012

Measuring B-fields: Faraday Rotation

Sun

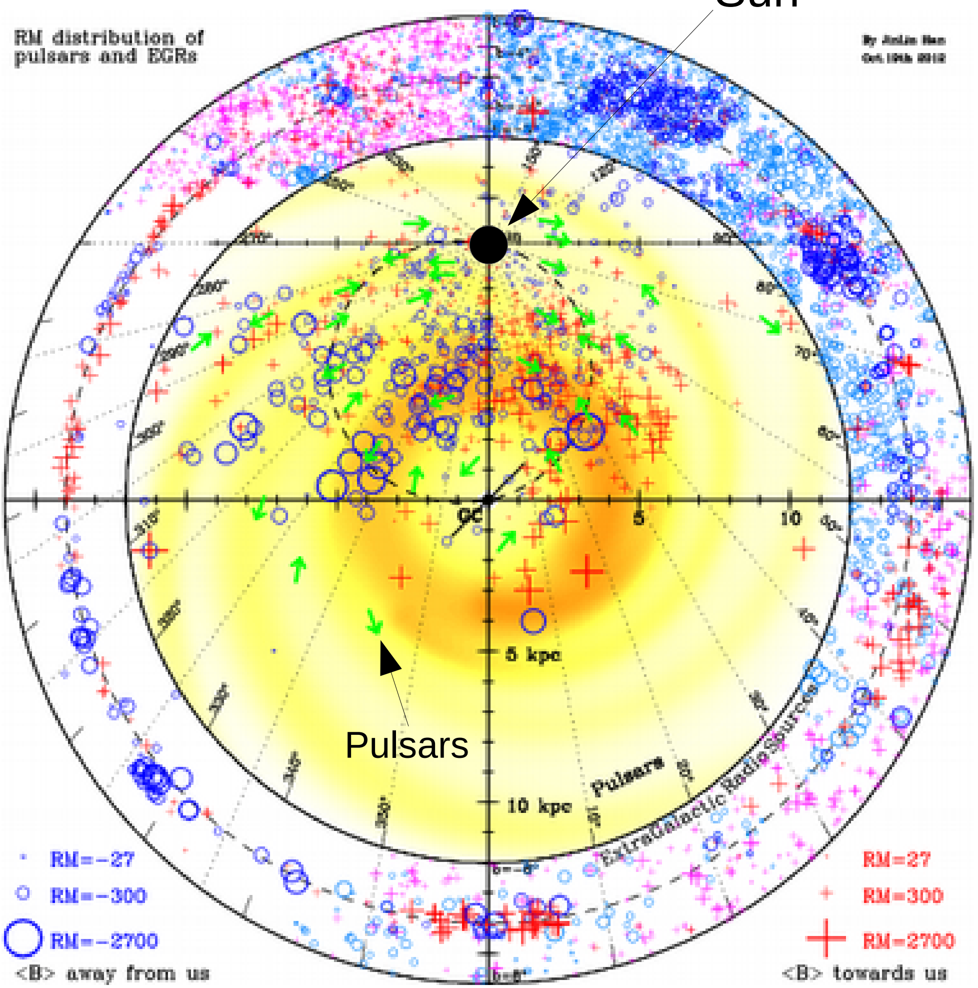

Pulsars

JinLin Han, 2013

Two most recent models of the Galactic B-field:

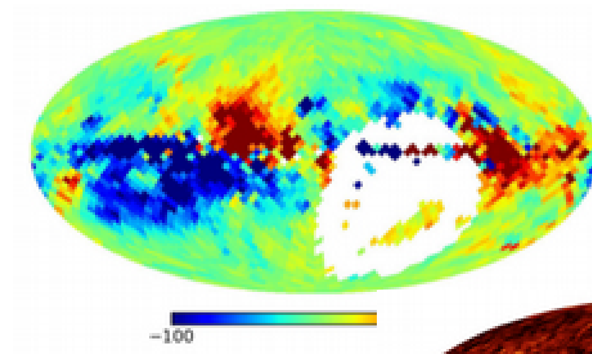

Binned
RM data

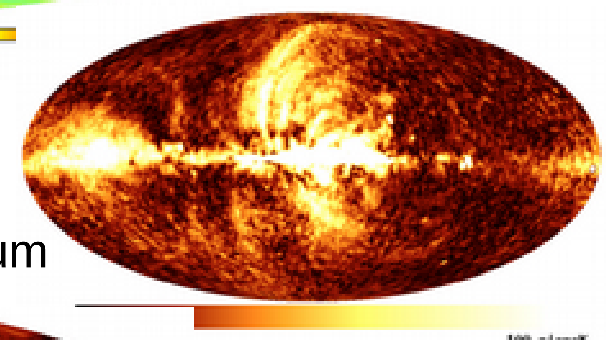

Polarised
radio-continuum

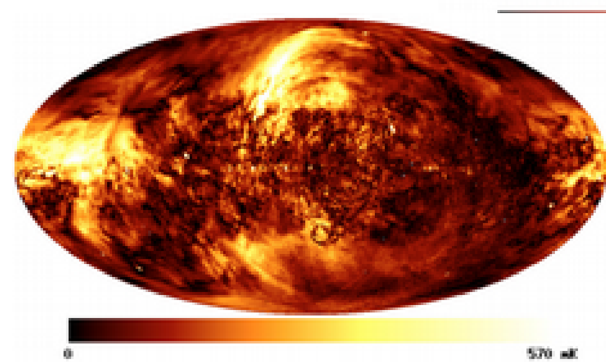

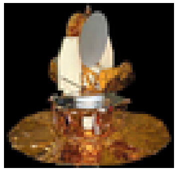

WMAP

Sun et al. 2008 **Jansson & Farrar 2012**

Measuring B-fields: Faraday Rotation

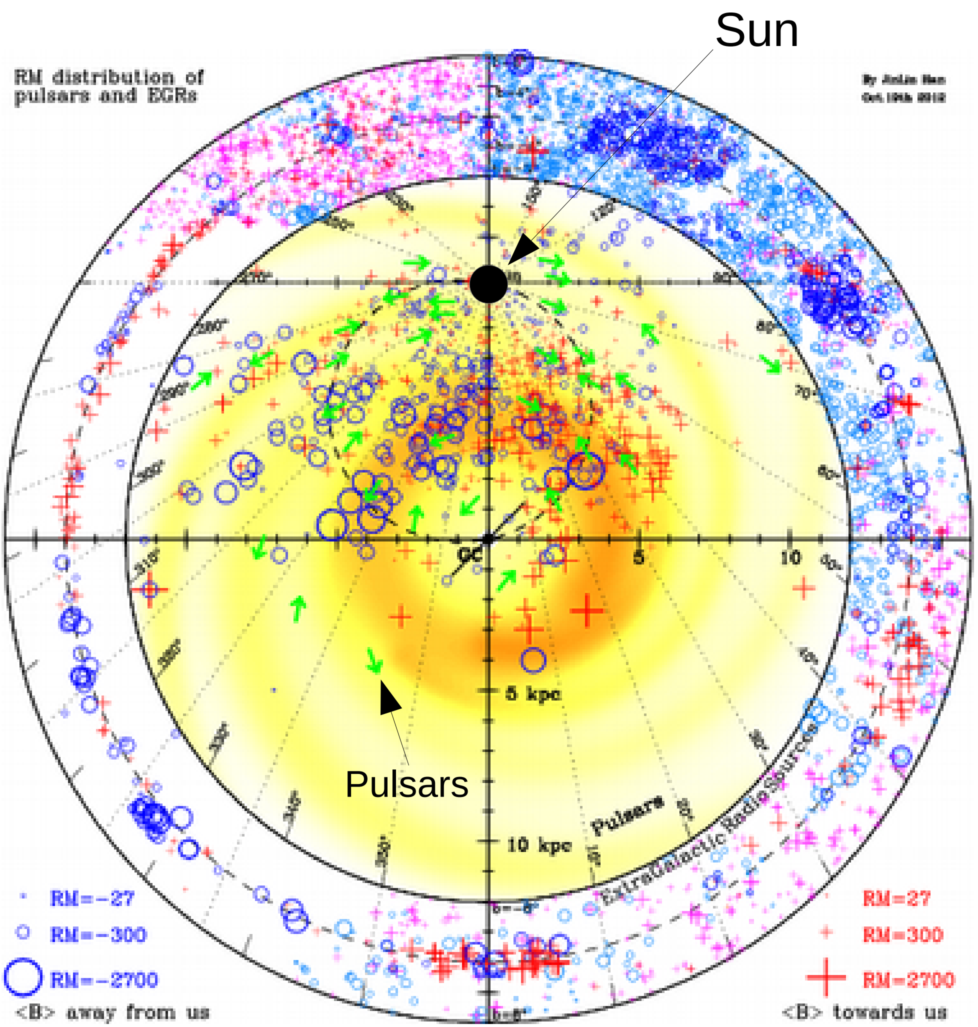

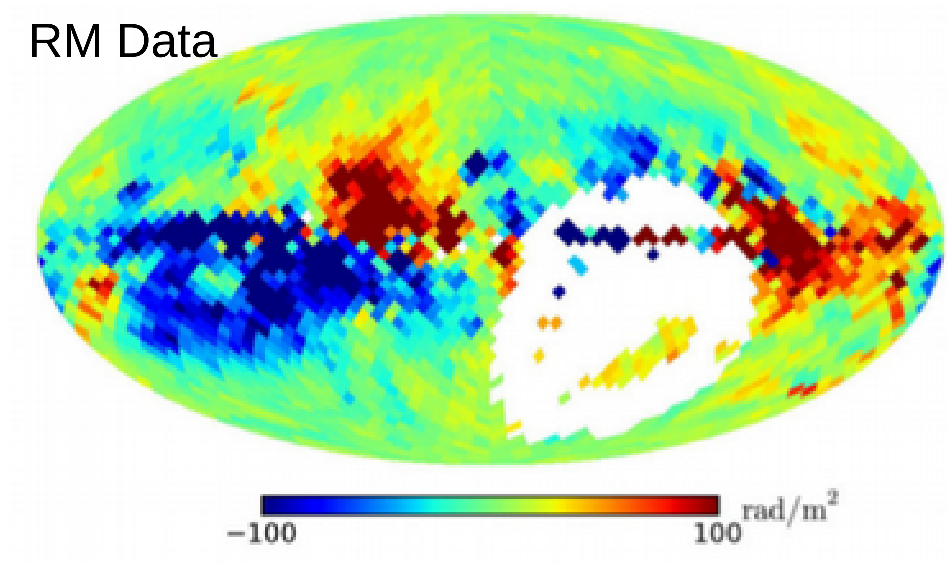

JinLin Han, 2013

Jansson & Farrar 2012

Measuring B-fields: Faraday Rotation

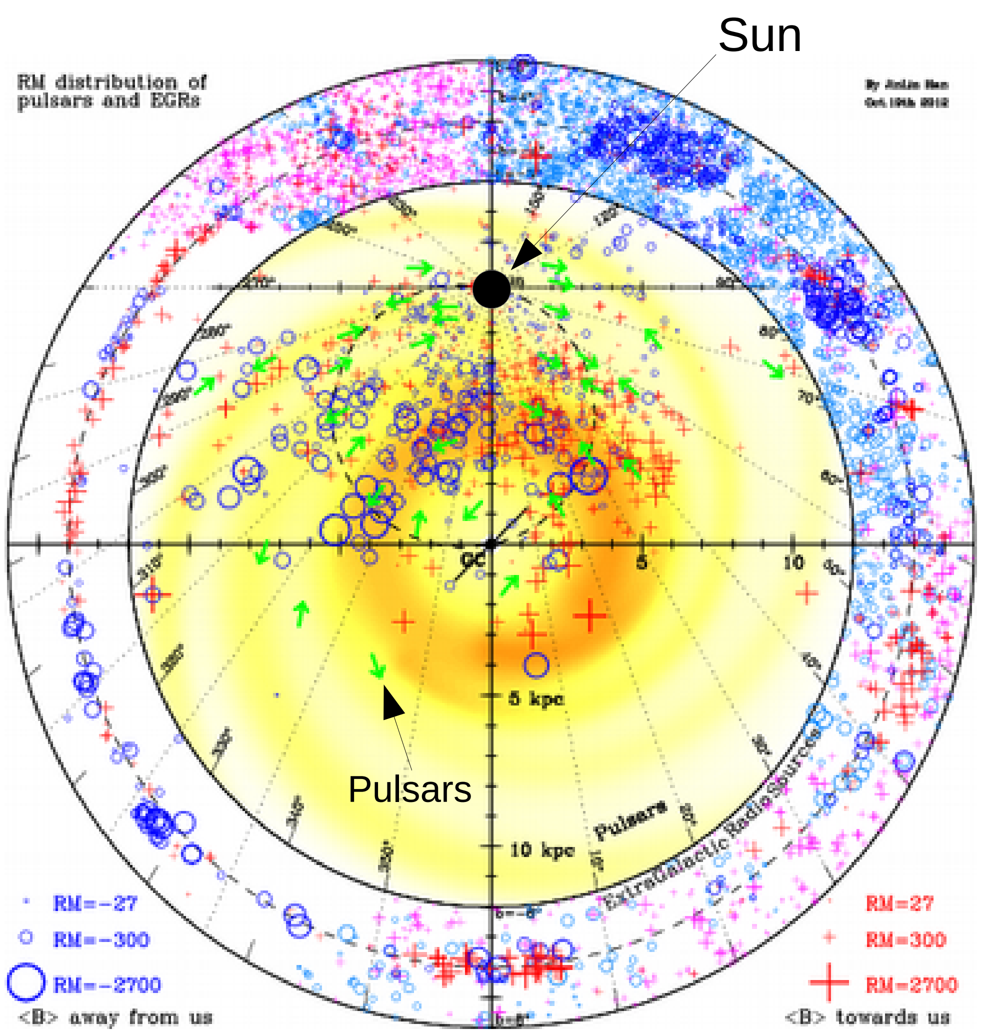

JinLin Han, 2013

RM Data

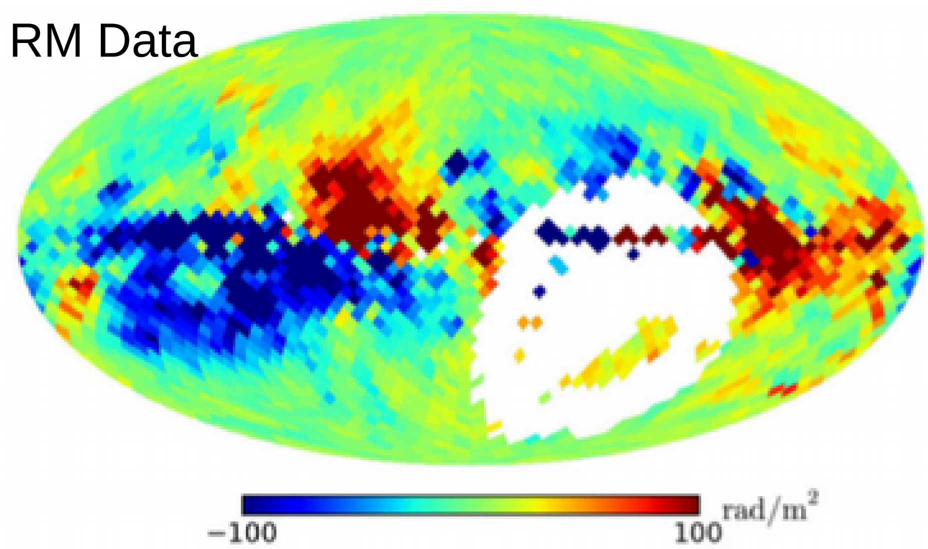

Model

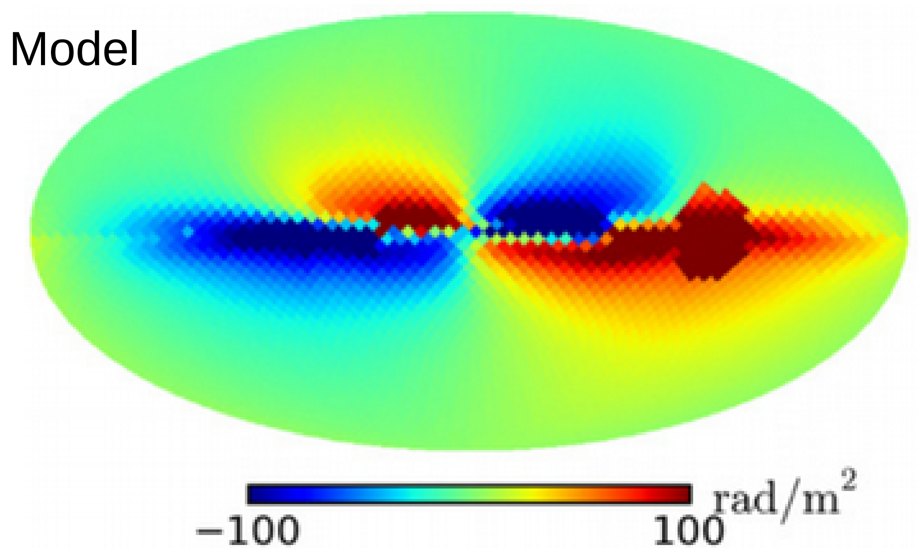

Jansson & Farrar 2012

Measuring B-fields: Faraday Rotation

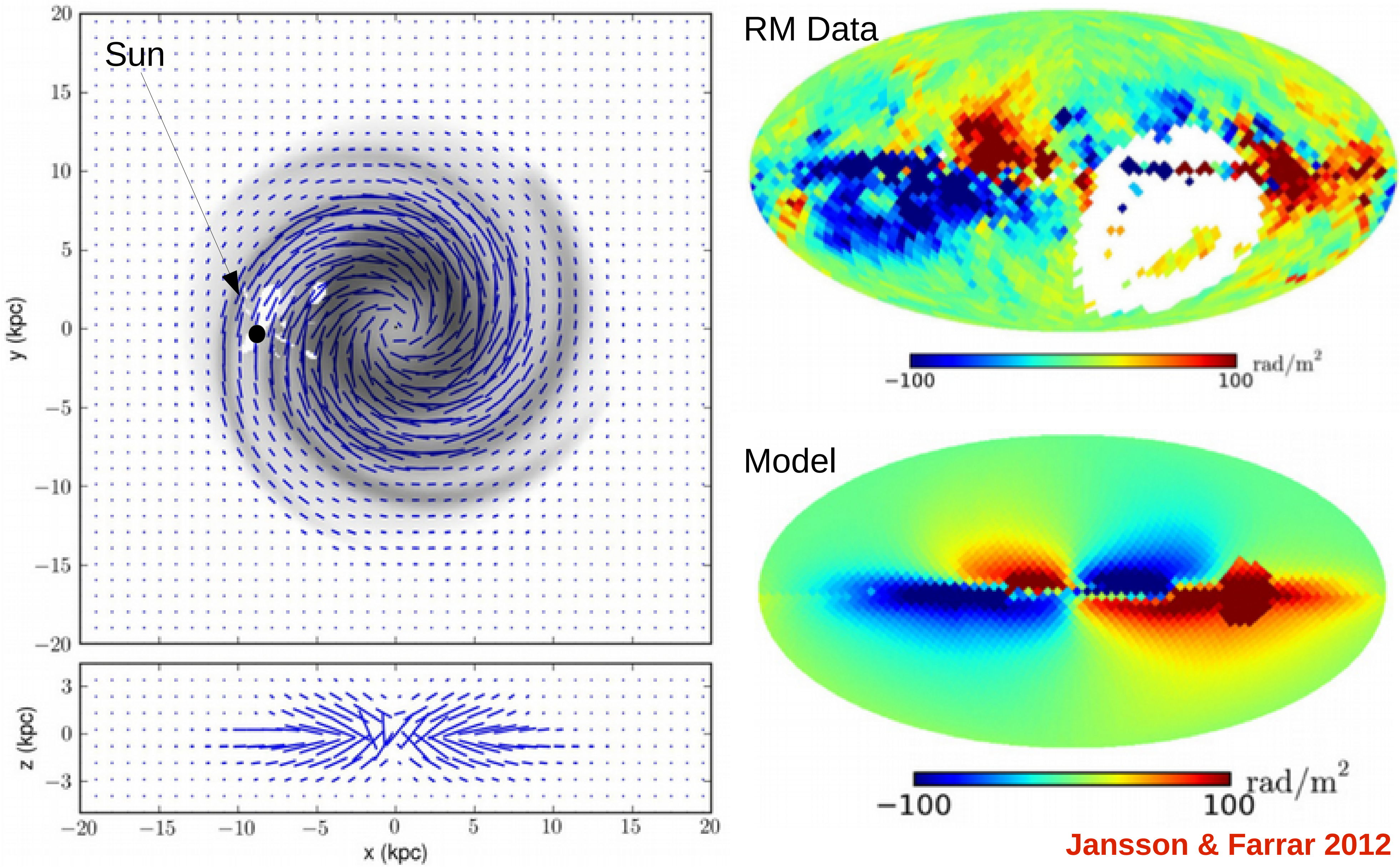

Jansson & Farrar 2012

Measuring B-fields: Faraday Rotation

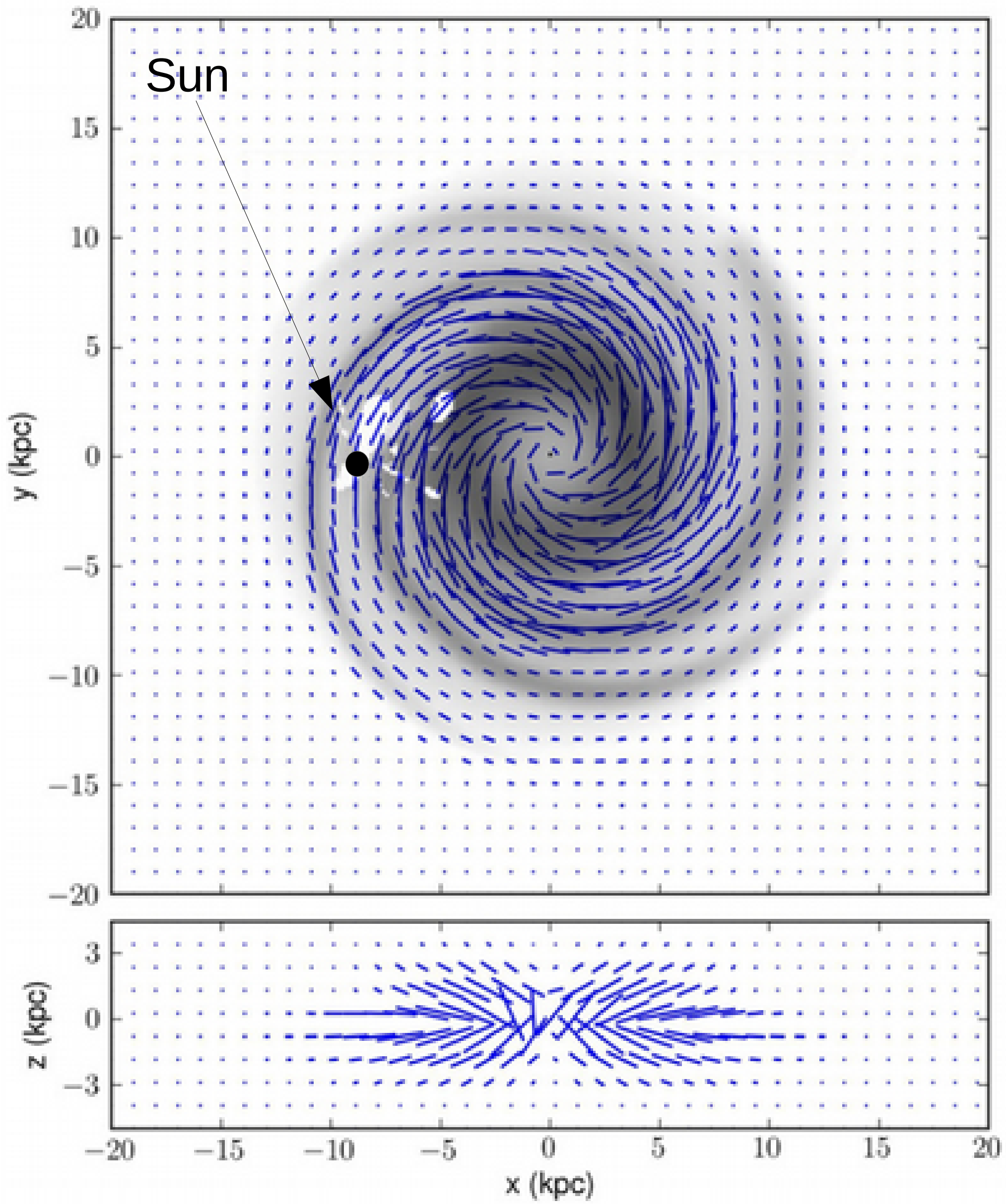

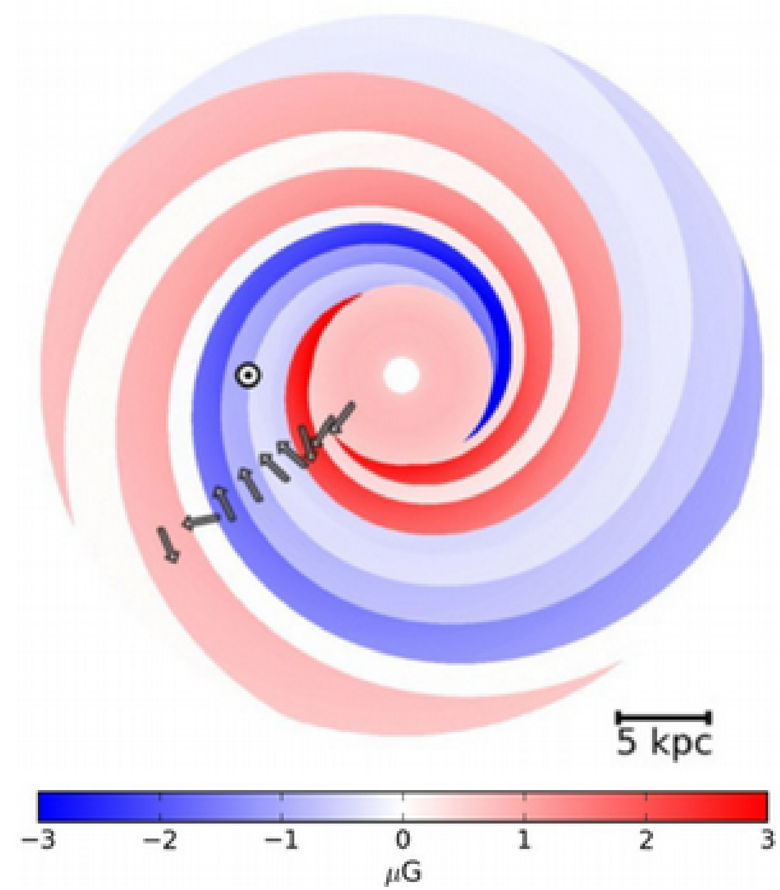

Jansson & Farrar 2012

Measuring B-fields: Faraday Rotation

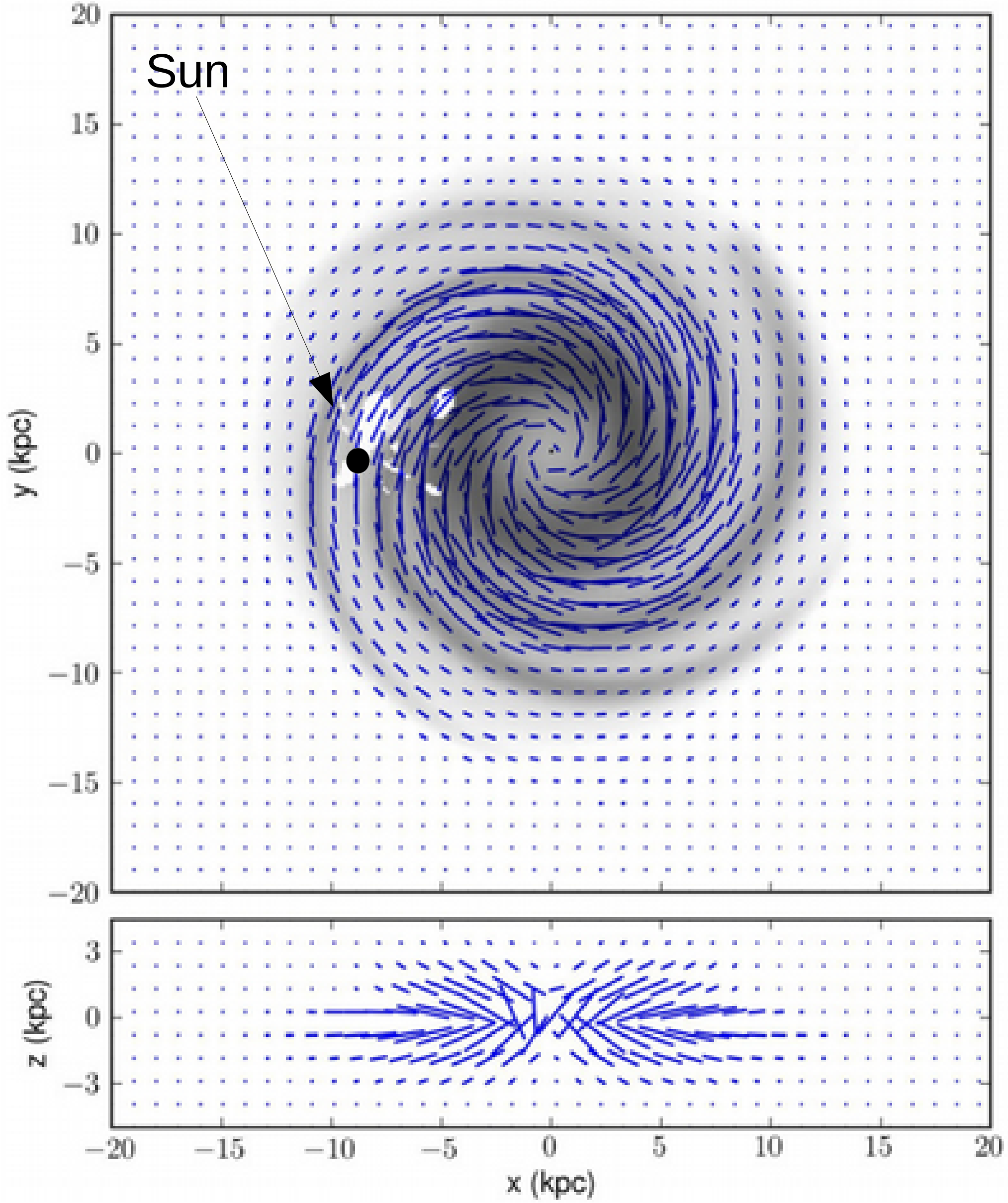

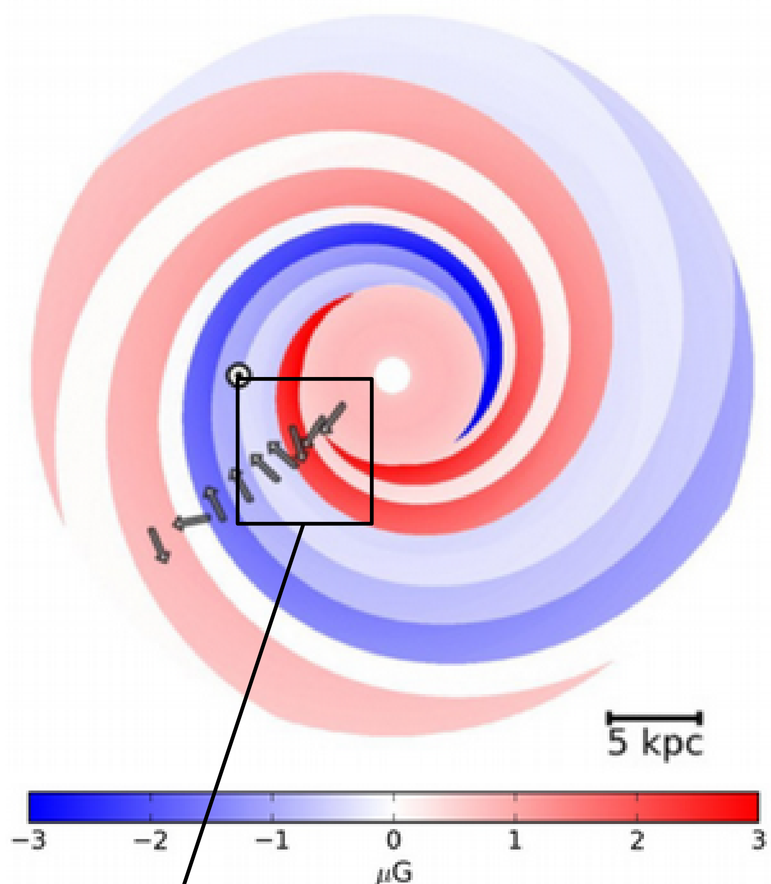

Evidence for field reversals between arms
Not seen in external galaxies – are these real?

Jansson & Farrar 2012

Measuring B-fields: Faraday Rotation

- Additional anchor-points *within the Galaxy* crucial for next generation of models

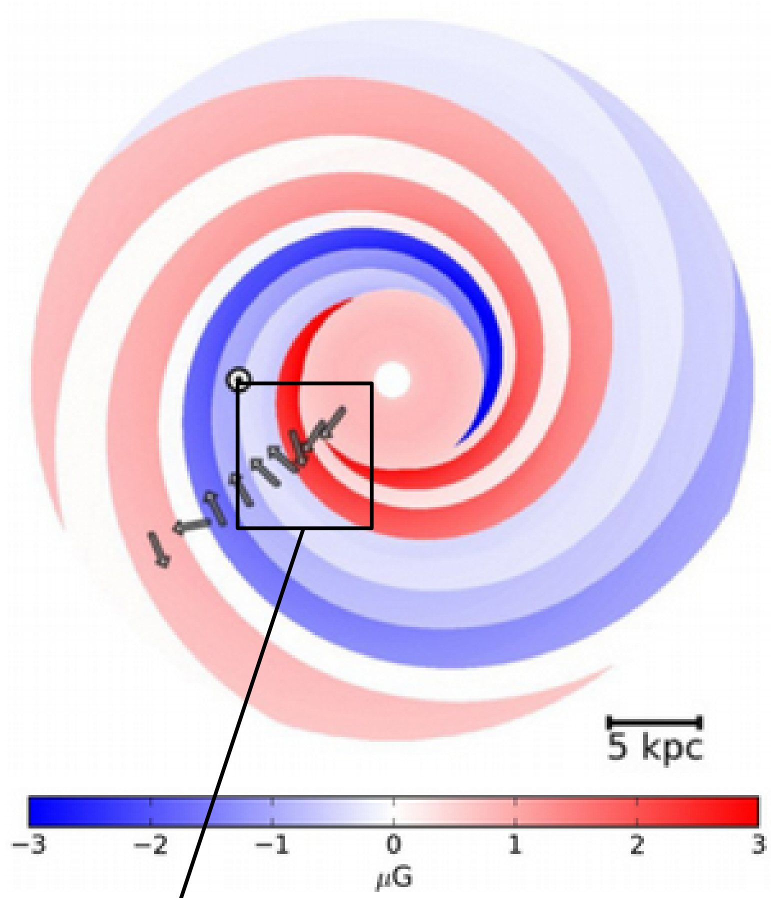

Evidence for field reversals between arms
Not seen in external galaxies – **are these real?**

Jansson & Farrar 2012

Measuring B-fields: Faraday Rotation

- Additional anchor-points *within the Galaxy* crucial for next generation of models

  Pulsars (with accurate distances) or other local magnetic phenomena – **interstellar bubbles**

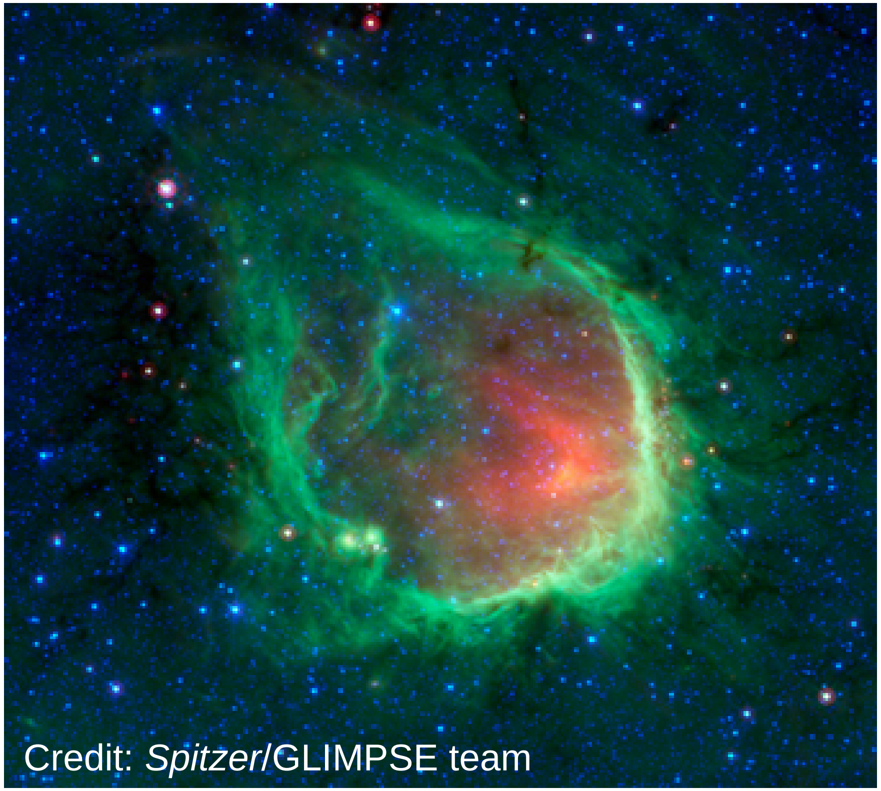

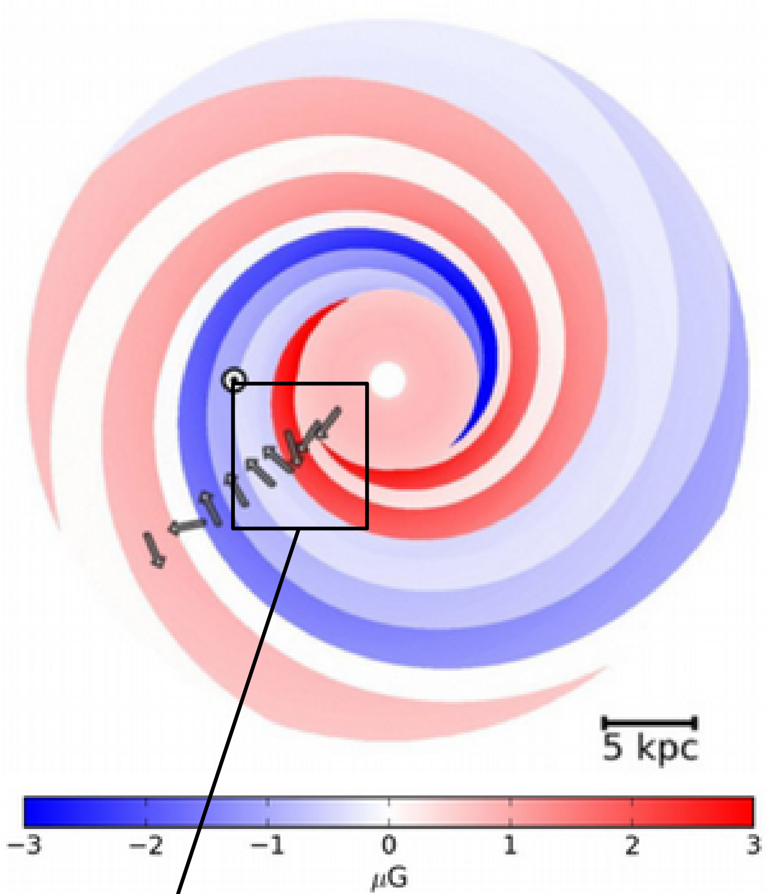

Evidence for field reversals between arms
Not seen in external galaxies – **are these real?**

Jansson & Farrar 2012

Measuring B-fields: bubbles

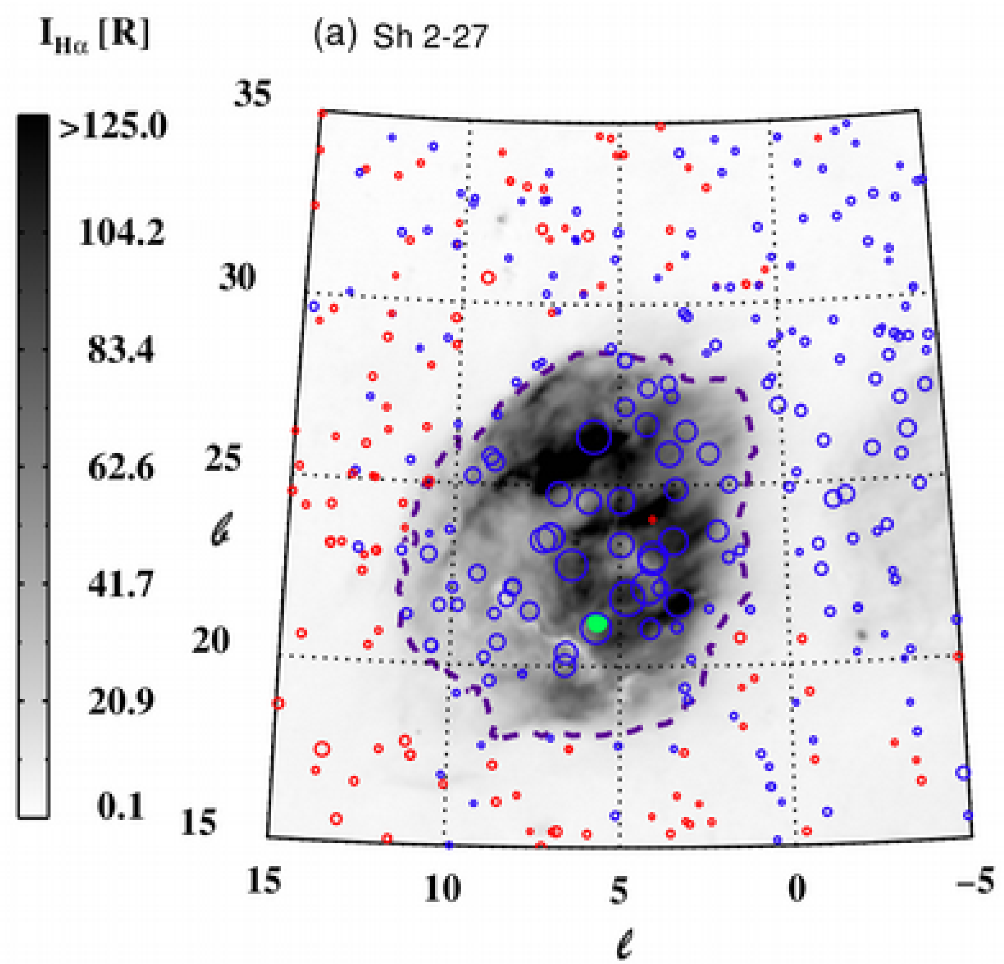

Harvey-Smith et al. 2011

- Discrete ionised objects in the Galaxy impose their own RM-signature on the large scale map of Rotation Measures
- The net RM compared to the surrounding background is due to the environment local to the object

Measuring B-fields: bubbles

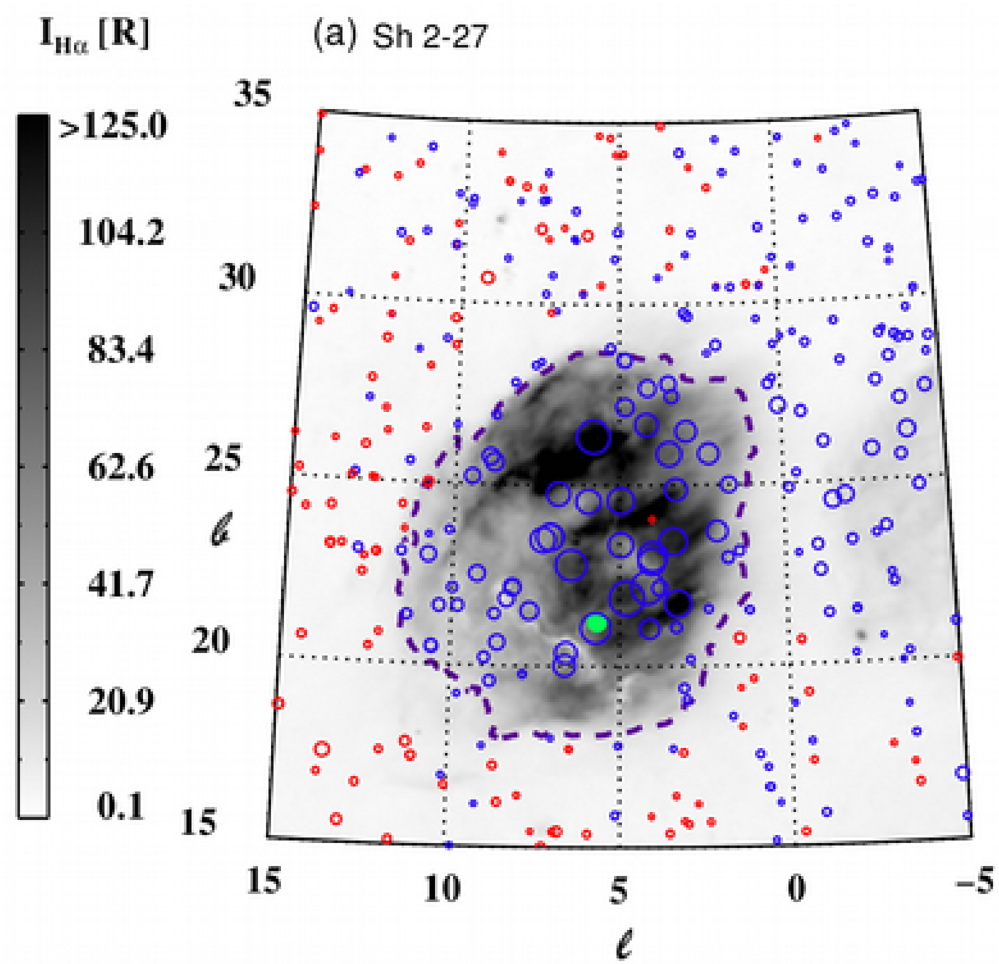

Harvey-Smith et al. 2011

- Discrete ionised objects in the Galaxy impose their own RM-signature on the large scale map of Rotation Measures
- The net RM compared to the surrounding background is due to the environment local to the object
- Can use individial objects as probes of *local* B and n_e
- Ultimate goal – use many objects at different distances to build up a 3D picture of the Galactic B-field

Measuring B-fields: bubbles: SNR

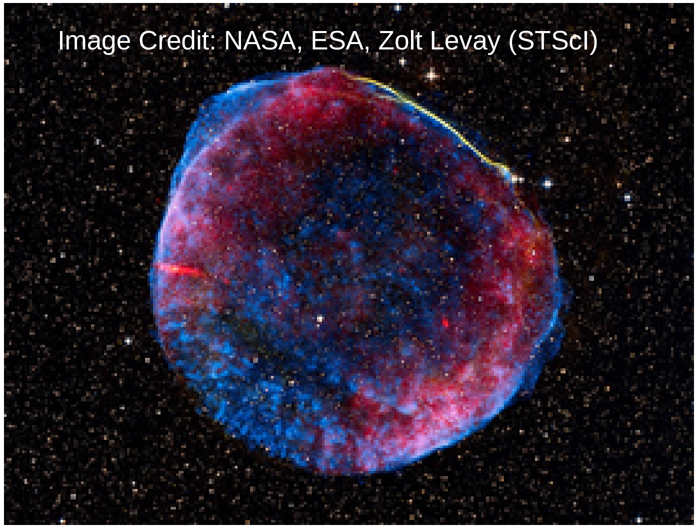

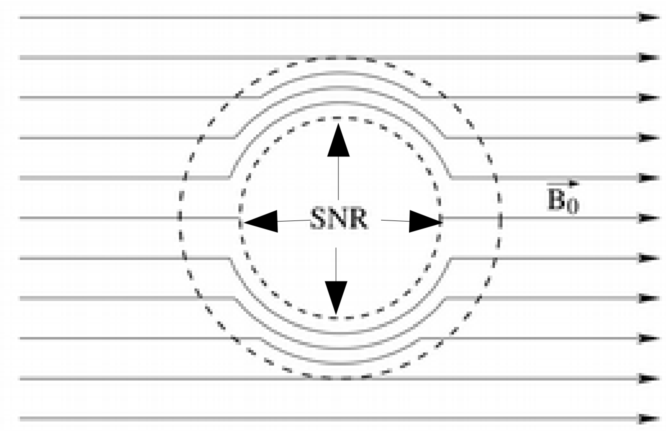

- Fast expansion: shock waves compresses and amplify the swept up magnetic field

Measuring B-fields: bubbles: SNR

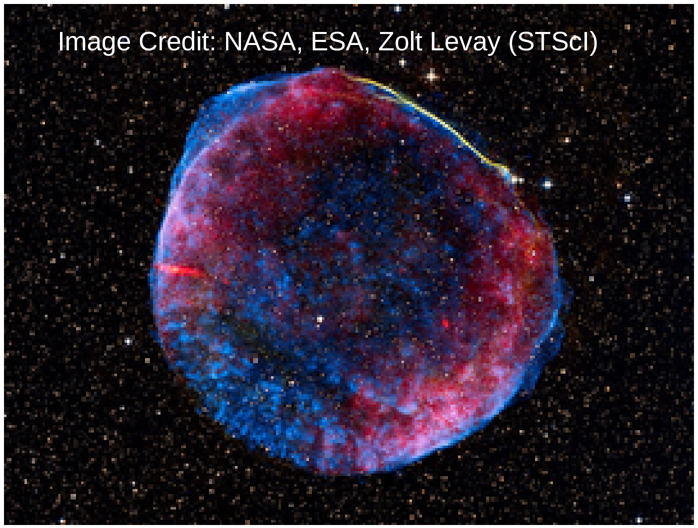

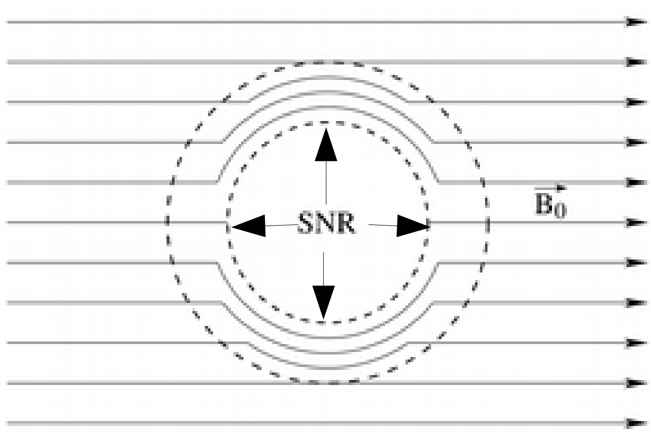

Kothes & Brown 2009

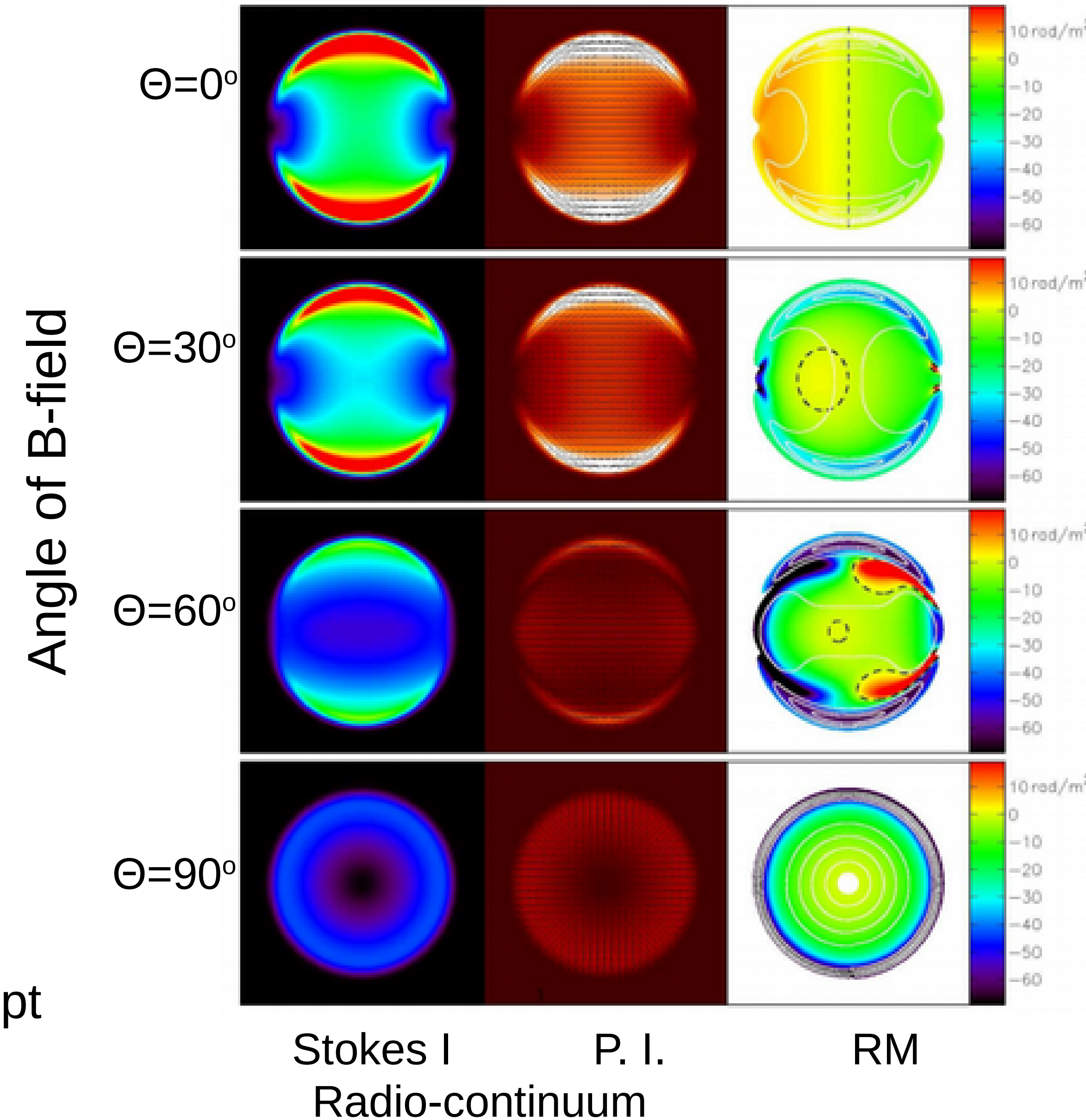

- Fast expansion: shock waves compresses and amplify the swept up magnetic field

Measuring B-fields: bubbles: HII regions

Image: Andreas Fink / wikimedia

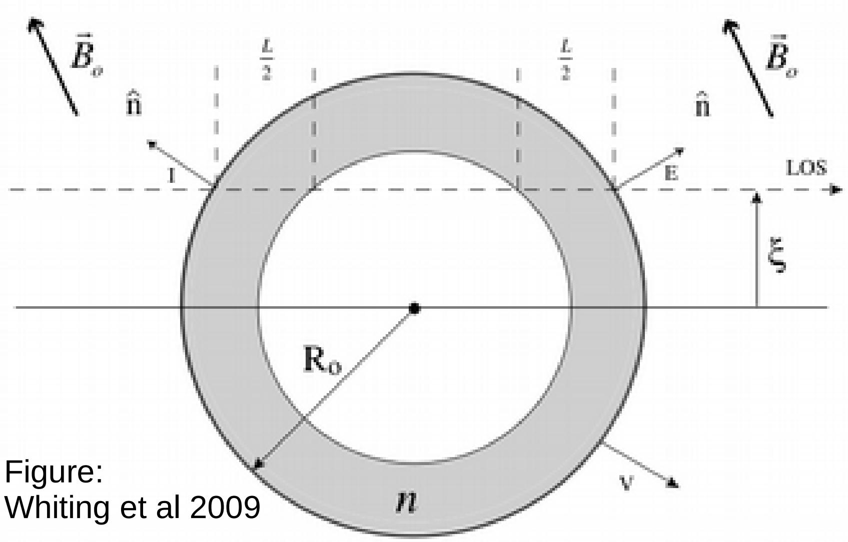

Figure:
Whiting et al 2009

Measuring B-fields: bubbles: HII regions


Rosette Nebula

Image: Andreas Fink / wikimedia

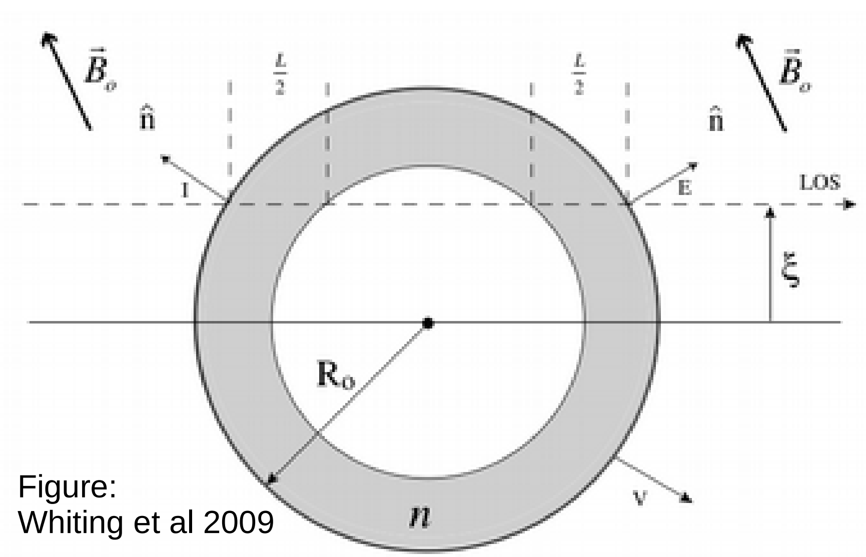

Figure:
Whiting et al 2009

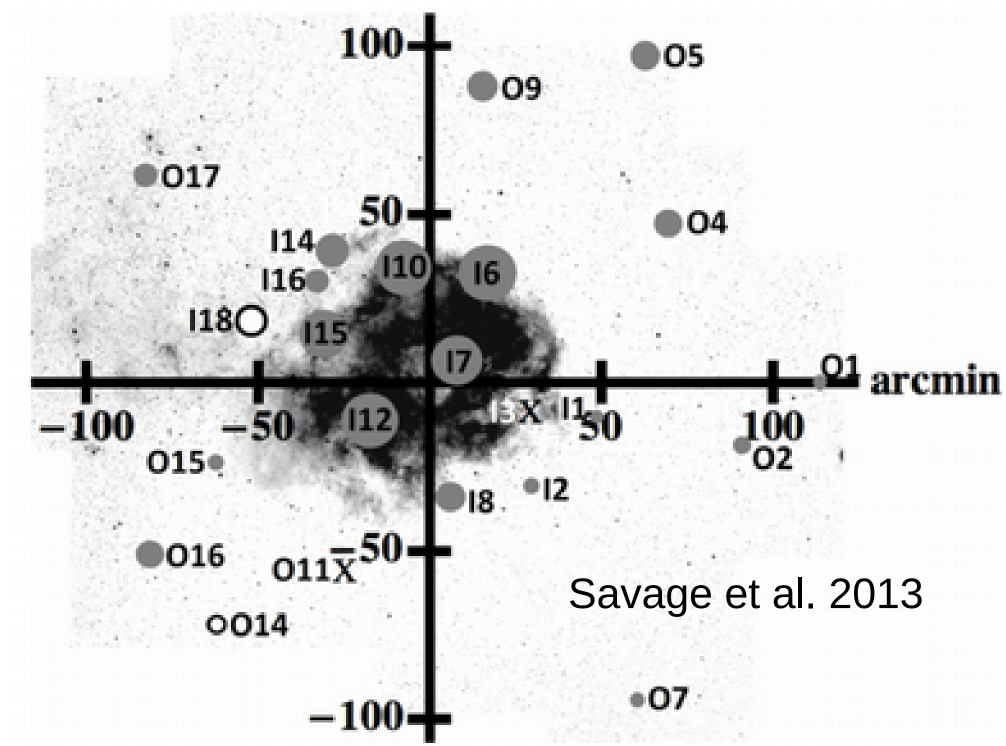

Savage et al. 2013

Measuring B-fields: bubbles: HII regions

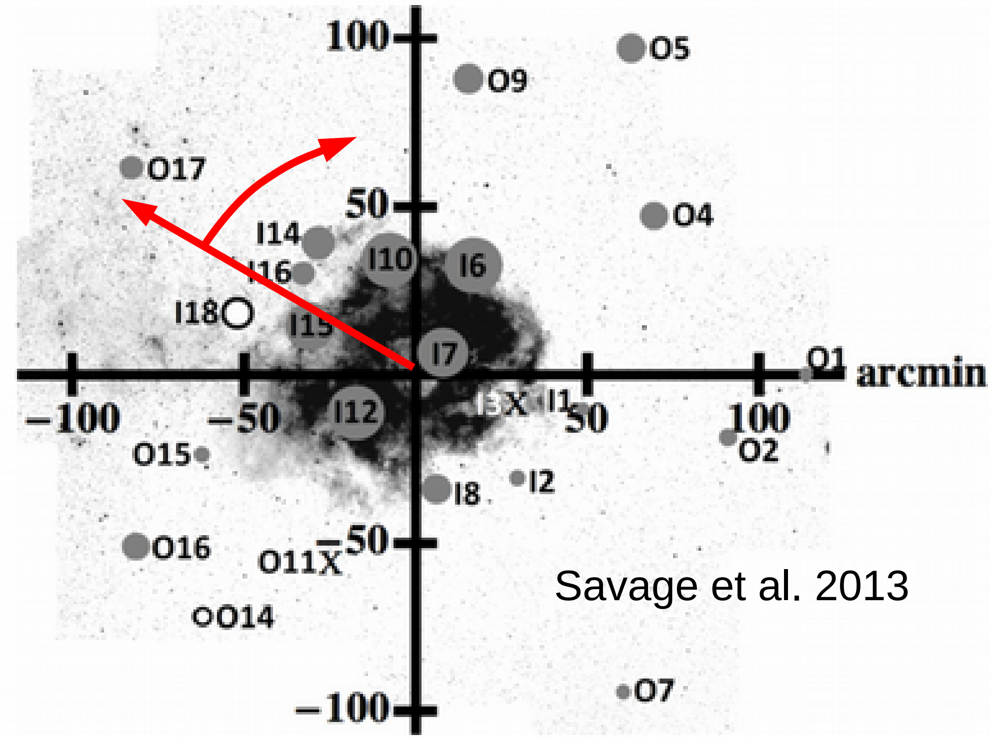

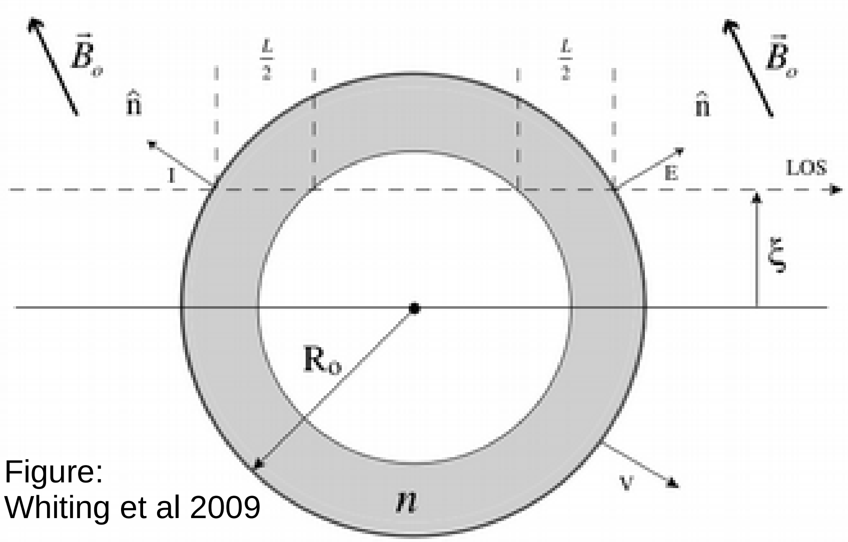

Figure:
Whiting et al 2009

Measuring B-fields: bubbles: HII regions

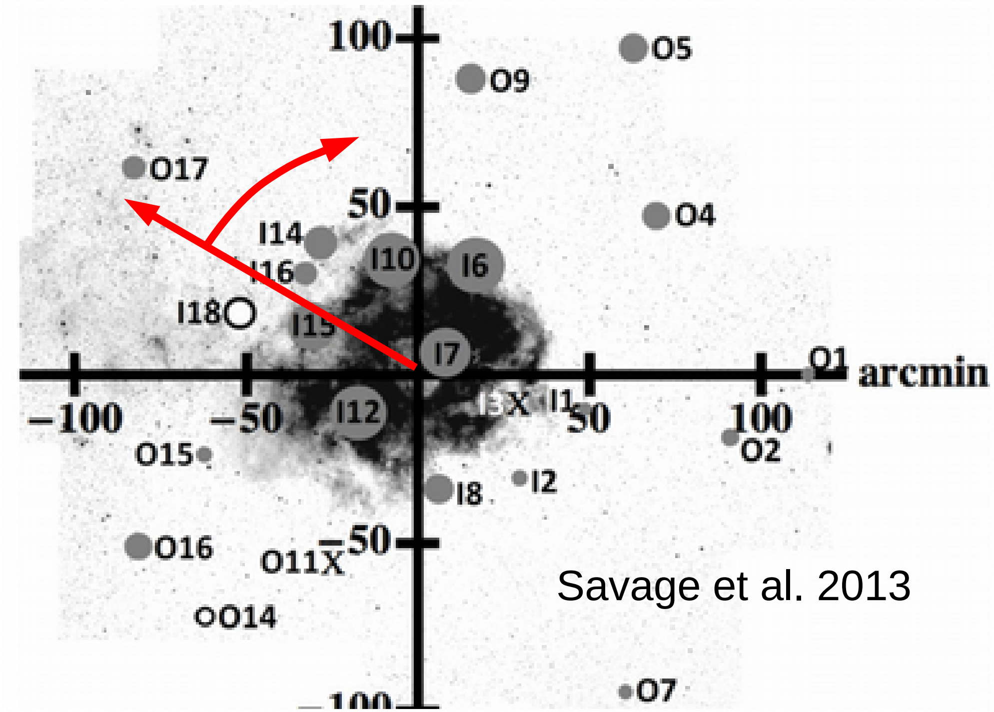

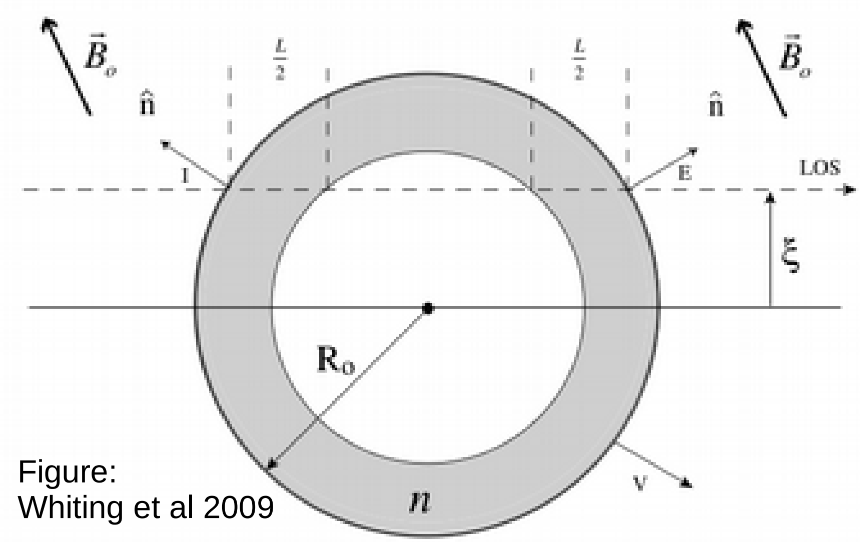

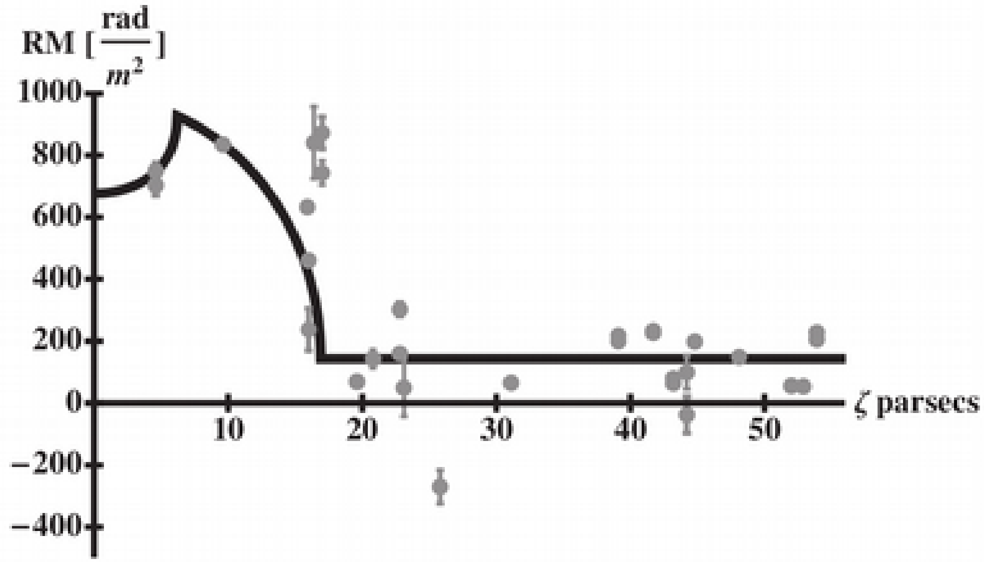

Measuring B-fields: bubbles: HII regions

Rosette Nebula

Image: Andreas Fink / wikimedia

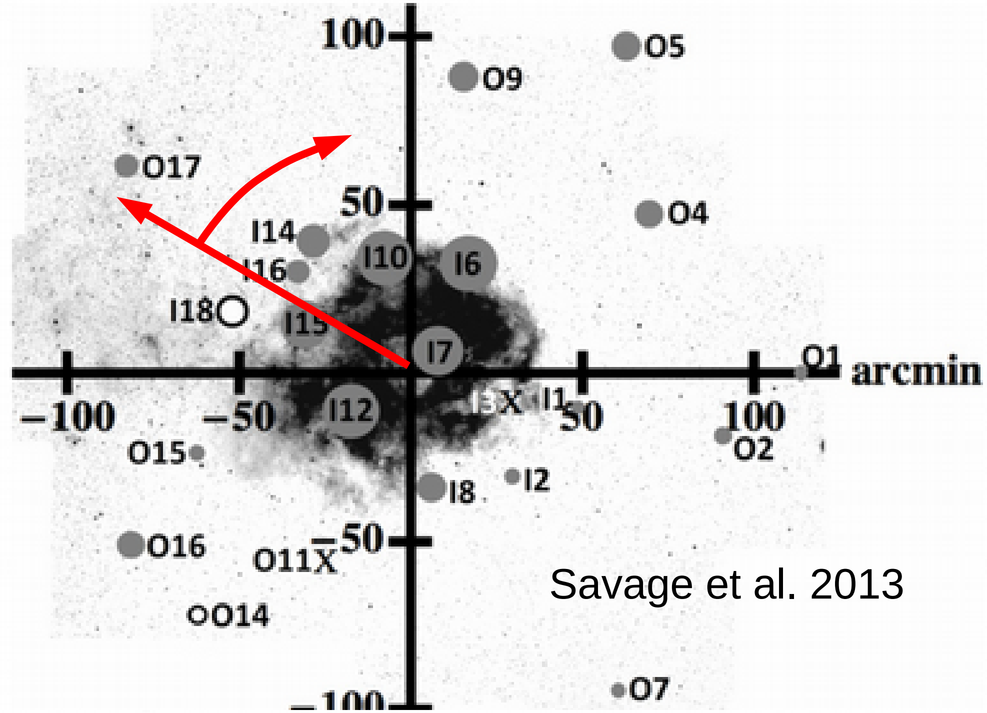

Savage et al. 2013

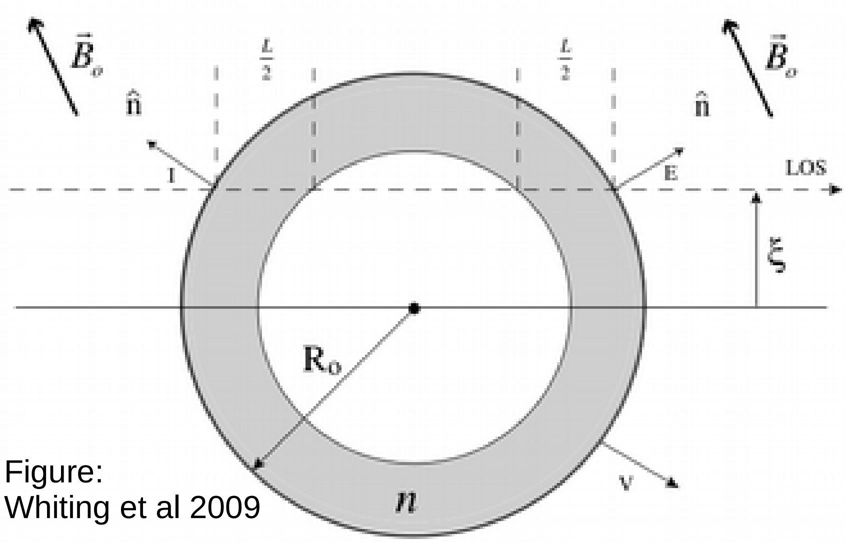

Figure:
Whiting et al 2009

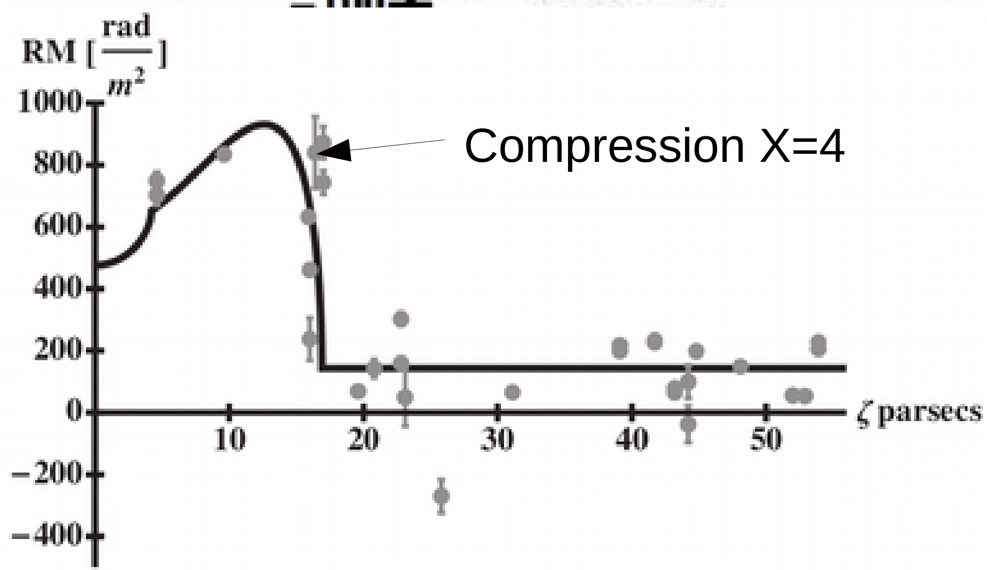

The Gum Nebula: A magnetic bubble?

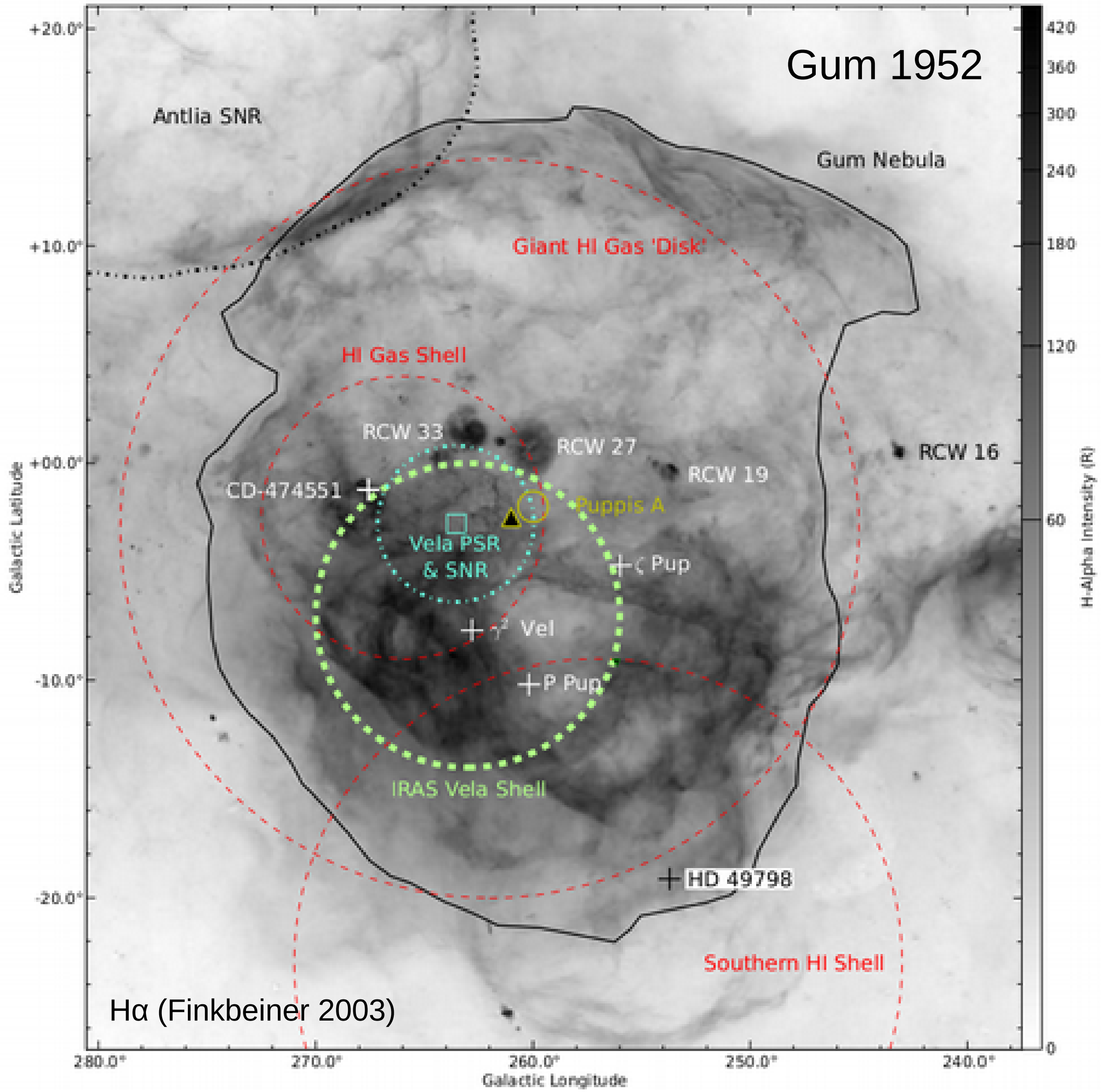

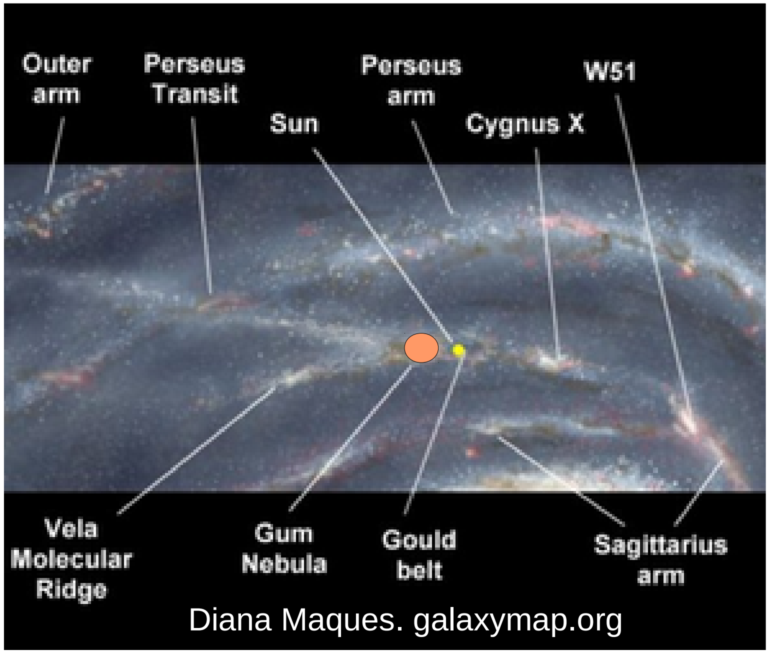

The Gum Nebula: A magnetic bubble?

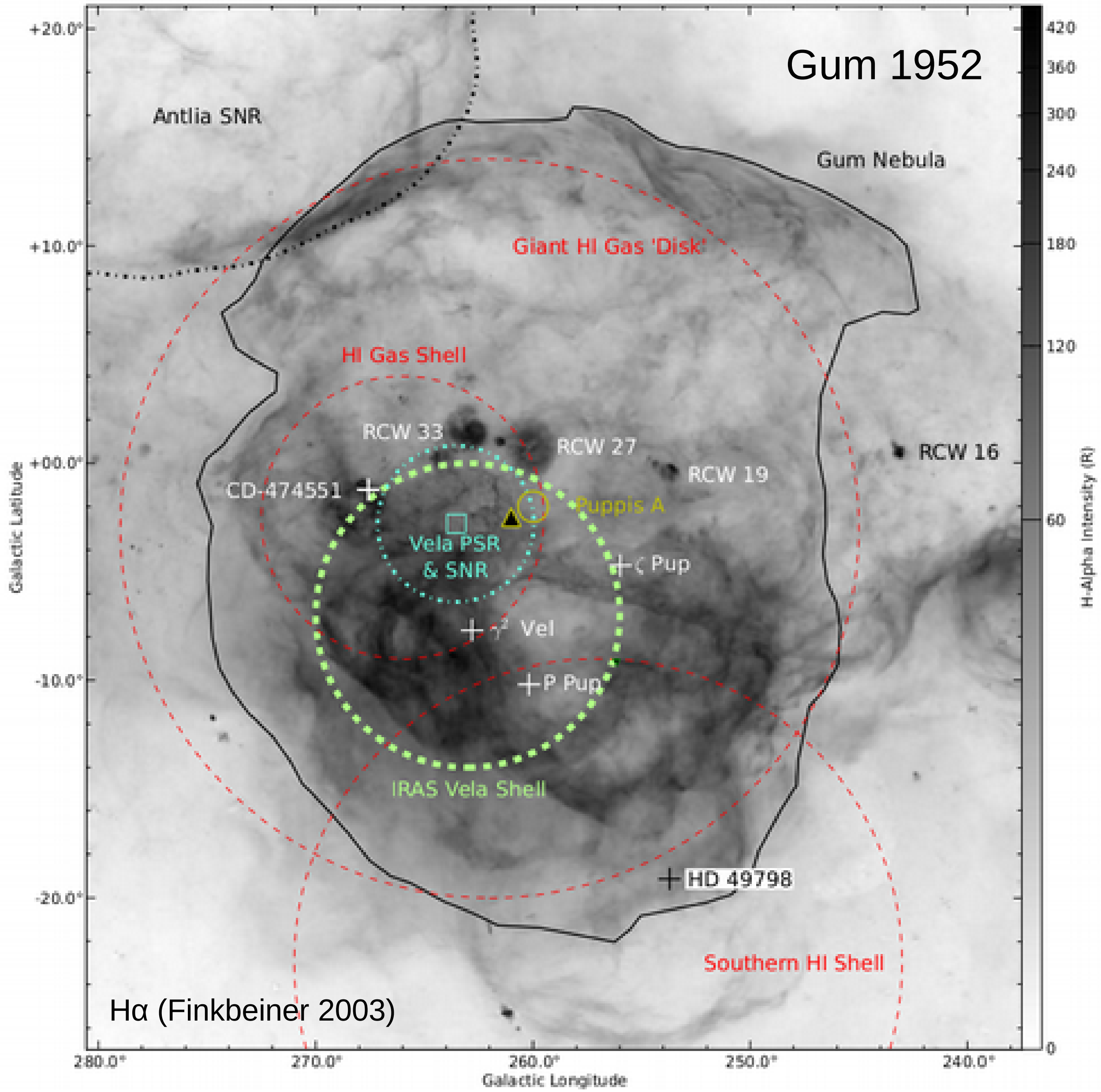

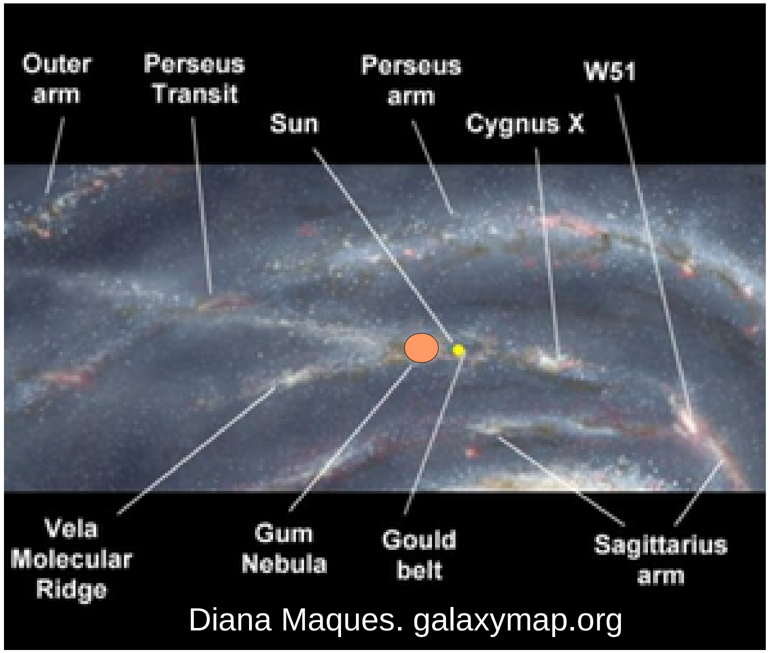

Uncertain origin:

- Fossil Stromgren sphere Brandt et al. (1971)
- Old HII region Gum (1956), Beurmann (1972)
- Stellar wind bubble Weaver (1977)
- Old supernova remnant Reynolds (1976)

The Gum Nebula: A magnetic bubble?

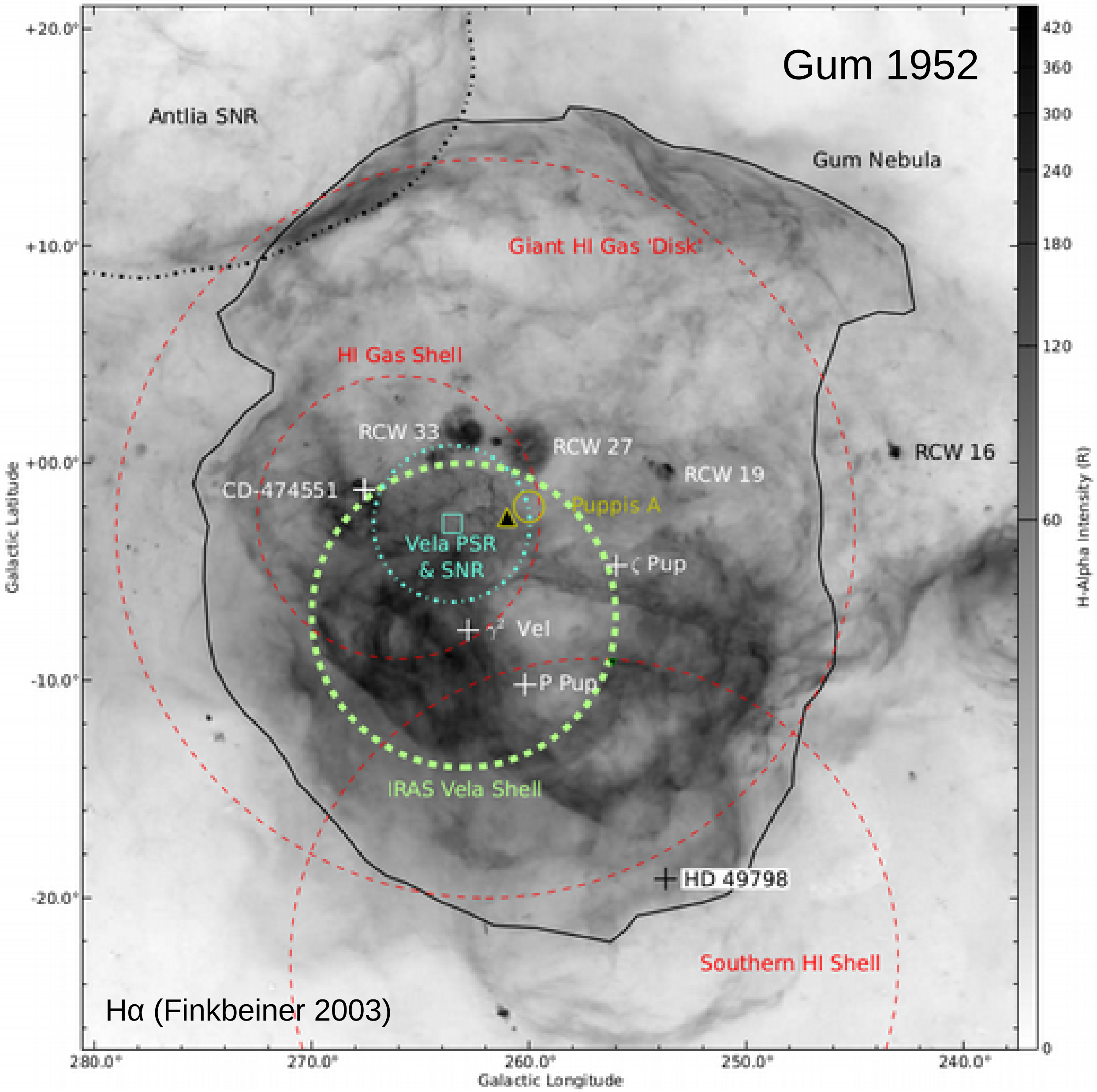

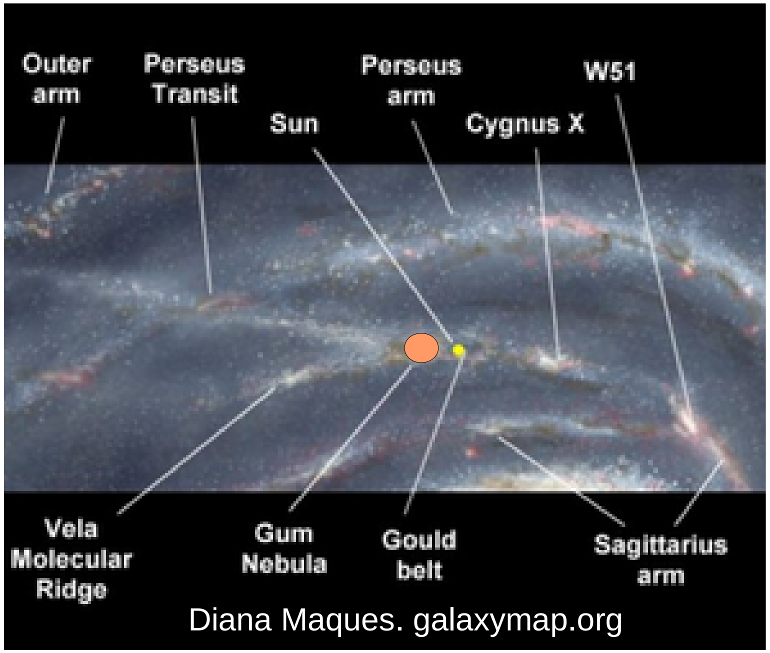

Uncertain origin:

- Fossil Stromgren sphere Brandt et al. (1971)
- Old HII region Gum (1956), Beurmann (1972)
- Stellar wind bubble Weaver (1977)
- Old supernova remnant Reynolds (1976)
  current consensus

The Gum Nebula: A magnetic bubble?

- Kinematics of the neutral gas:

  Fit kinematic shell model to associated cometary globules

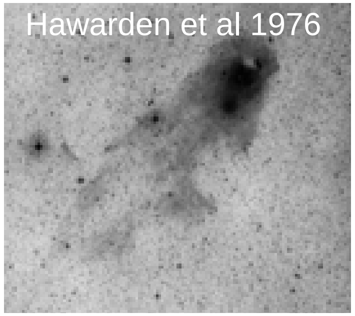

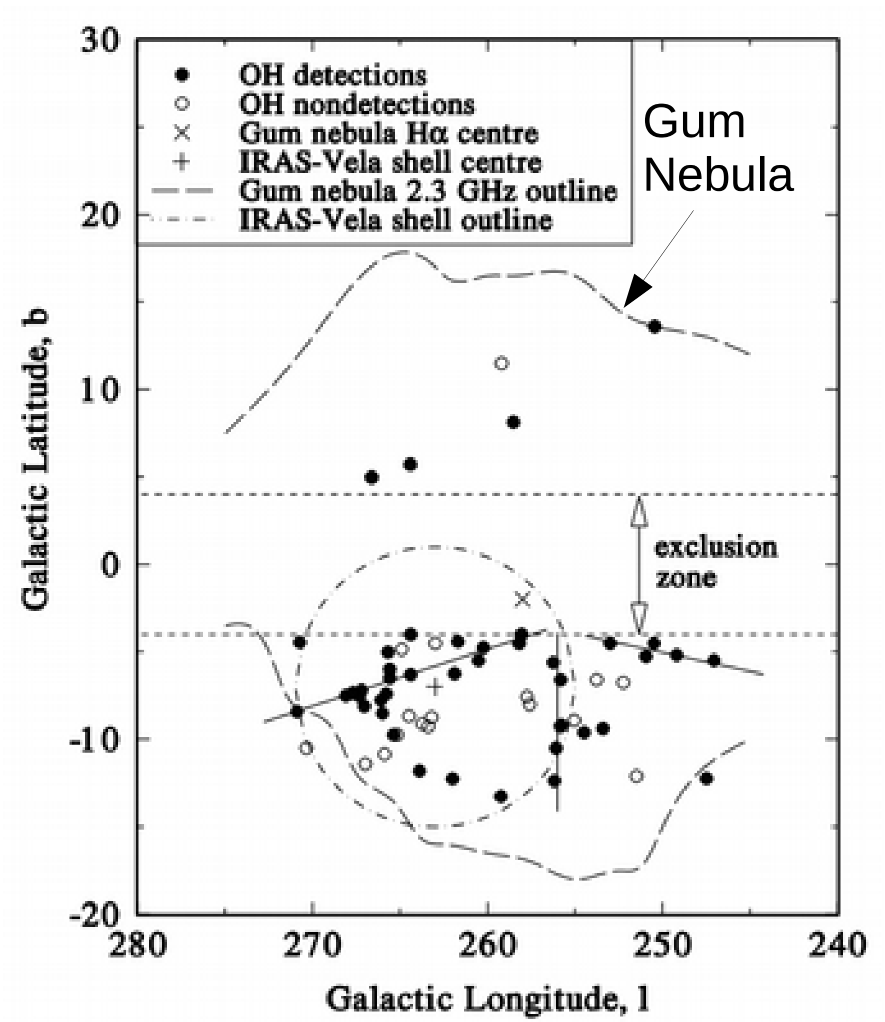

Woermann et al. 2001

The Gum Nebula: A magnetic bubble?

- Kinematics of the neutral gas:

  Fit kinematic shell model to associated cometary globules

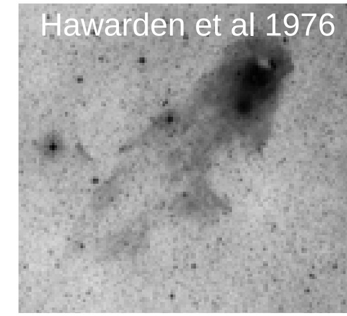

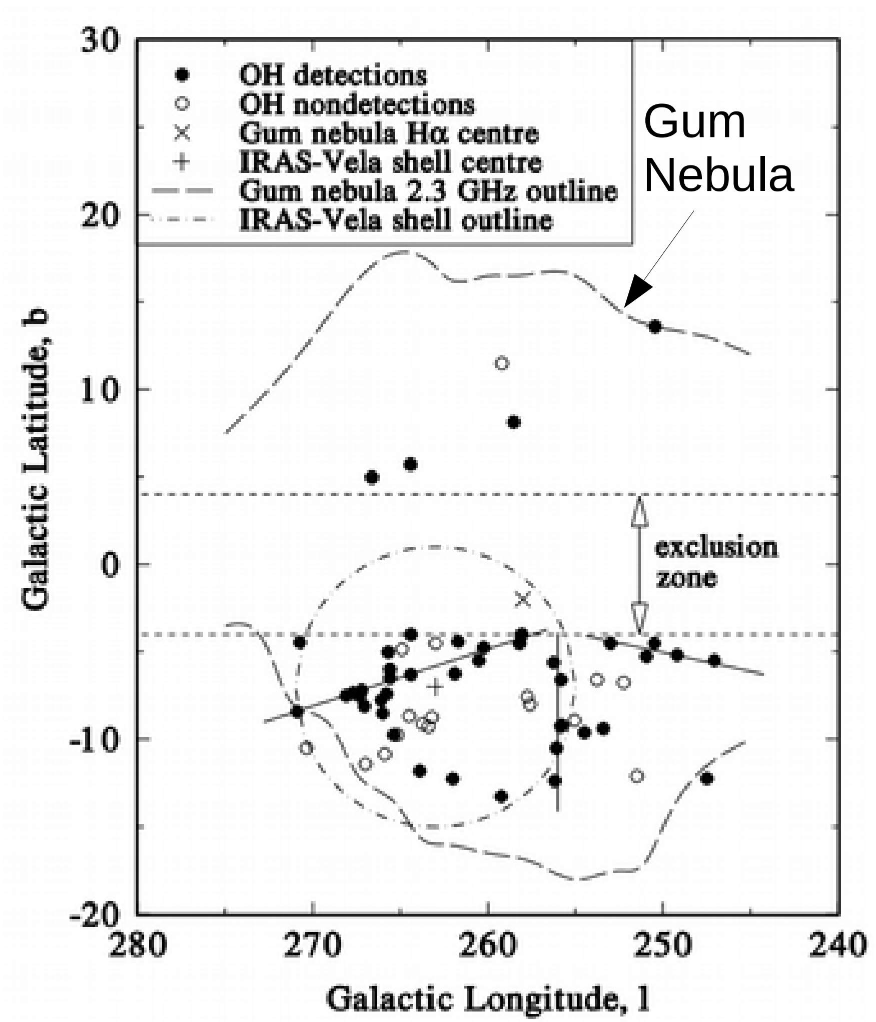

Woermann et al. 2001

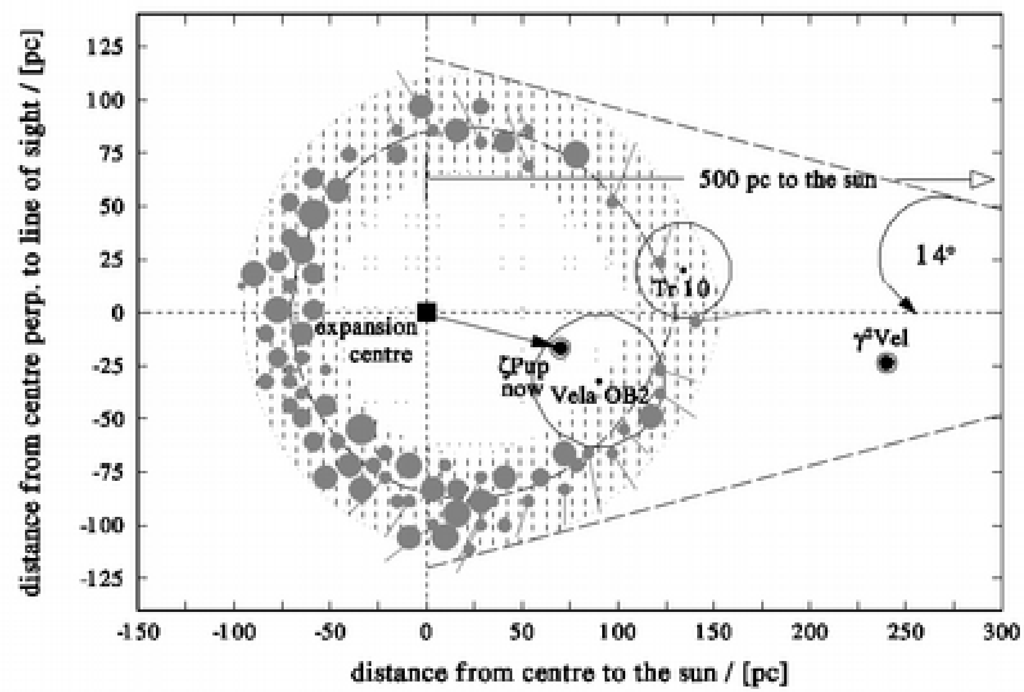

- ~10 km/s expansion velocity
- Suggests Zeta Pup's companion a likely SN progenitor ~1.5 Myr ago

The Gum Nebula: A magnetic bubble?

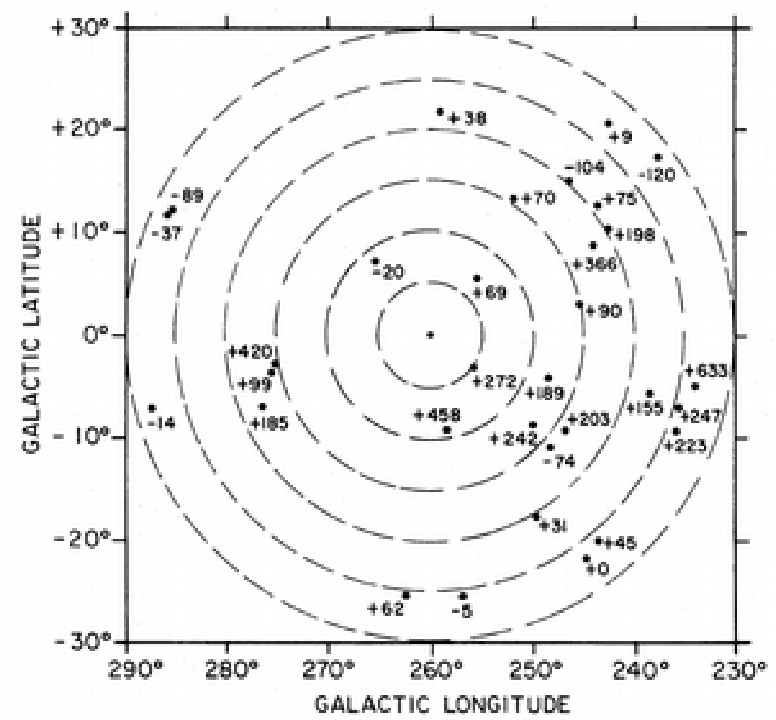

- First systematic study of the B-field in the Gum was by Vallee et al. (1983)
- 32 RMs sampled across the Gum

The Gum Nebula: A magnetic bubble?

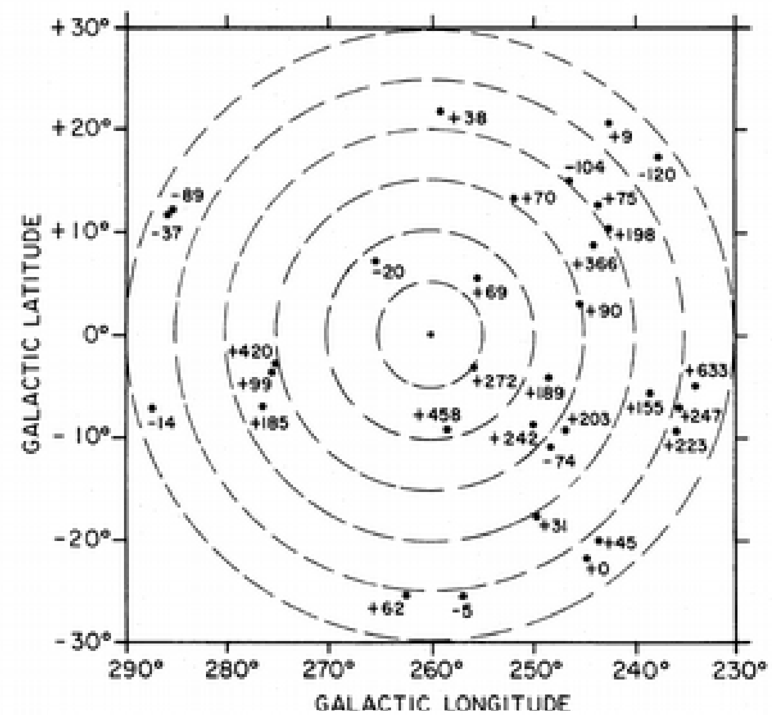

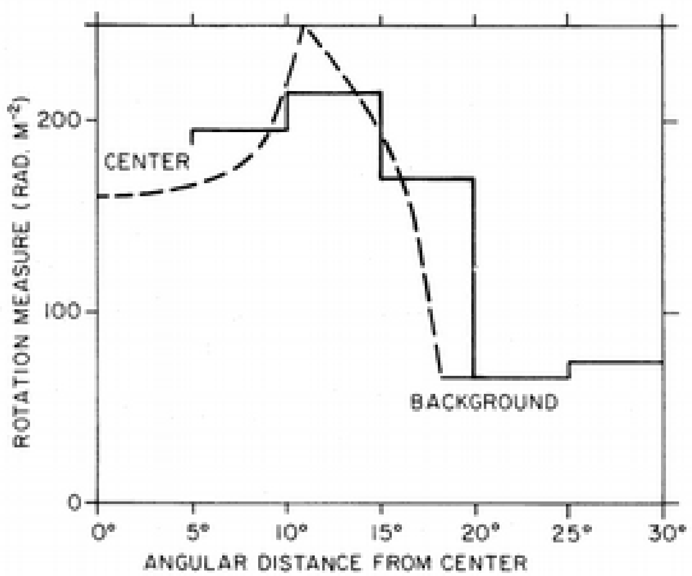

- First systematic study of the B-field in the Gum was by Vallee et al. (1983)
- 32 RMs sampled across the Gum
- Found to be consistent with a simple shell model where B = 2 μGauss

The Gum Nebula: A magnetic bubble?

- First systematic study of the B-field in the Gum was by Vallee et al. (1983)
- 32 RMs sampled across the Gum
- Found to be consistent with a simple shell model where B = 2 μGauss

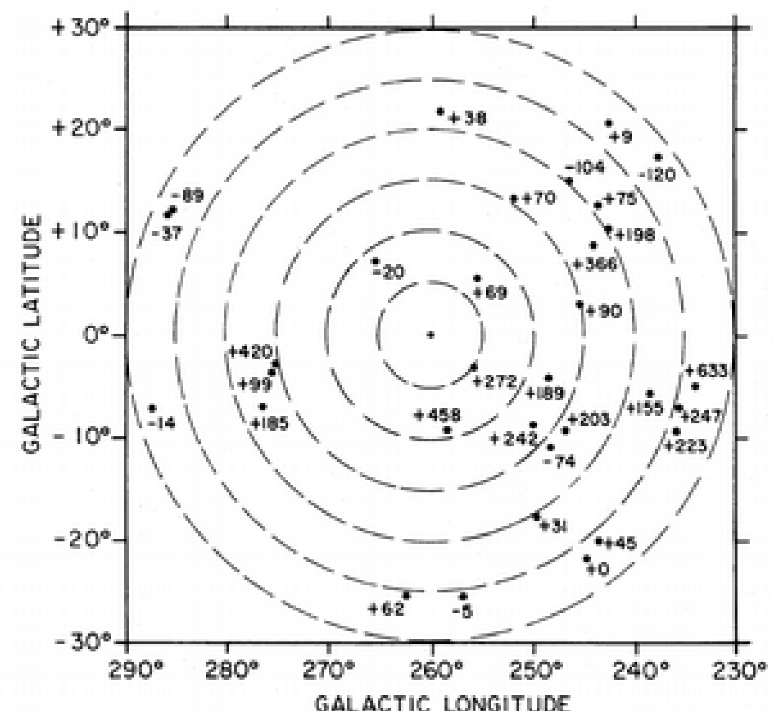

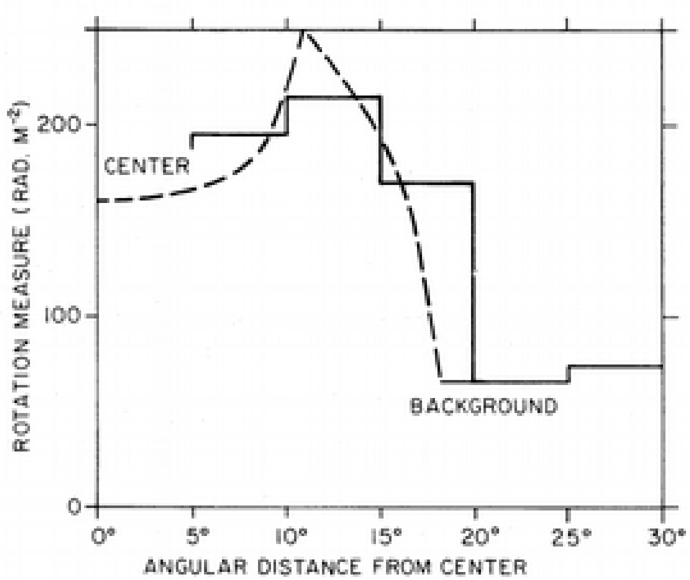

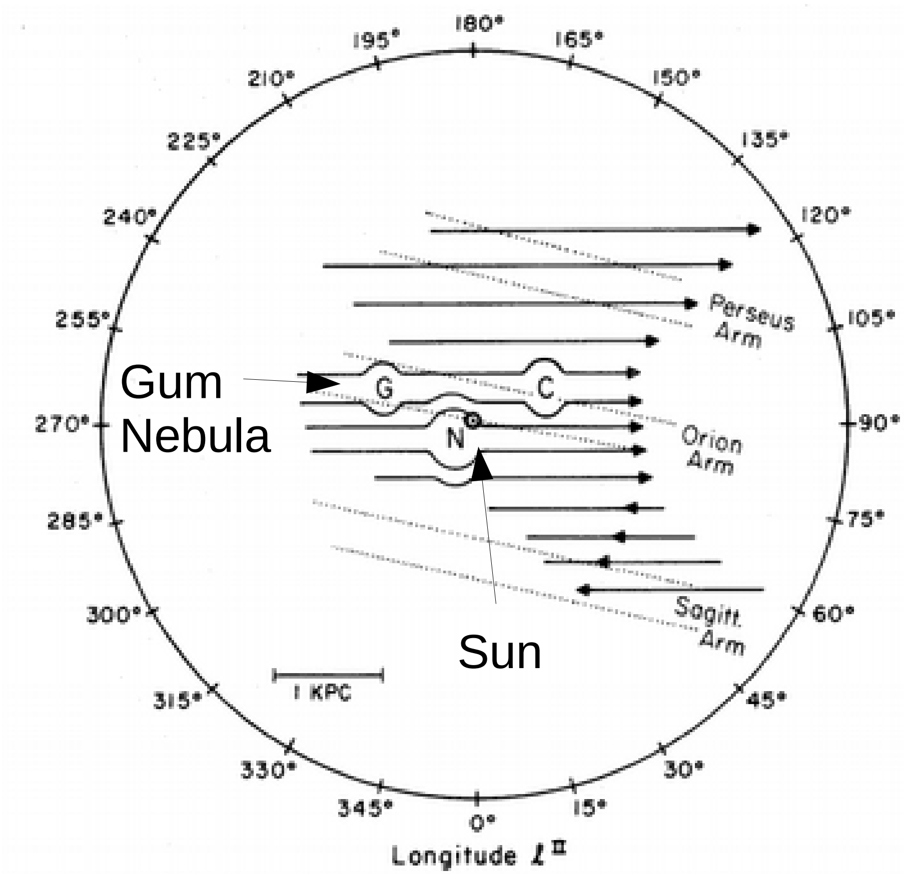

RMs through the nebula

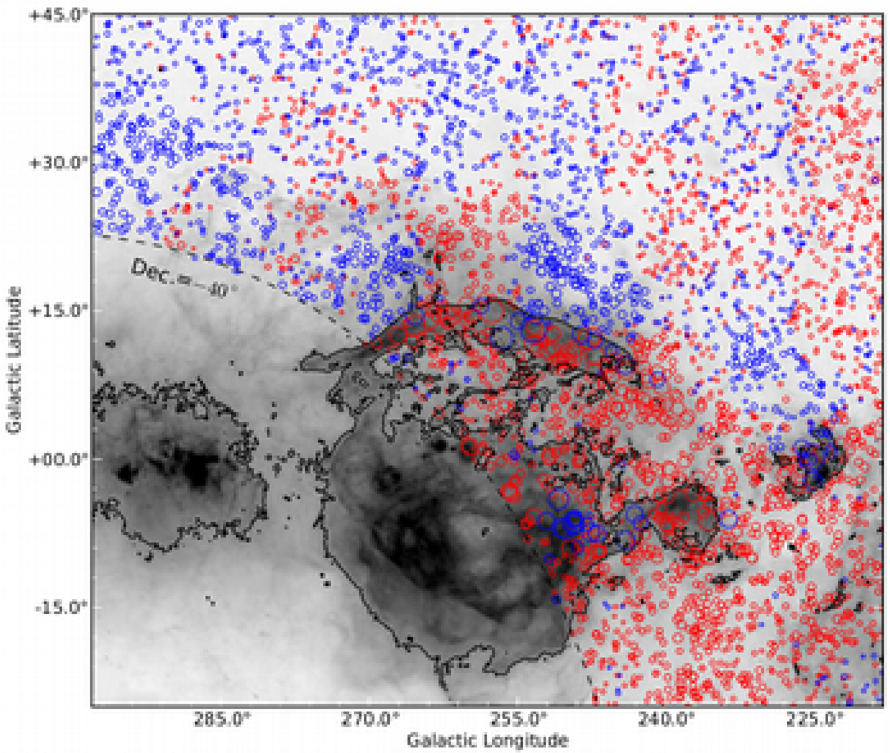

- NVSS Taylor et al. 2009 currently the best RM-grid covering the Gum Nebula

RMs through the nebula

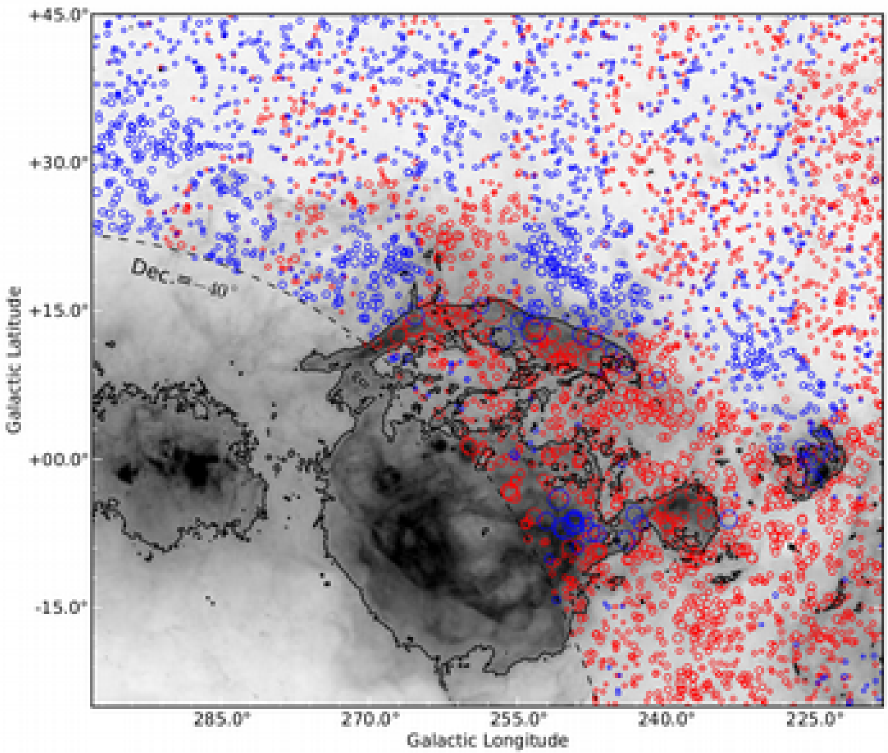

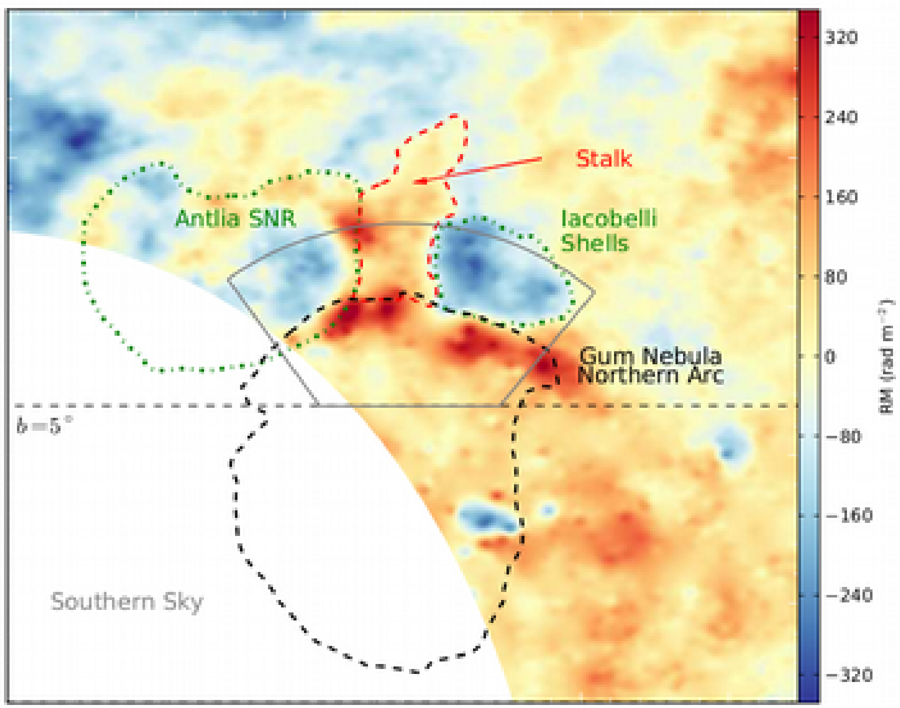

- NVSS Taylor et al. 2009 currently the best RM-grid covering the Gum Nebula
- Focus on the (relatively) unconfused upper region above b=5 deg

RMs through the nebula

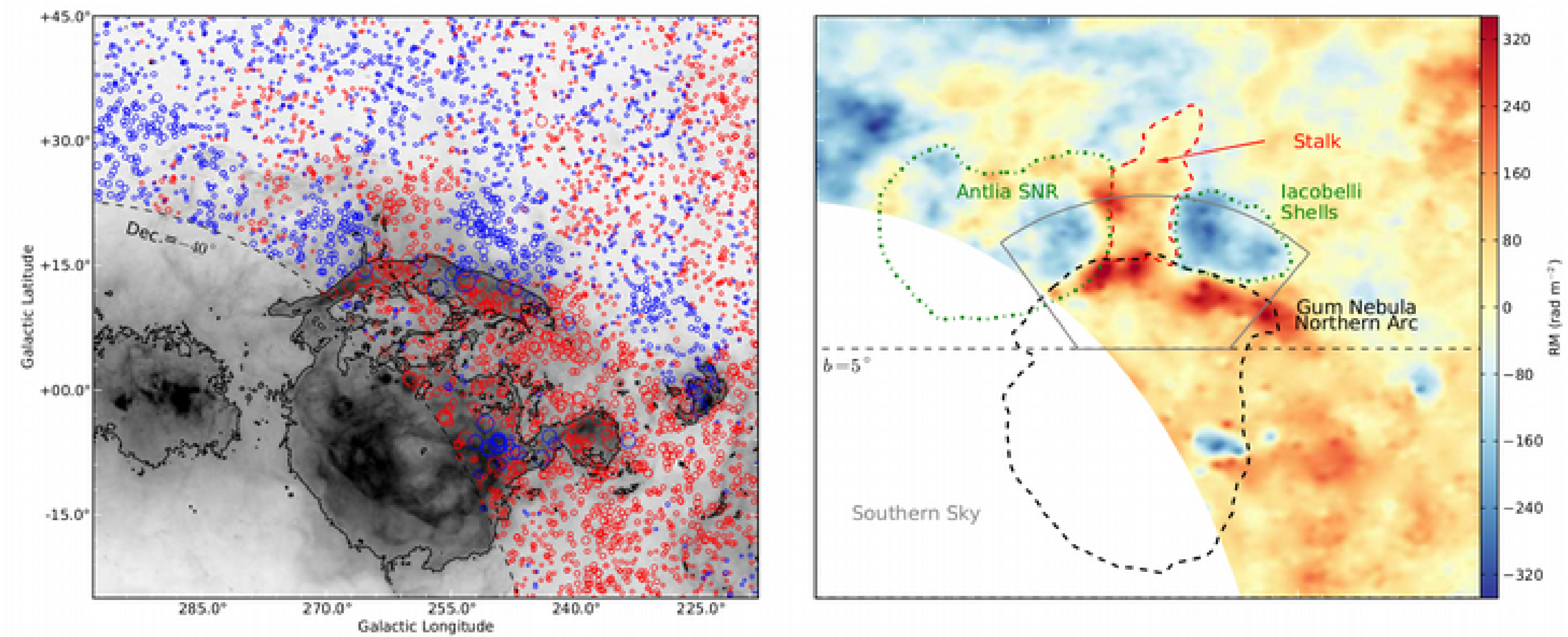

- NVSS Taylor et al. 2009 currently the best RM-grid covering the Gum Nebula
- Focus on the (relatively) unconfused upper region above b=5 deg
- Despite height above the plane (5 deg < b < 15 deg), RMs still require corrections for compact objects identified other data.

RMs through the nebula

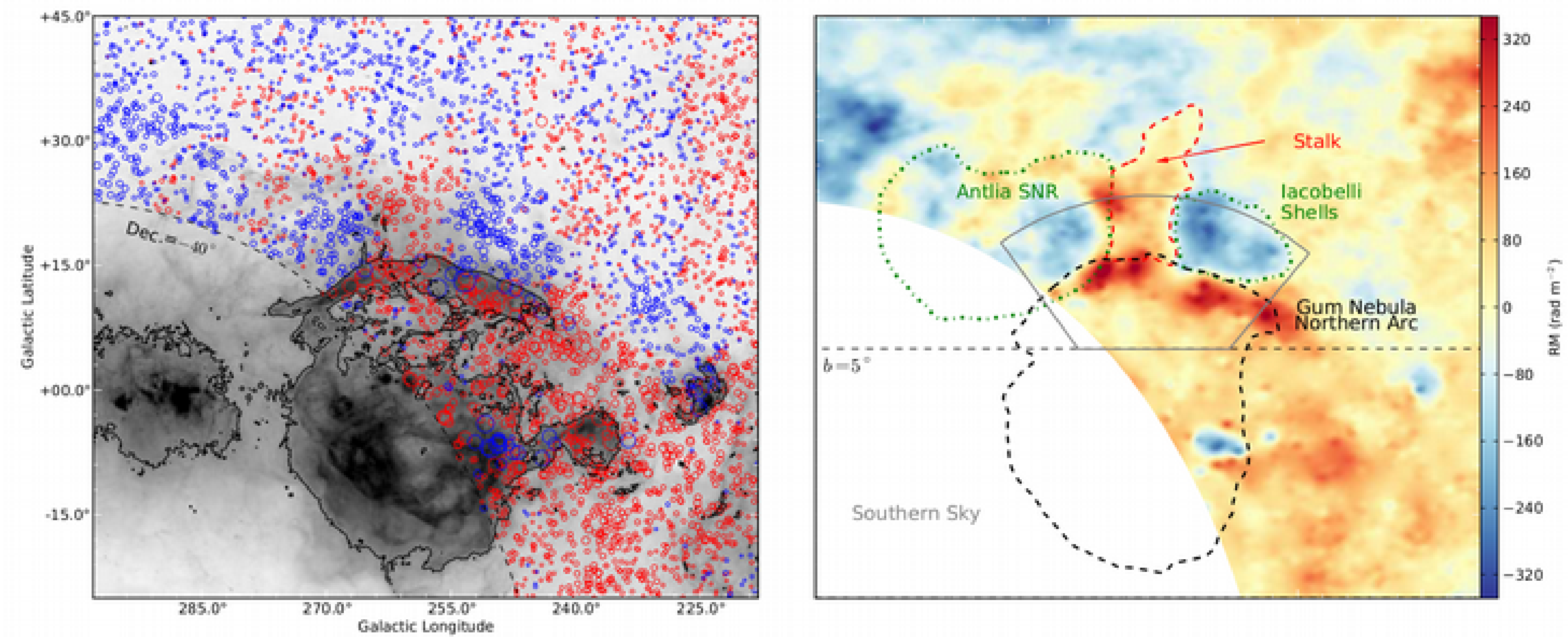

- NVSS Taylor et al. 2009 currently the best RM-grid covering the Gum Nebula
- Focus on the (relatively) unconfused upper region above b=5 deg
- Despite height above the plane (5 deg < b < 15 deg), RMs still require corrections for compact objects identified other data.
- Main assumption is the large-scale gradient behind the selected region.

RMs through the nebula

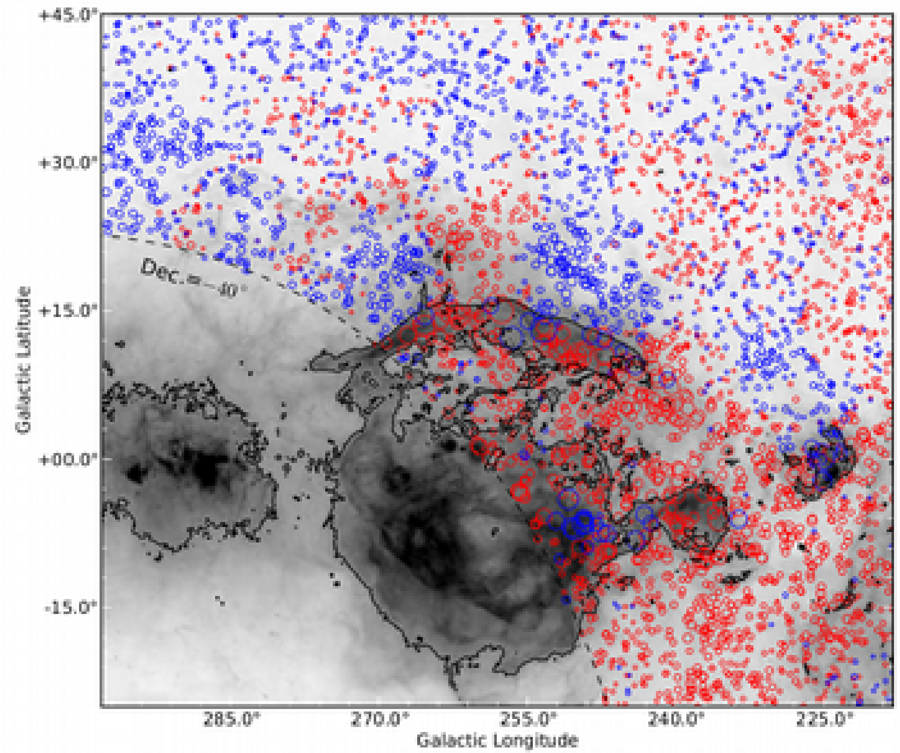

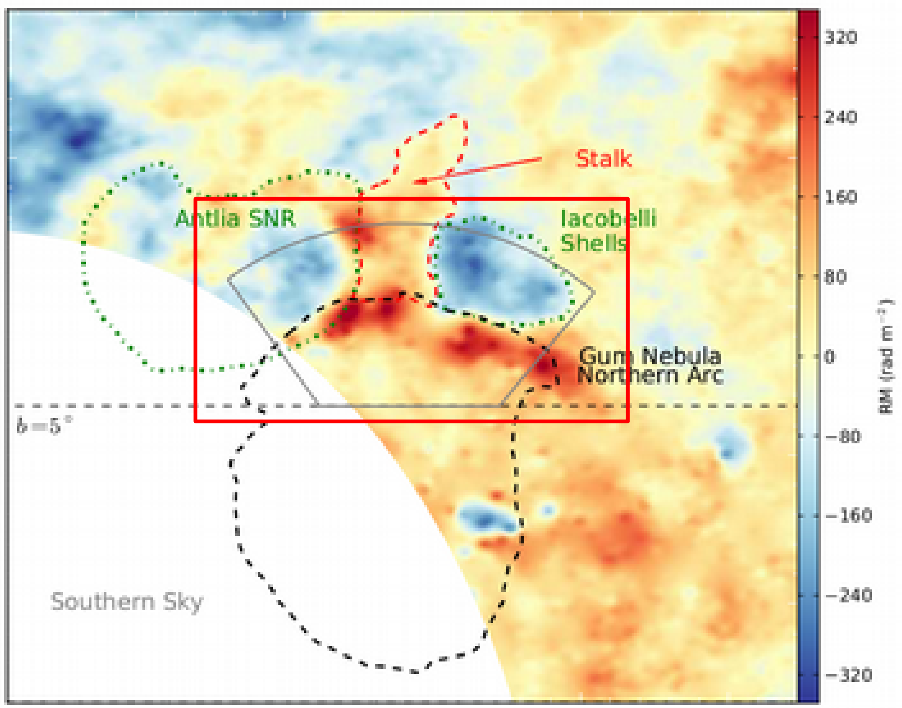

- NVSS Taylor et al. 2009 currently the best RM-grid covering the Gum Nebula
- Focus on the (relatively) unconfused upper region above b=5 deg
- Despite height above the plane (5 deg < b < 15 deg), RMs still require corrections for compact objects identified other data.
- Main assumption is the large-scale gradient behind the selected region.

RMs through the nebula

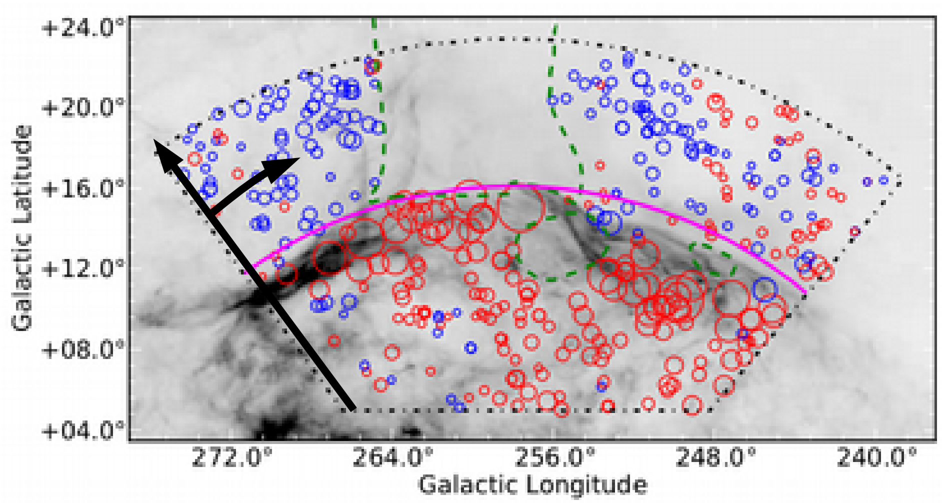

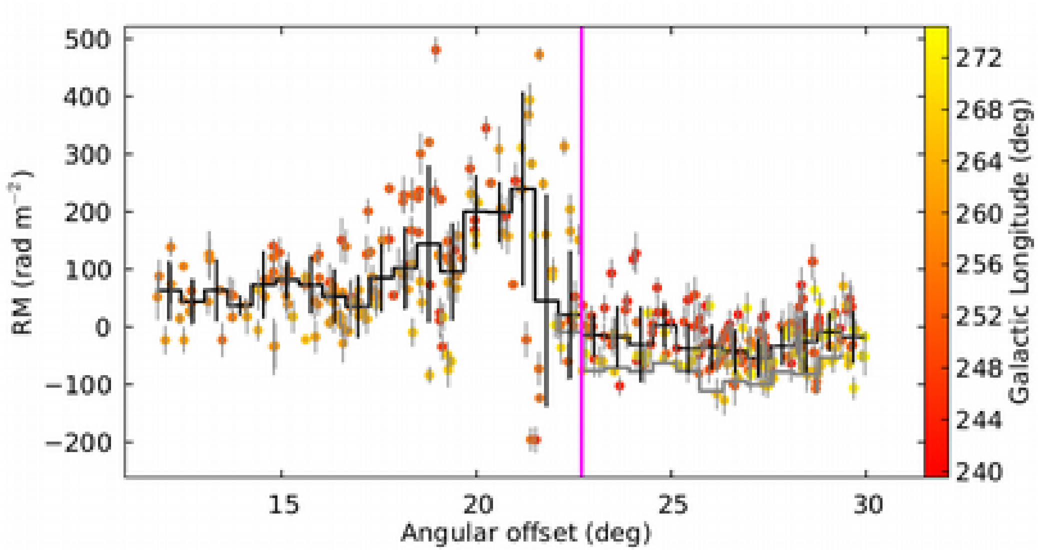

RMs through the nebula

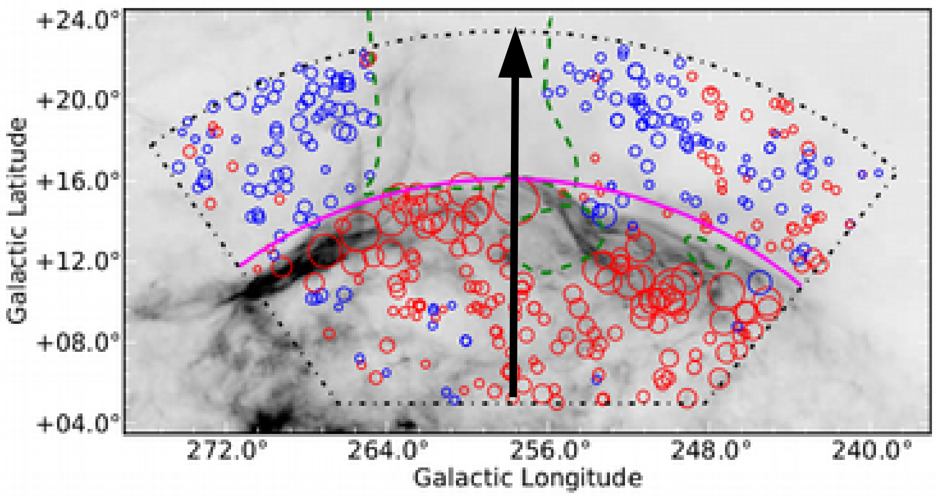

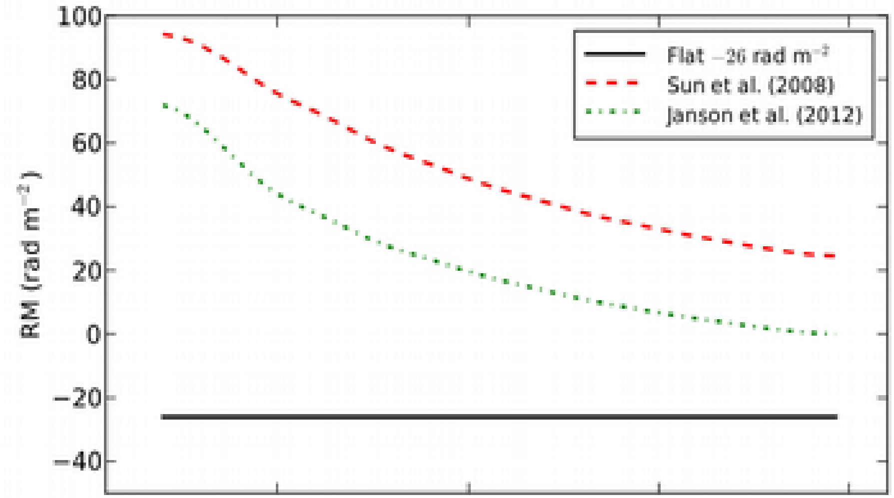

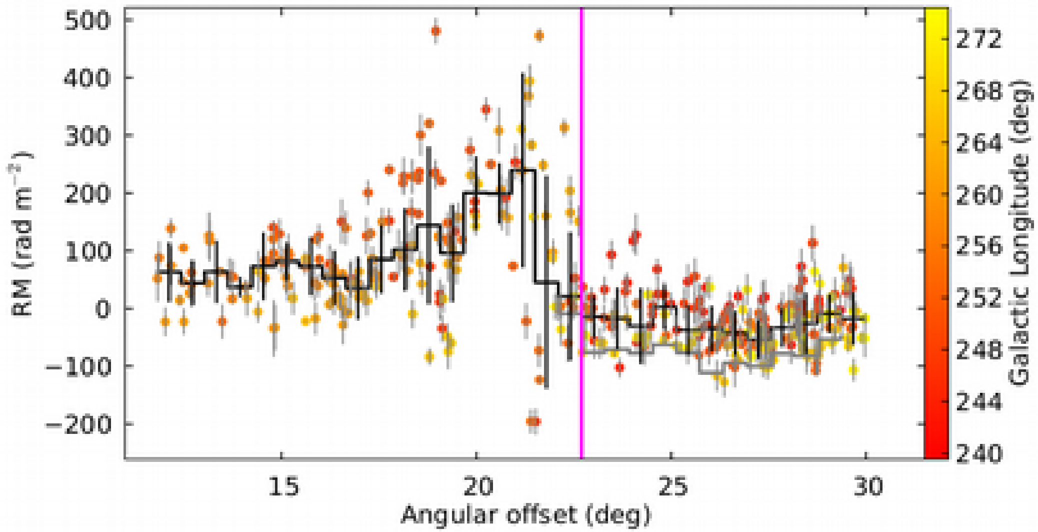

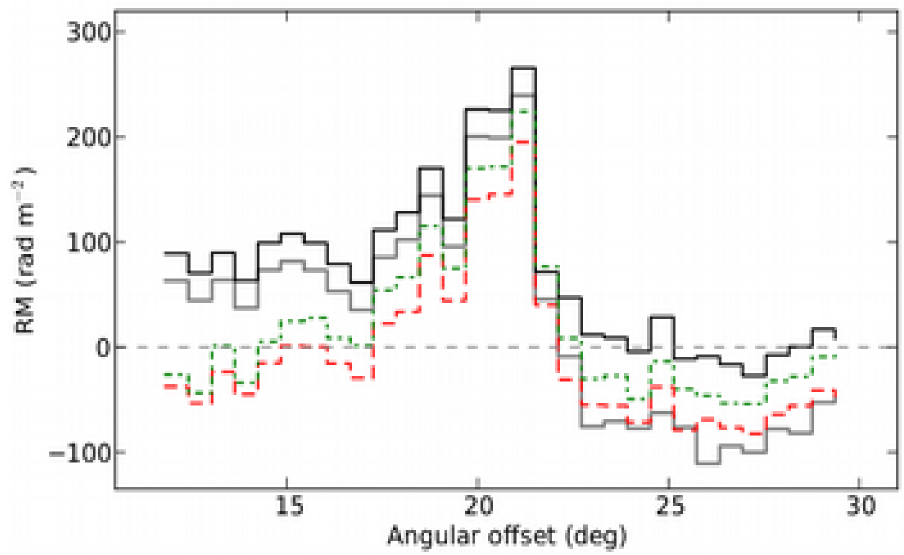

RMs through the nebula

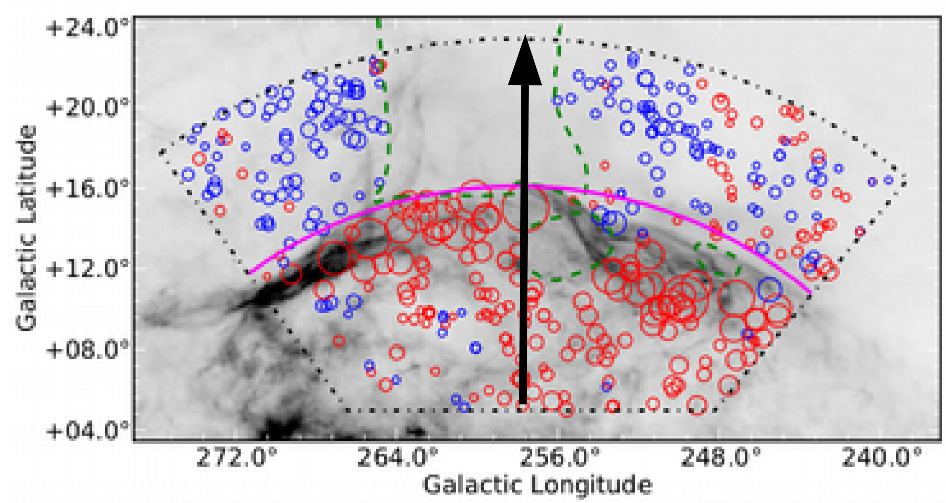

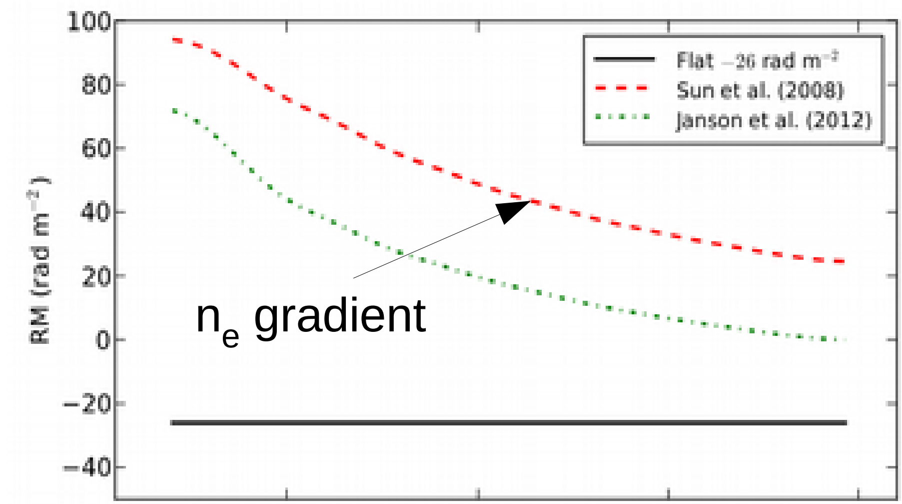

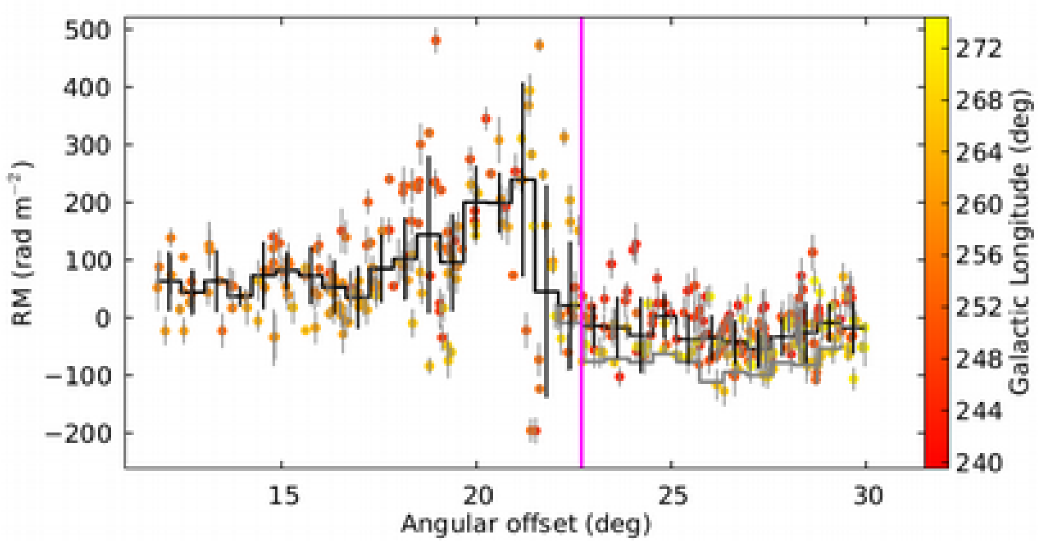

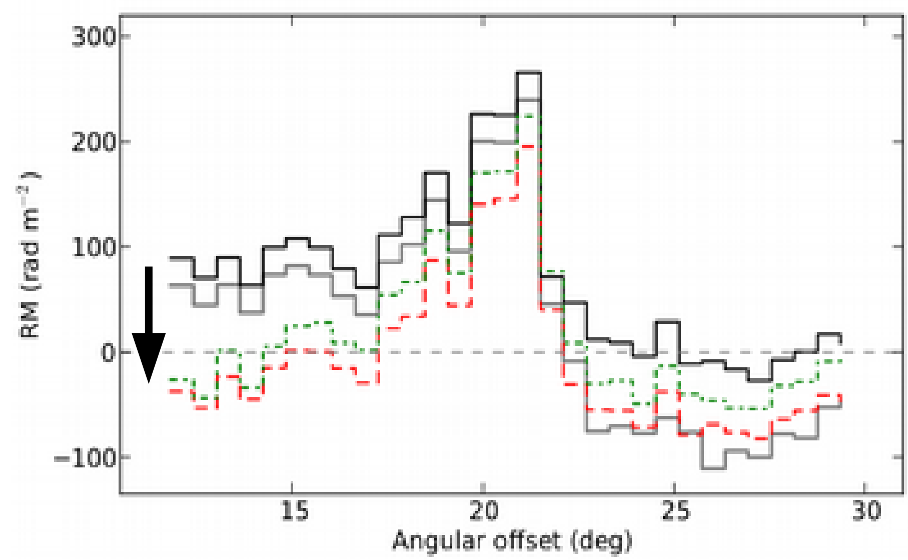

A near-field ionised shell model

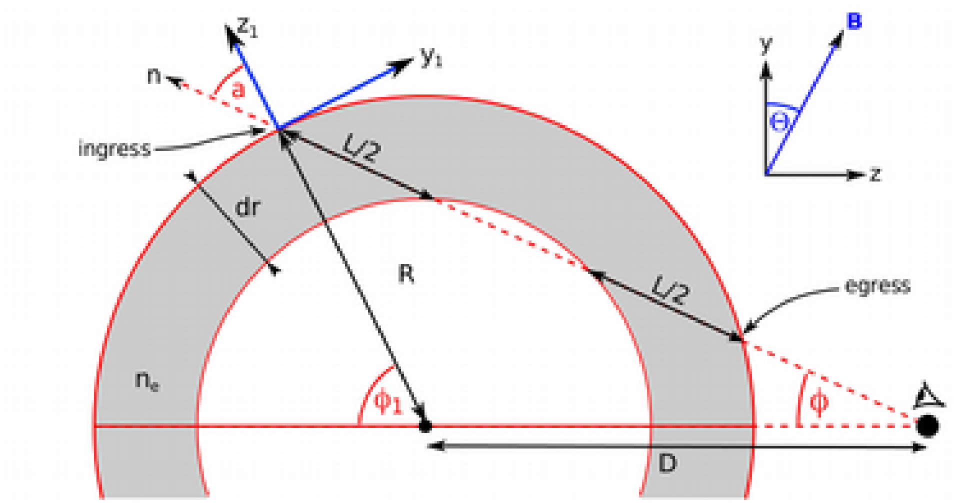

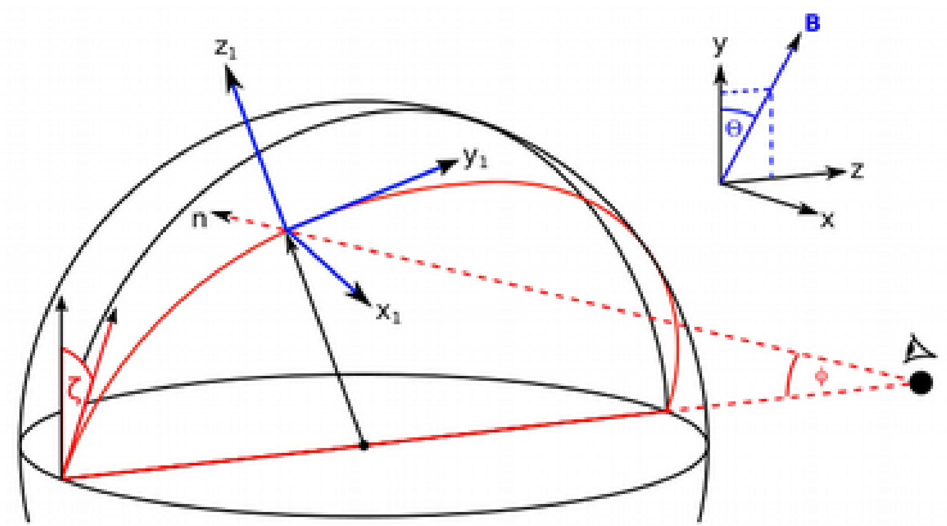

- We model the nebula as a spherical ionised shell straddling the plane
- Shell is in the near-field meaning that the RM-signature is asymmetric in az

A near-field ionised shell model

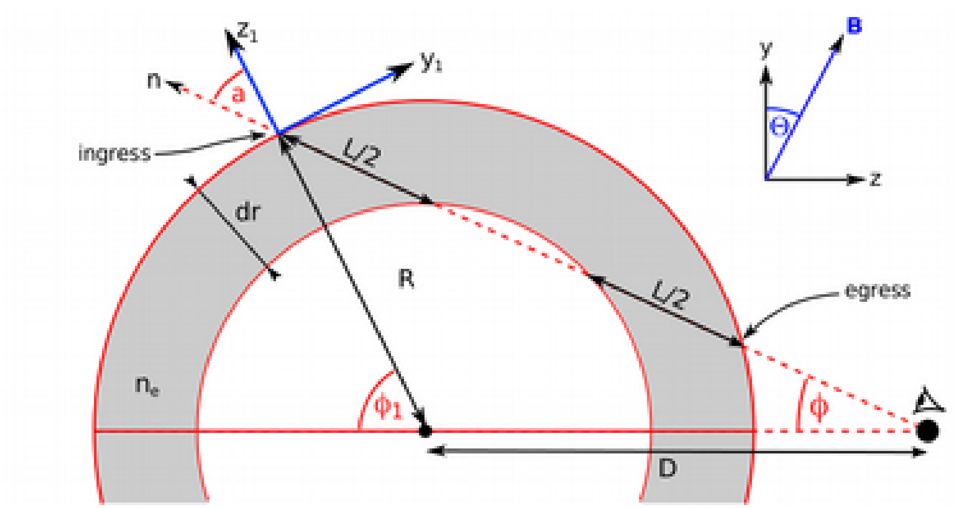

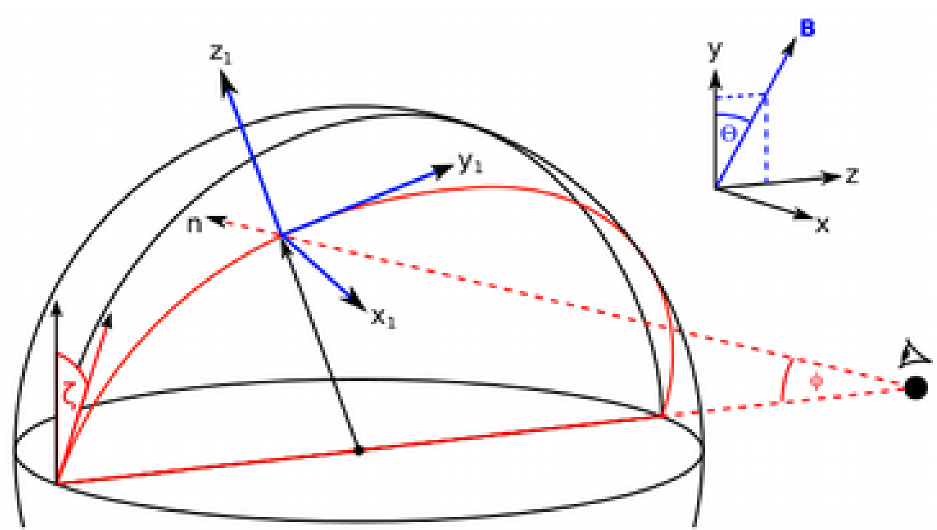

- We model the nebula as a spherical ionised shell straddling the plane
- Shell is in the near-field meaning that the RM-signature is asymmetric in az
- Free parameters in the model:
  - B_o … magnetic field strength
  - Θ … B-field angle
  - dr … thickness of shell
  - Φ_{outer} … outer angular radius
  - n_e … electron density in shell
  - f … filling factor
  - X … compression factor
  - δ(RM) … scatter hyperparameter

$$\mathrm{RM} = 0.81\, f\, \left(\frac{B_{||}(\phi,\zeta,B_0,\Theta,X)}{\mu\mathrm{G}}\right)\left(\frac{n_e}{\mathrm{cm}^{-3}}\right)\left(\frac{L(\phi,dr)}{pc}\right)$$

A near-field ionised shell model

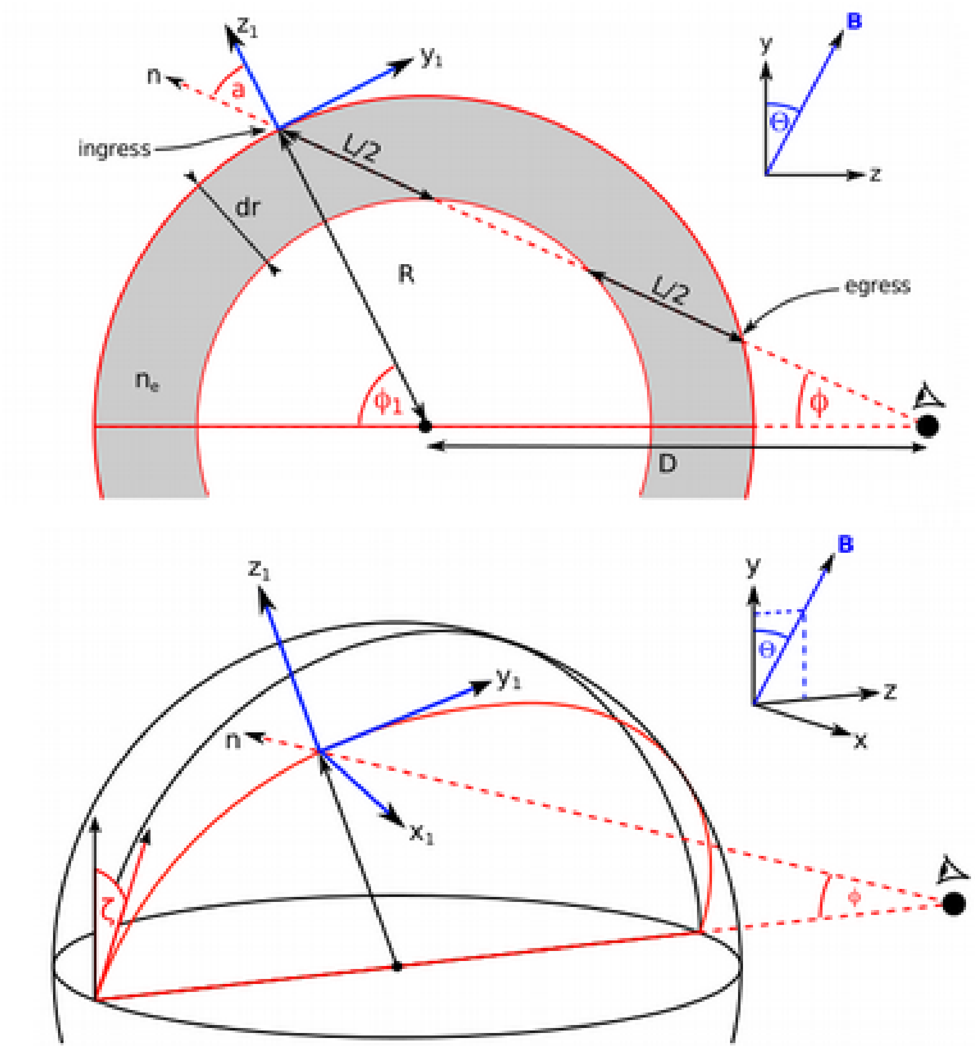

Magnetic field angle

Θ = 0 degrees

RM Image

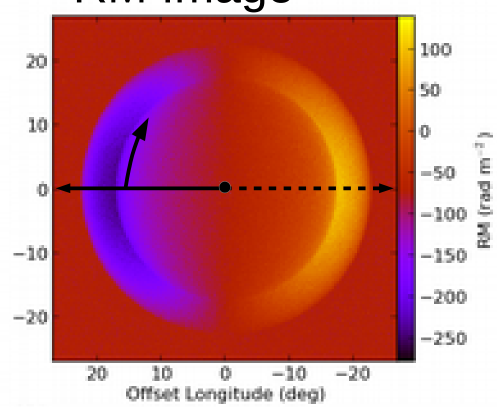

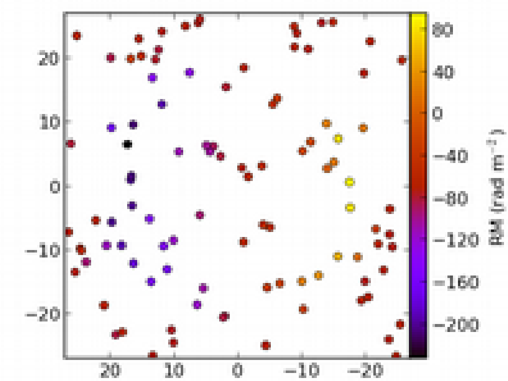

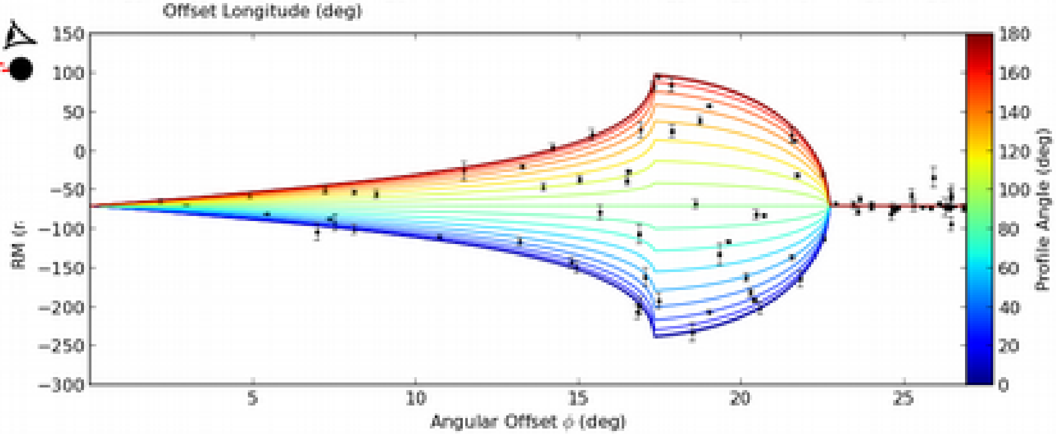

A near-field ionised shell model

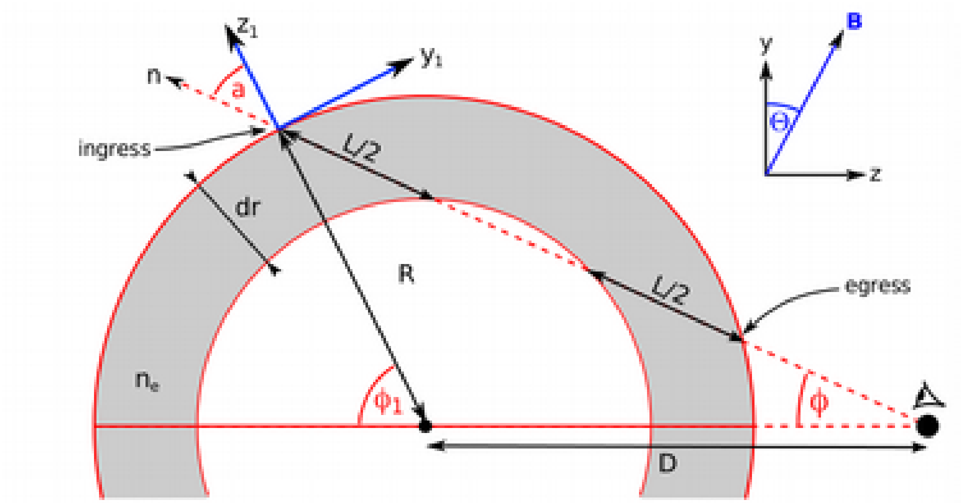

Magnetic field angle

Θ = 5 degrees

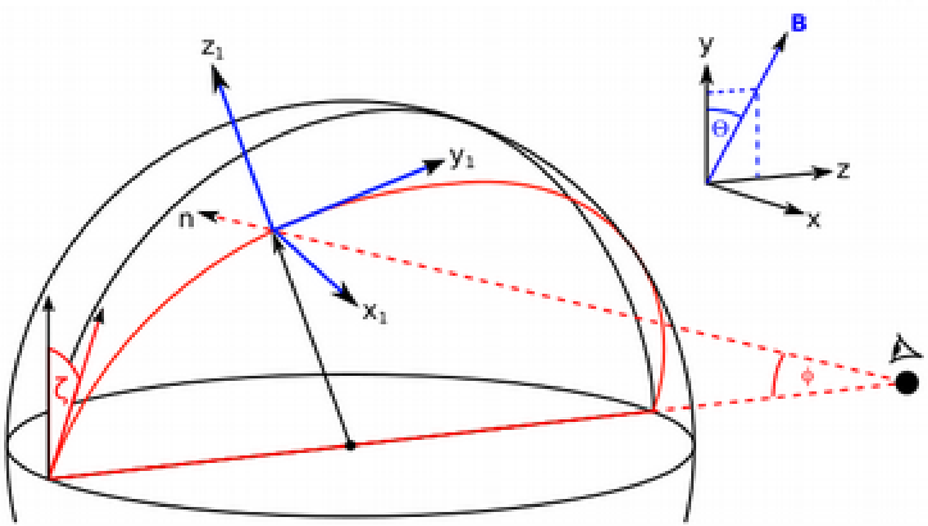

RM Image

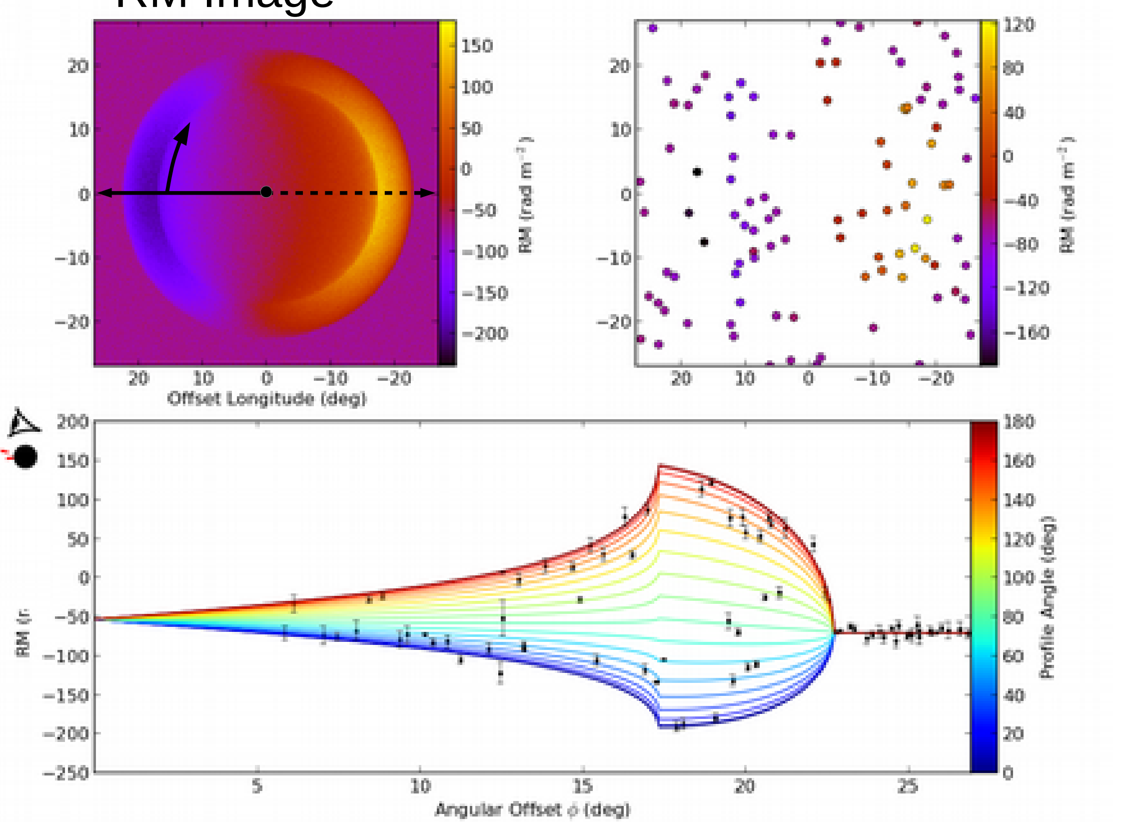

A near-field ionised shell model

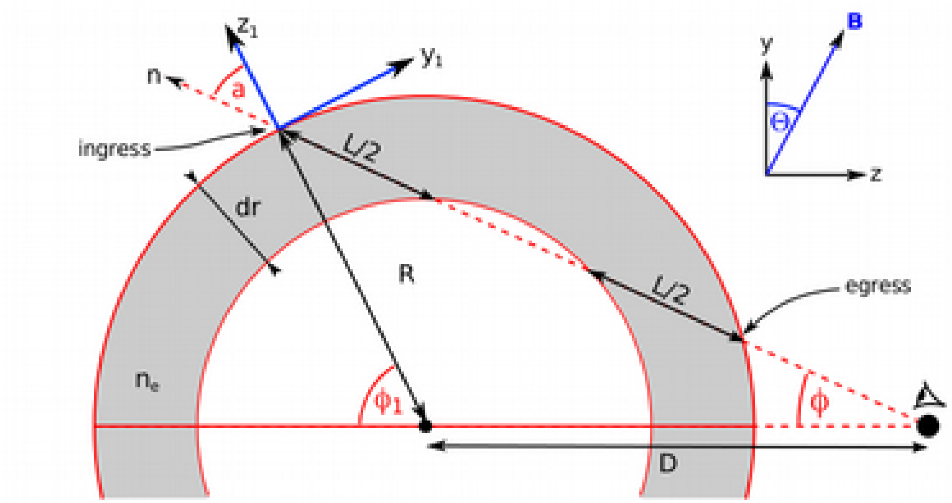

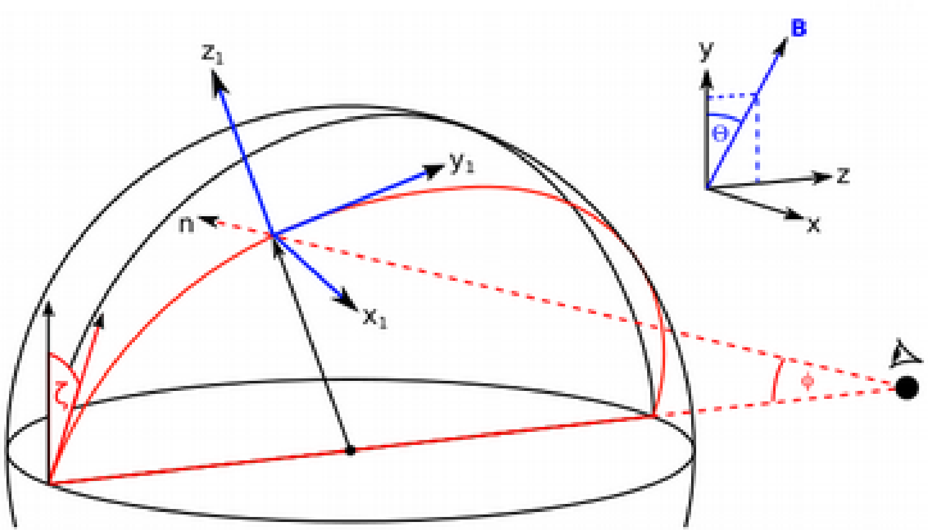

Magnetic field angle

Θ = 15 degrees

RM Image

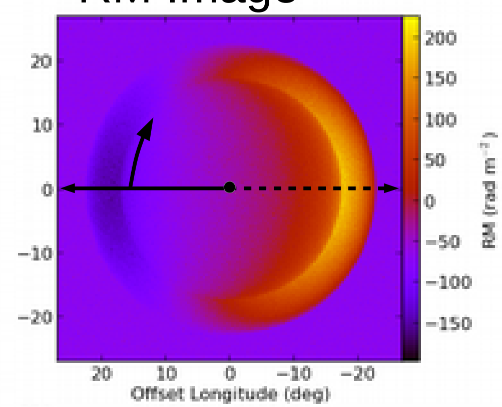

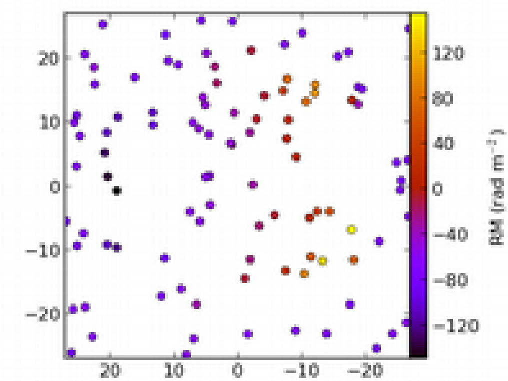

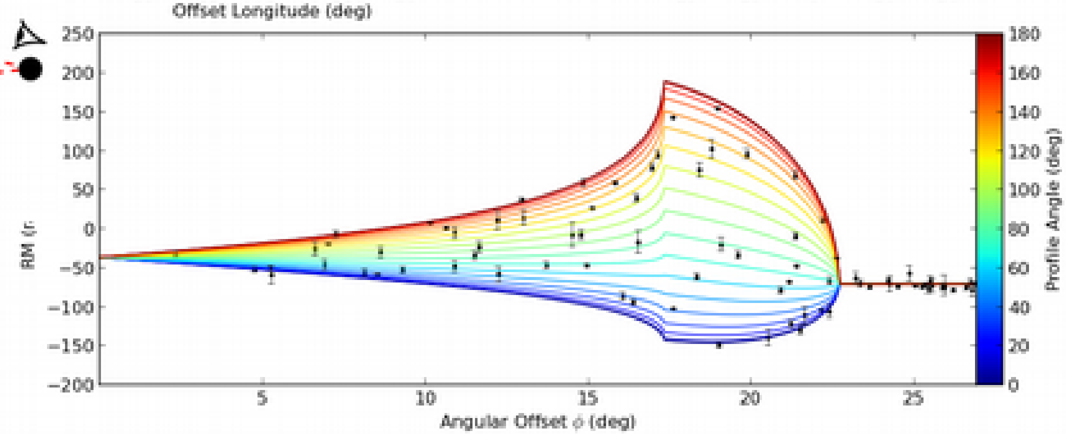

A near-field ionised shell model

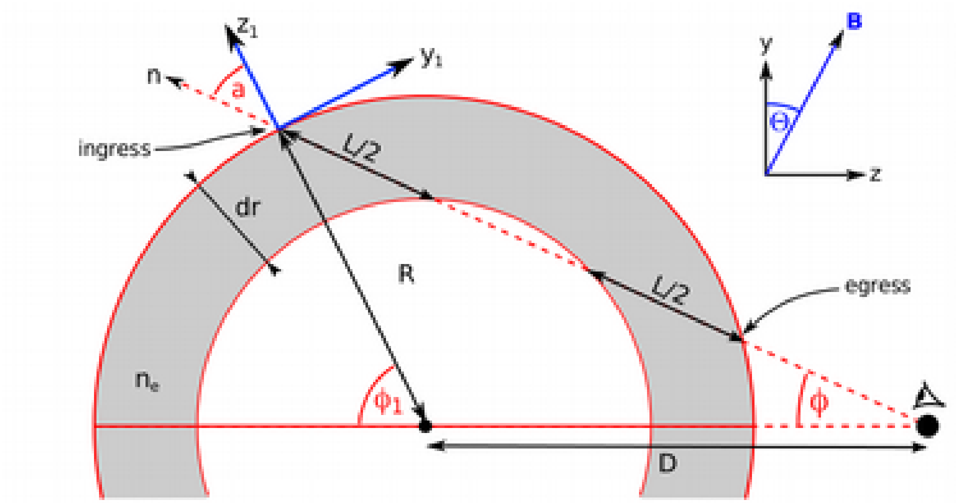

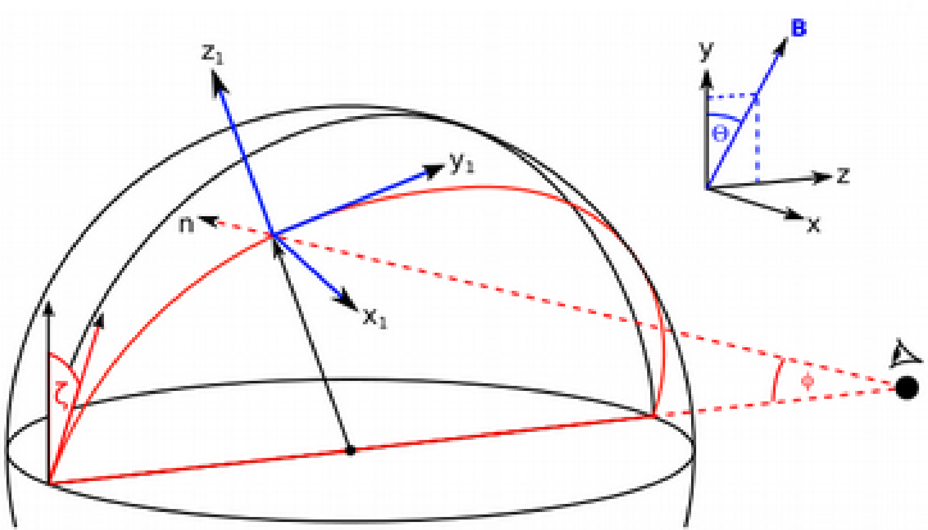

Magnetic field angle

Θ = 20 degrees

RM Image

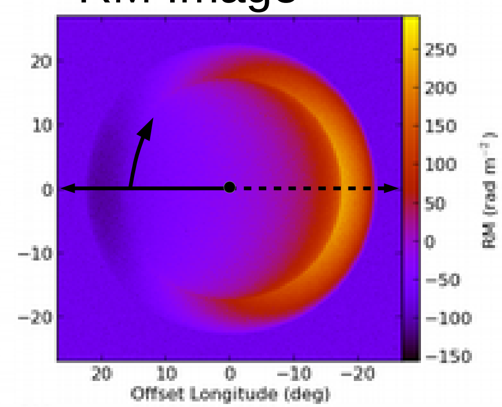

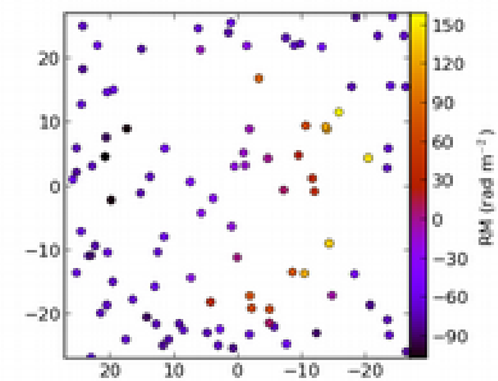

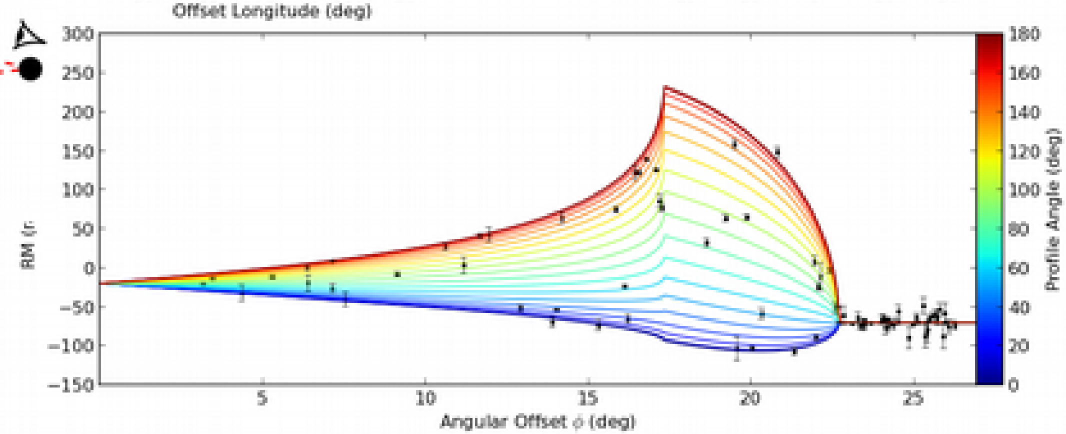

A near-field ionised shell model

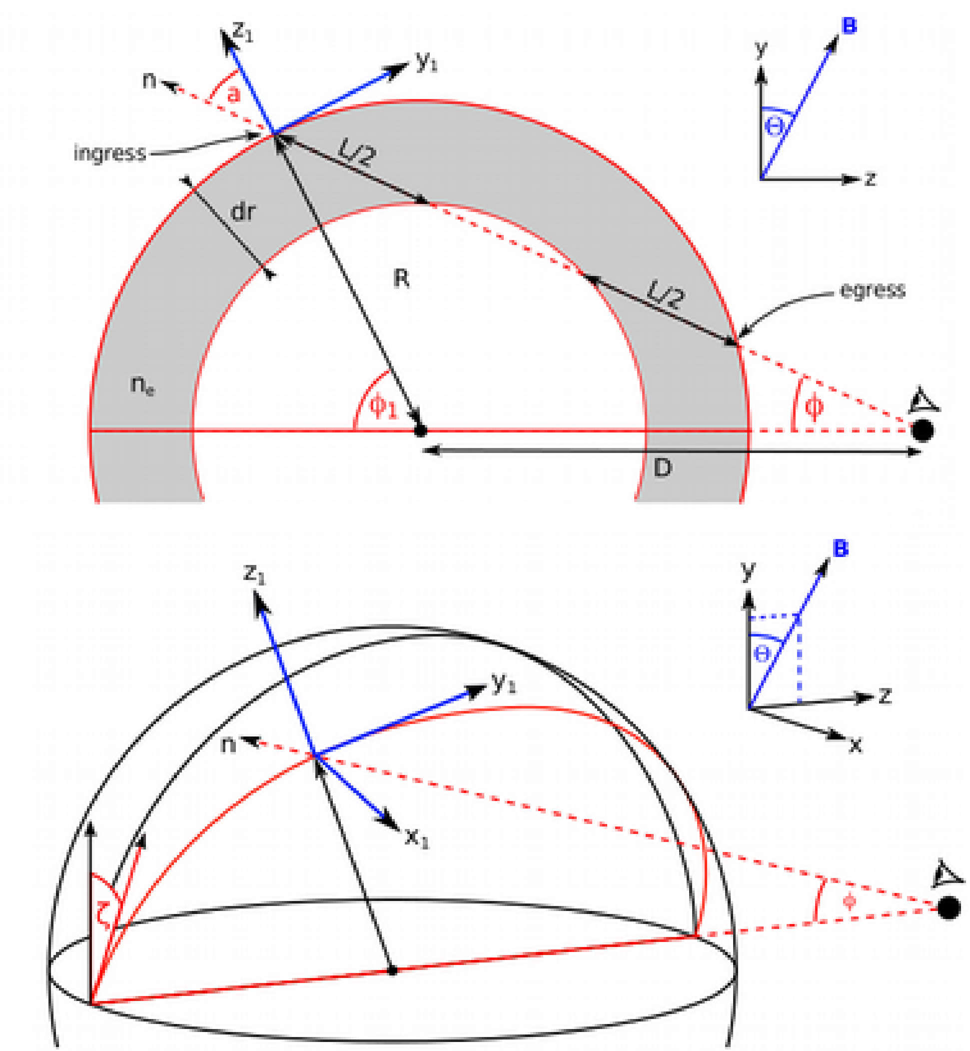

Magnetic field angle

Θ = 50 degrees

RM Image

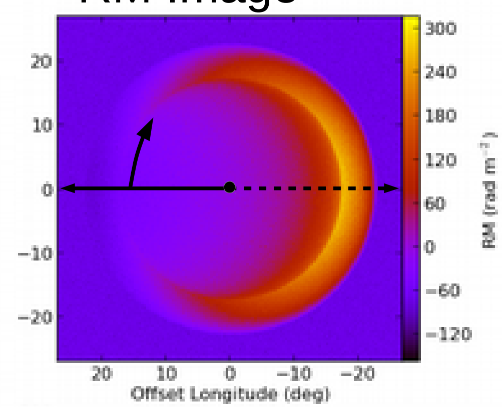

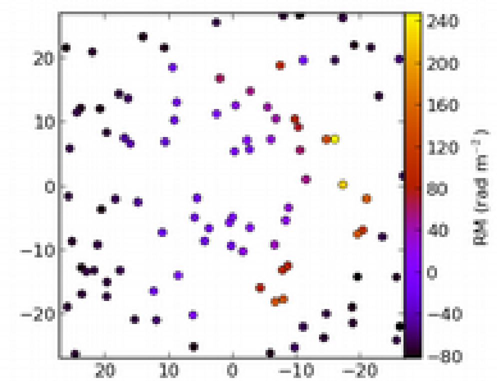

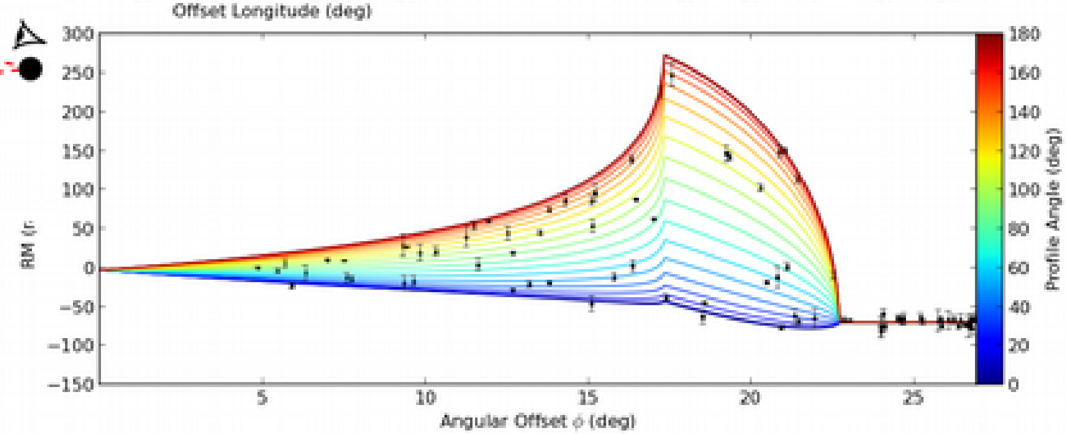

A near-field ionised shell model

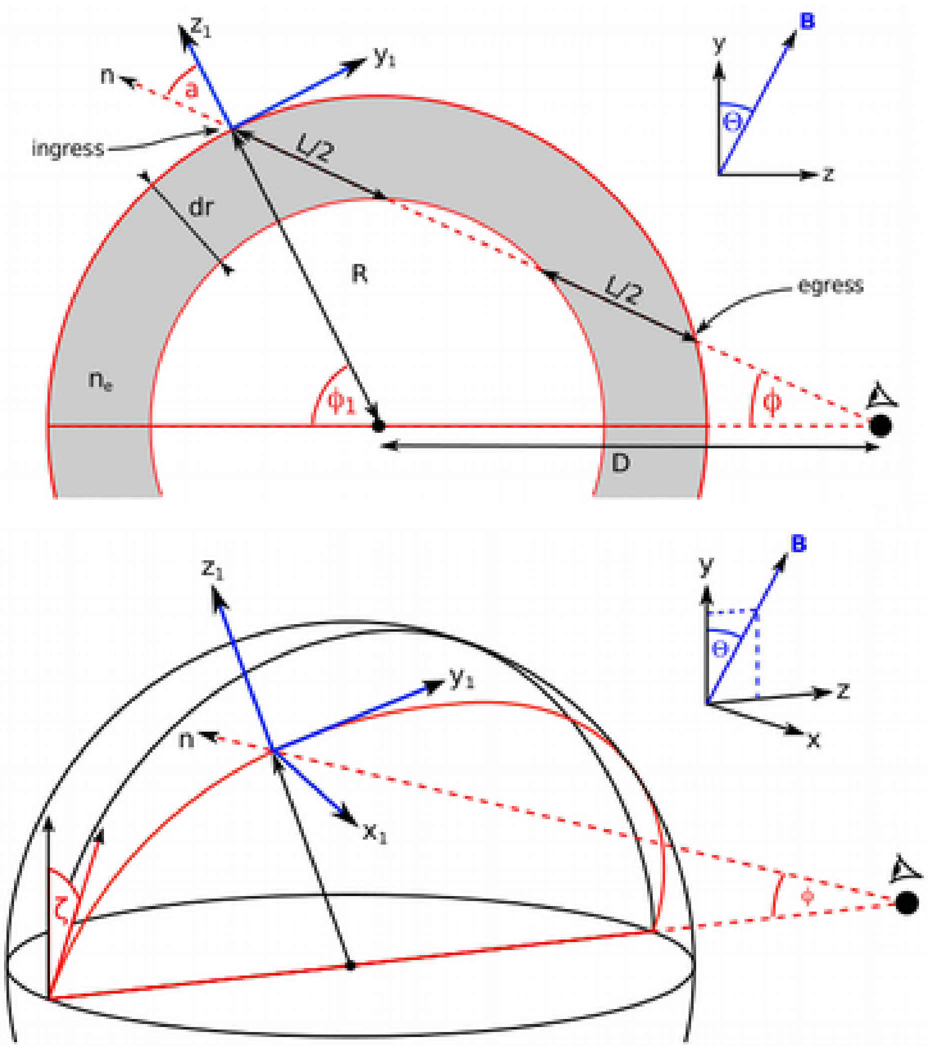

Magnetic field angle

Θ = 60 degrees

RM Image

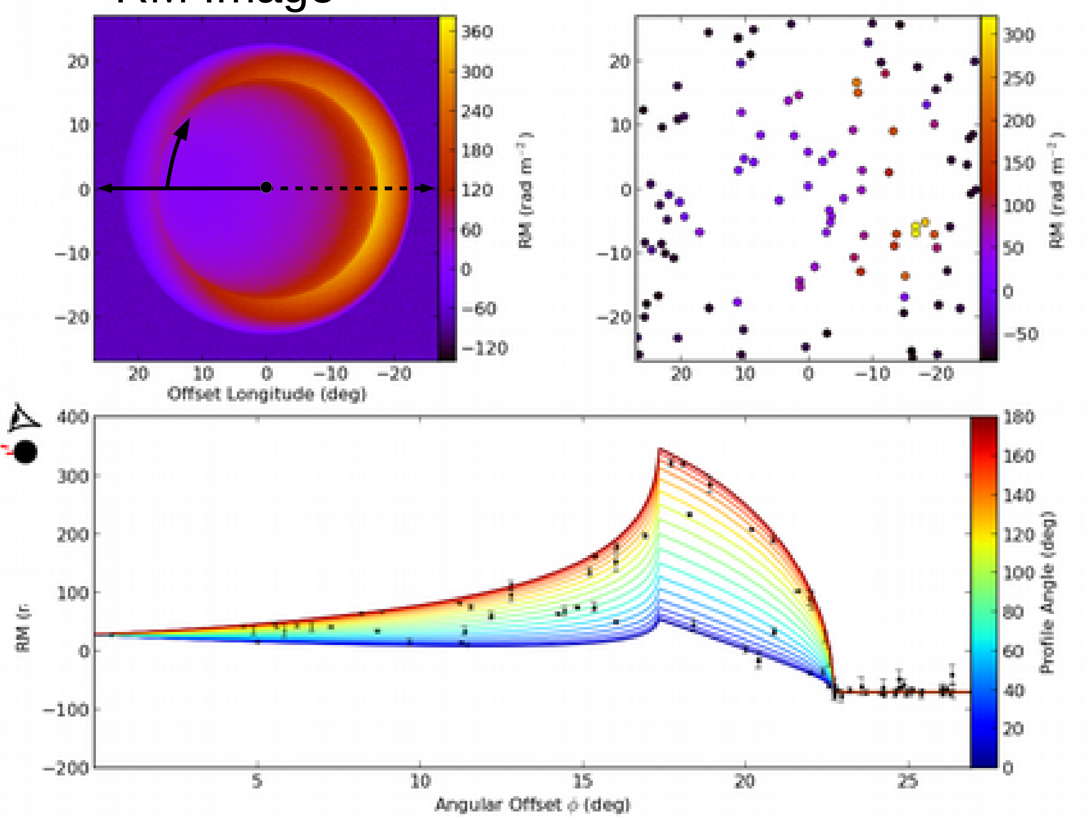

A near-field ionised shell model

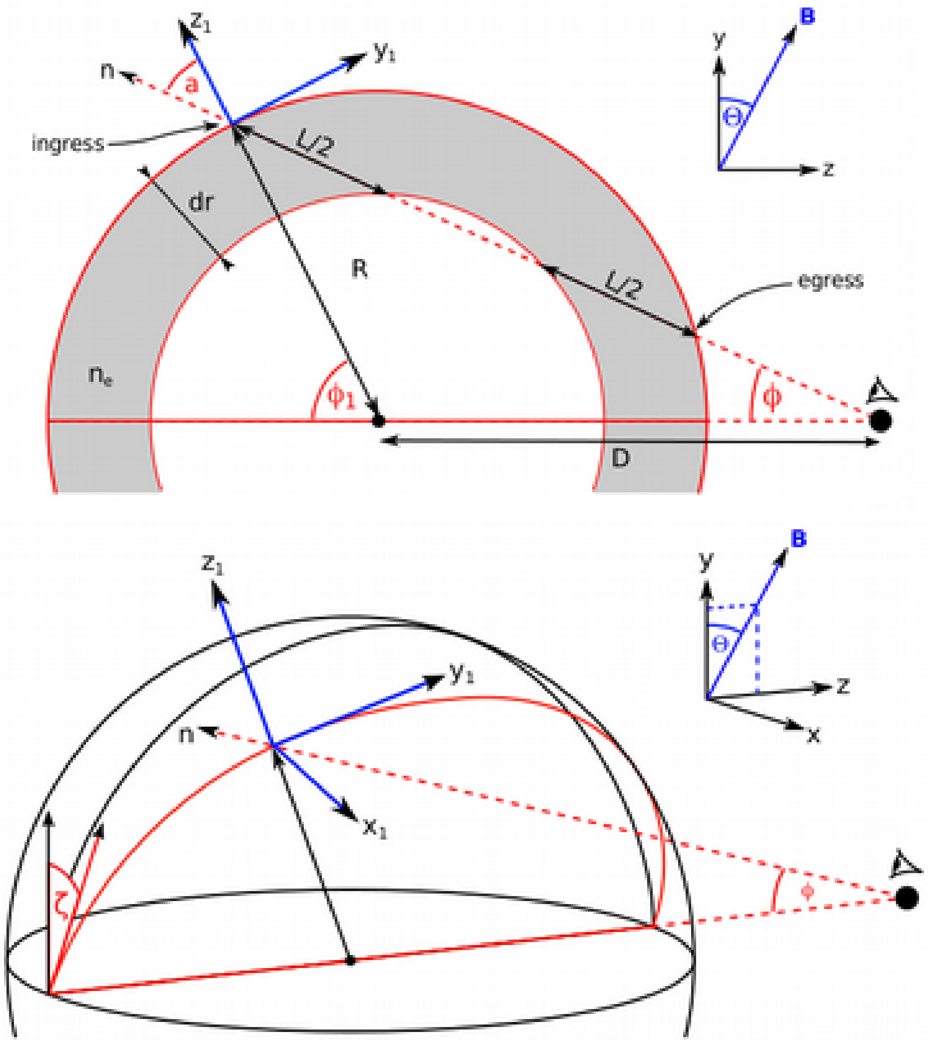

Magnetic field angle

Θ = 70 degrees

RM Image

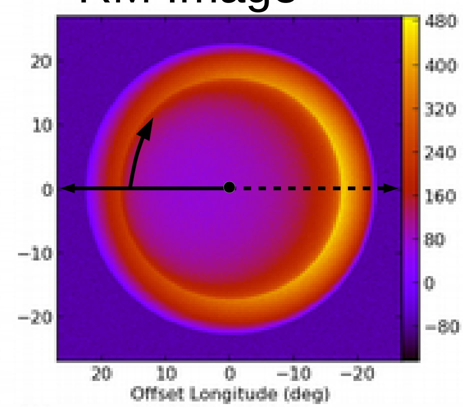

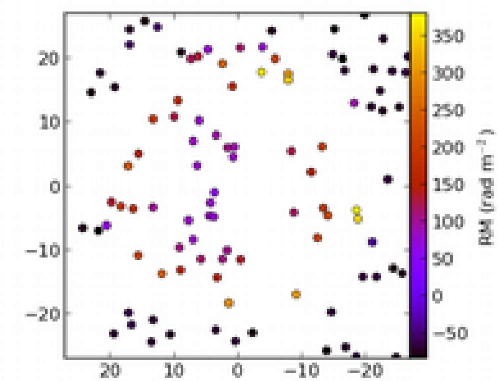

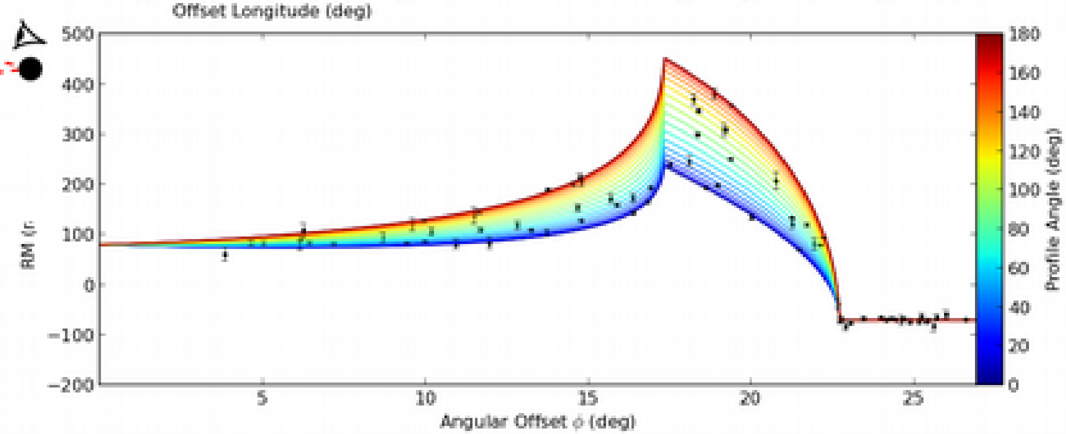

A near-field ionised shell model

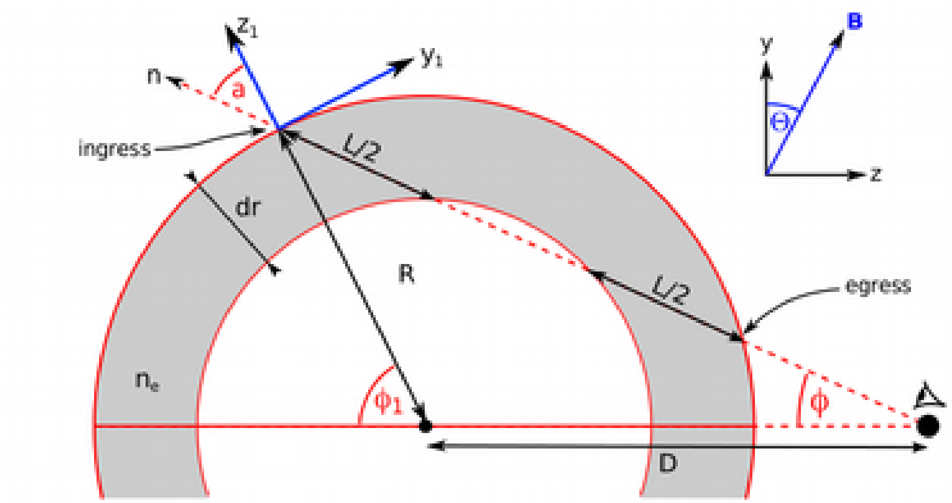

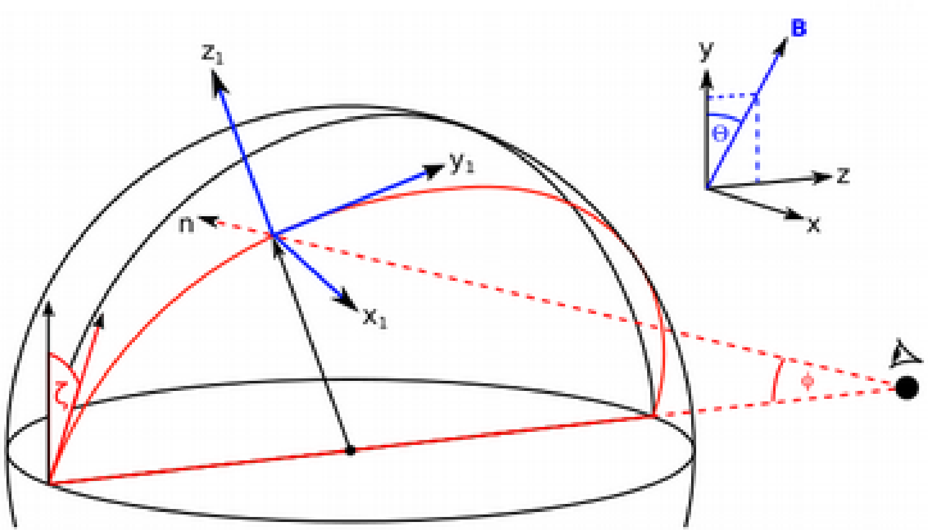

Magnetic field angle

Θ = 80 degrees

RM Image

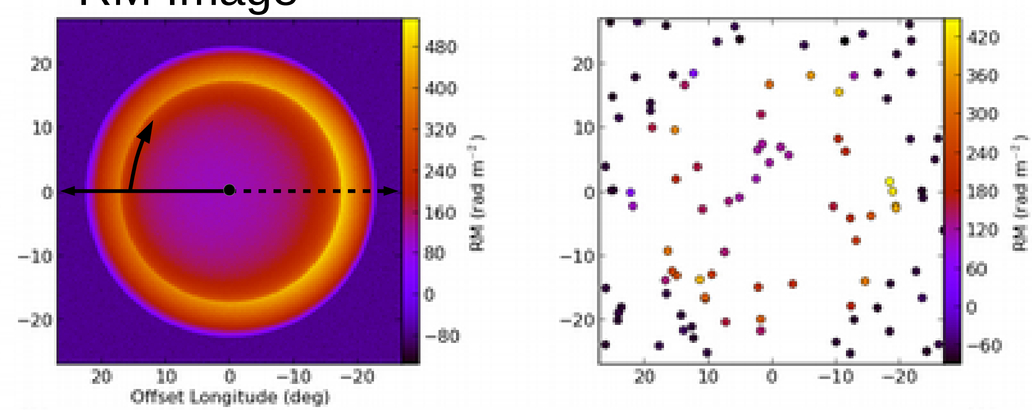

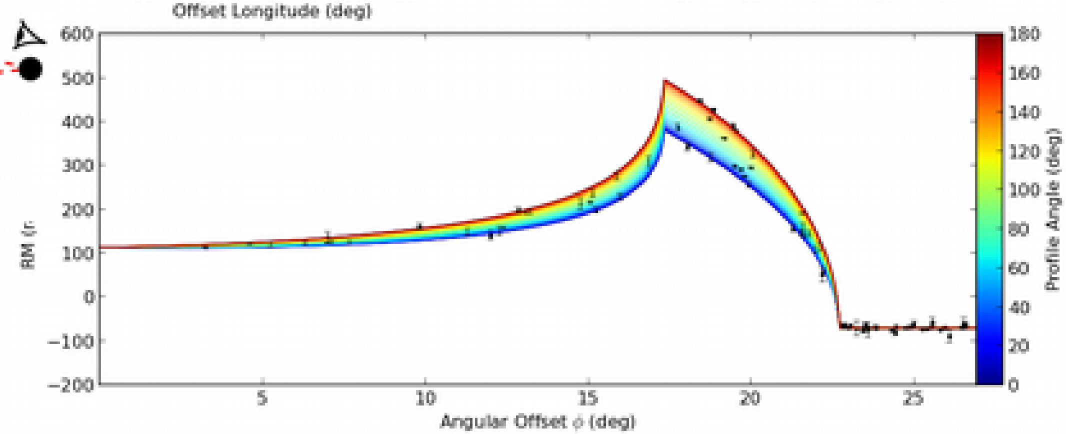

A near-field ionised shell model

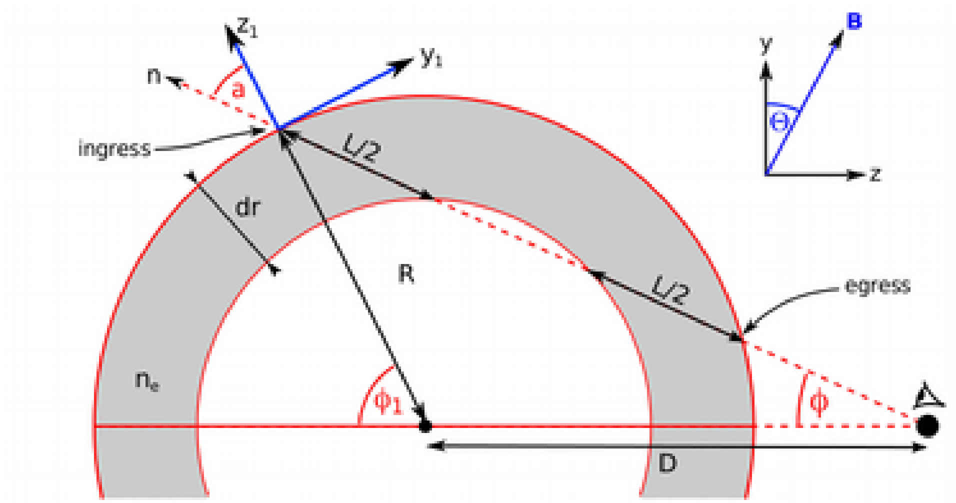

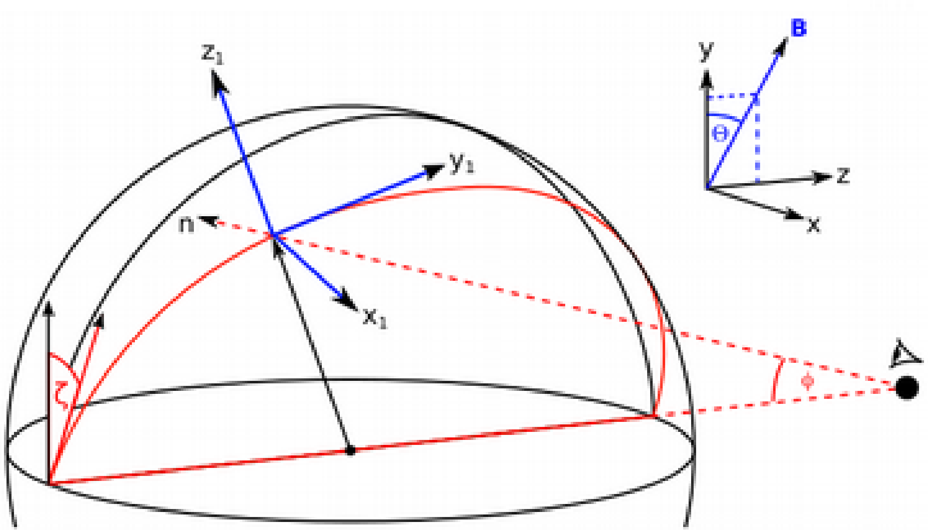

Magnetic field angle

Θ = 90 degrees

RM Image

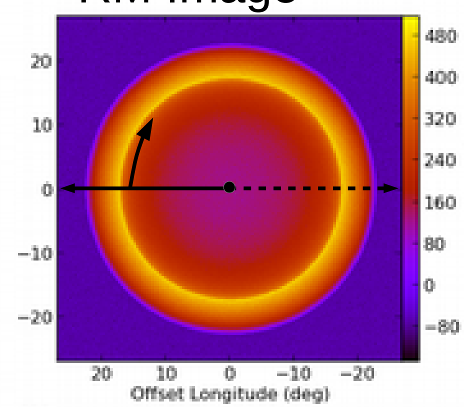

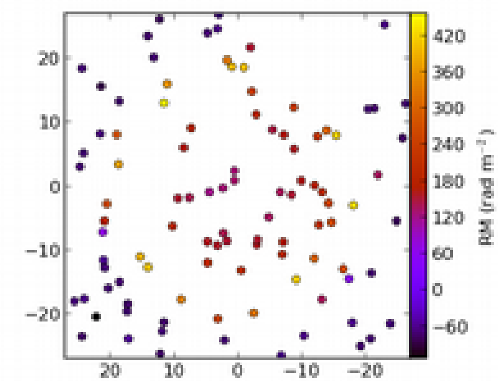

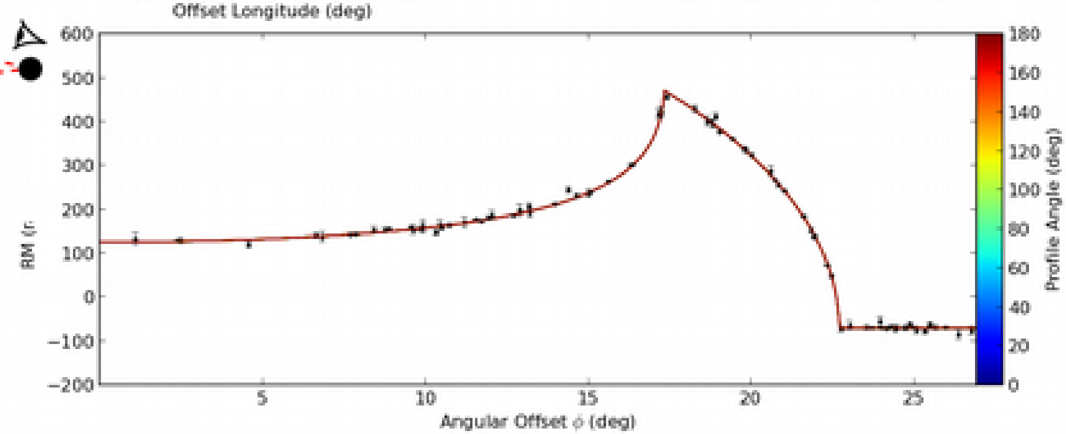

A near-field ionised shell model

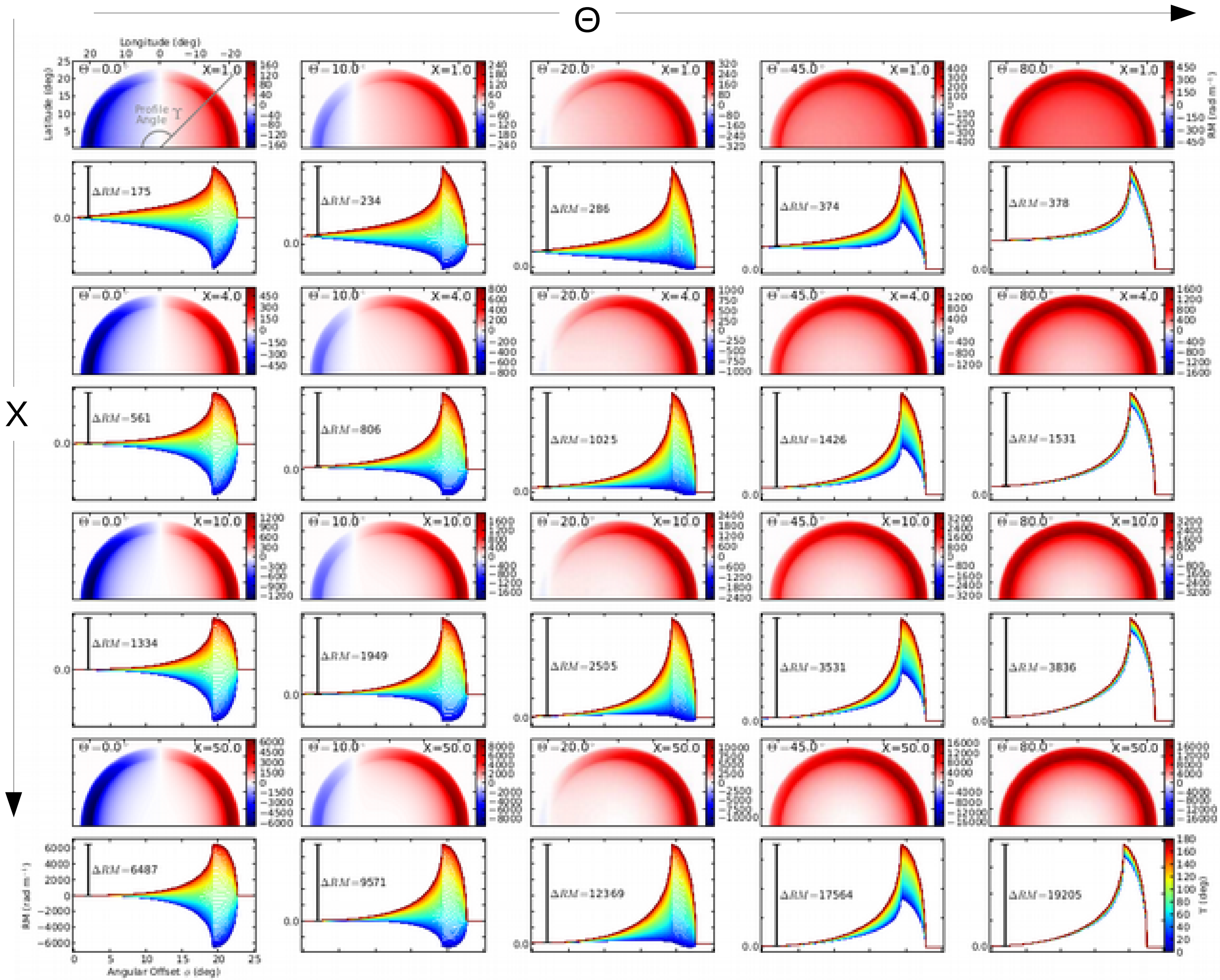

A near-field ionised shell model

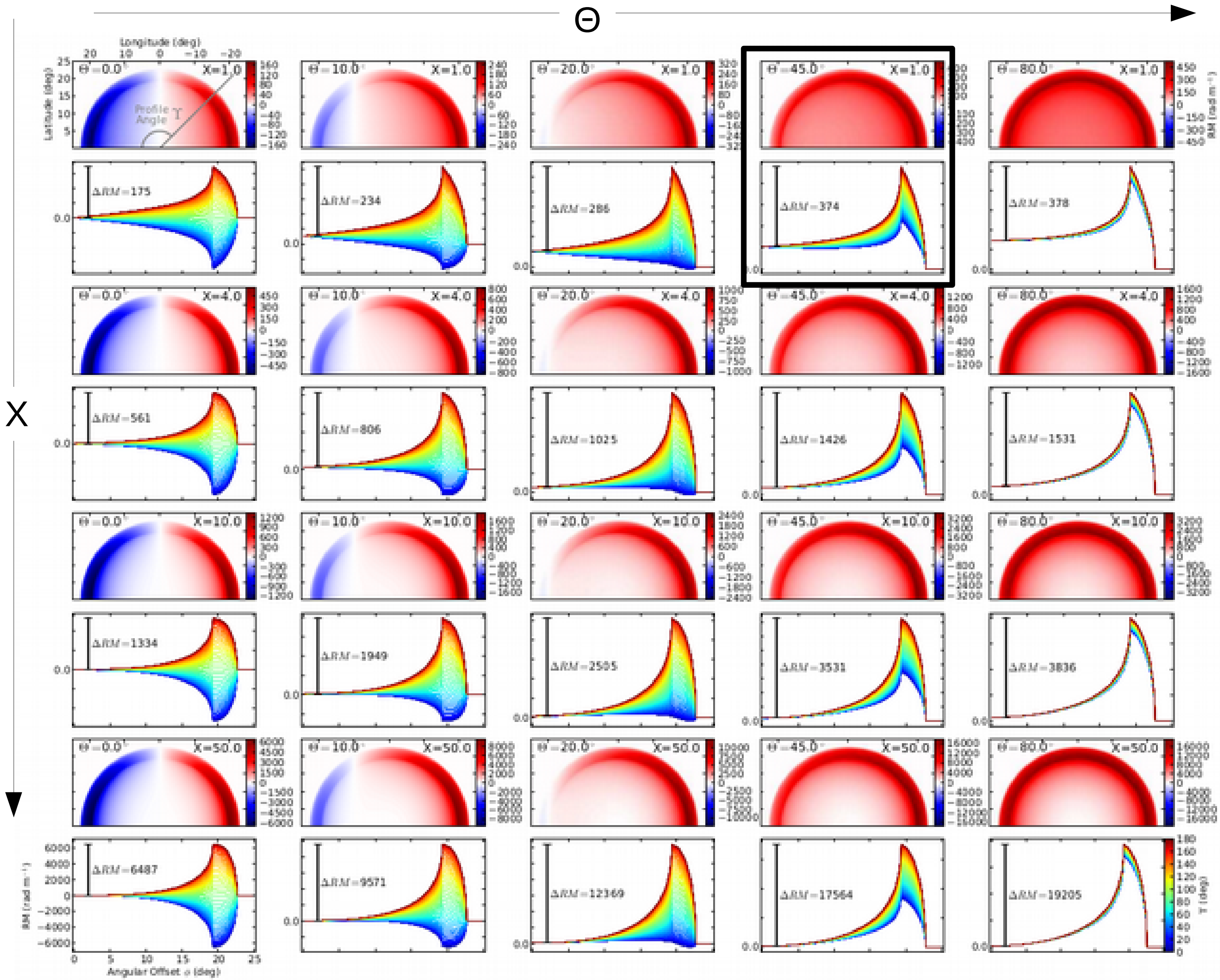

A near-field ionised shell model

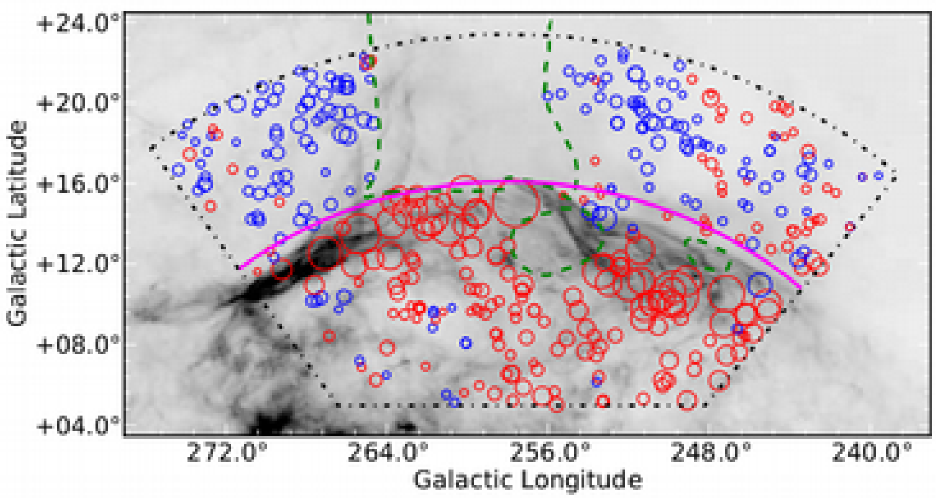

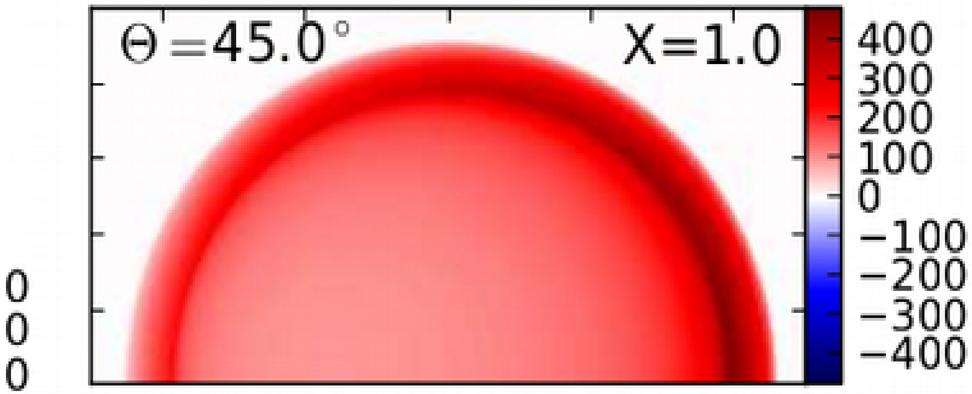

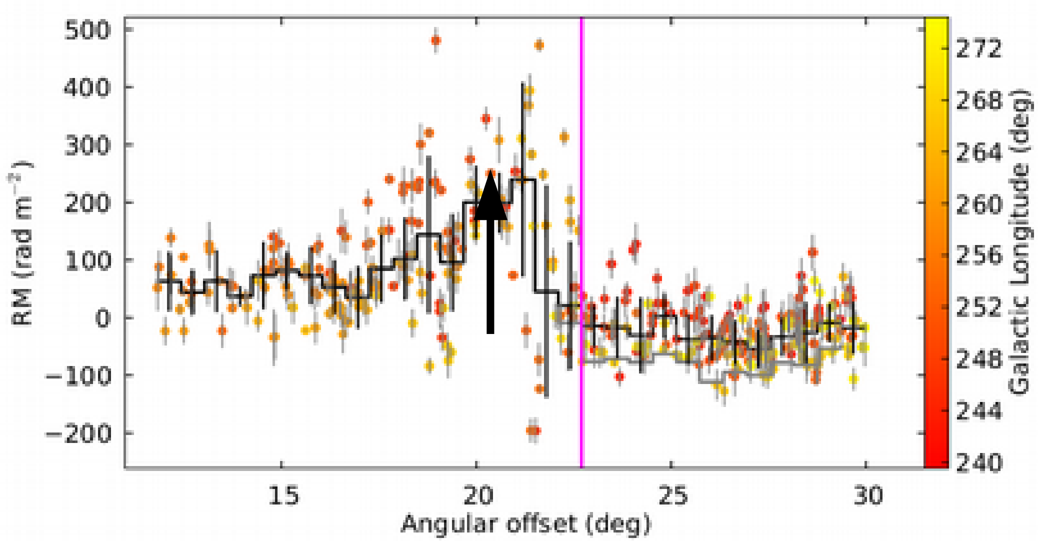

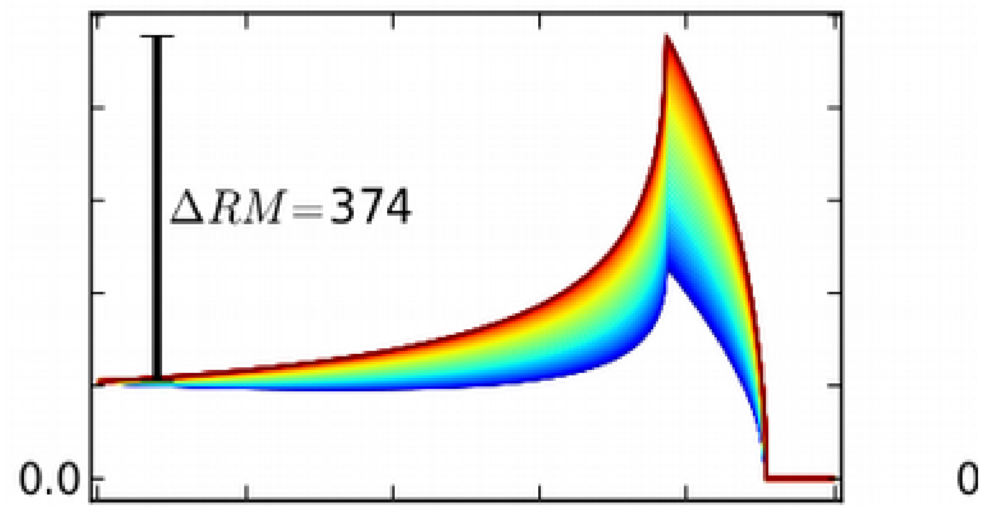

A near-field ionised shell model

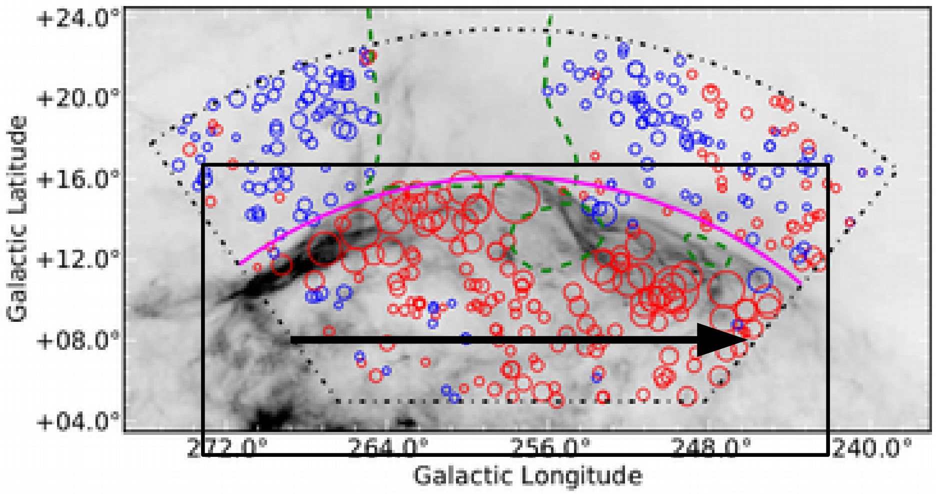

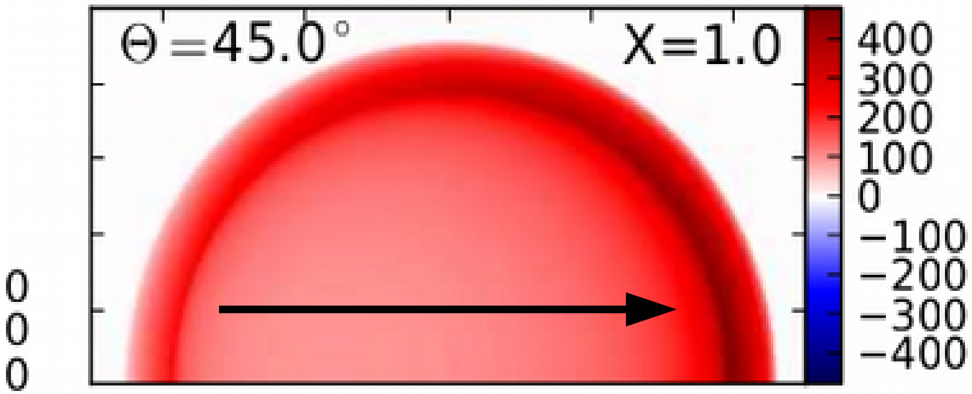

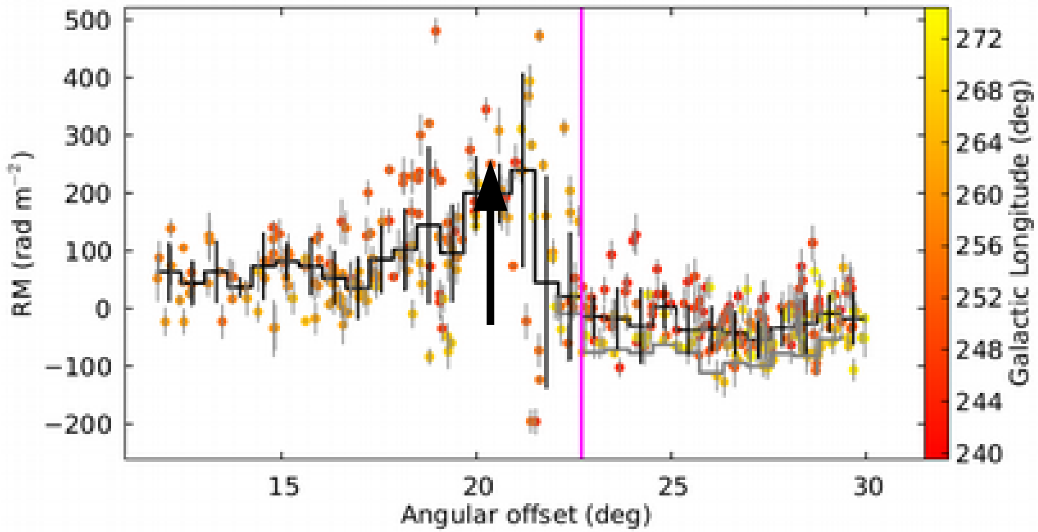

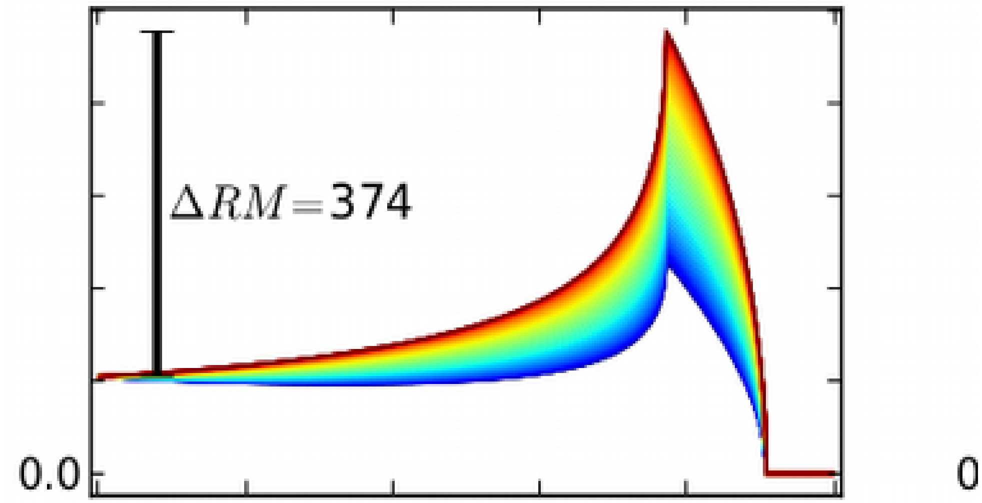

Aside: electron density

- B and n_e are degenerate, so must constrain n_e using other data

$$\mathrm{RM} = 0.81 \int_{obs}^{src} n_e B_{||} \, dl \quad \mathrm{rad\,m^{-2}}.$$

Aside: electron density

- B and n_e are degenerate, so must constrain n_e using other data

$$\mathrm{RM} = 0.81 \int_{obs}^{src} n_e \, B_{||} \, dl \quad \mathrm{rad\,m^{-2}}.$$

- Estimate electron-density from Hα

$$\mathrm{EM} = \int_0^{\infty} n_e^2 \, dl \quad \mathrm{cm^{-6}}.$$

Aside: electron density

- B and n_e are degenerate, so must constrain n_e using other data

$$\mathrm{RM} = 0.81 \int_{obs}^{src} n_e \, B_{||} \, dl \quad \mathrm{rad\,m^{-2}}.$$

- Estimate electron-density from Hα

$$\mathrm{EM} = \int_0^{\infty} n_e^2 \, dl \quad \mathrm{cm^{-6}}.$$

$$\mathrm{EM} = 2.75 \left(\frac{T_e}{10^4\,\mathrm{K}} \right)^{0.9} \left(\frac{I_{\mathrm{H}_\alpha}}{\mathrm{R}} \right) e^{\tau} \quad \mathrm{cm^{-6}\,pc}.$$

Aside: electron density

Extinction corrected Hα map:

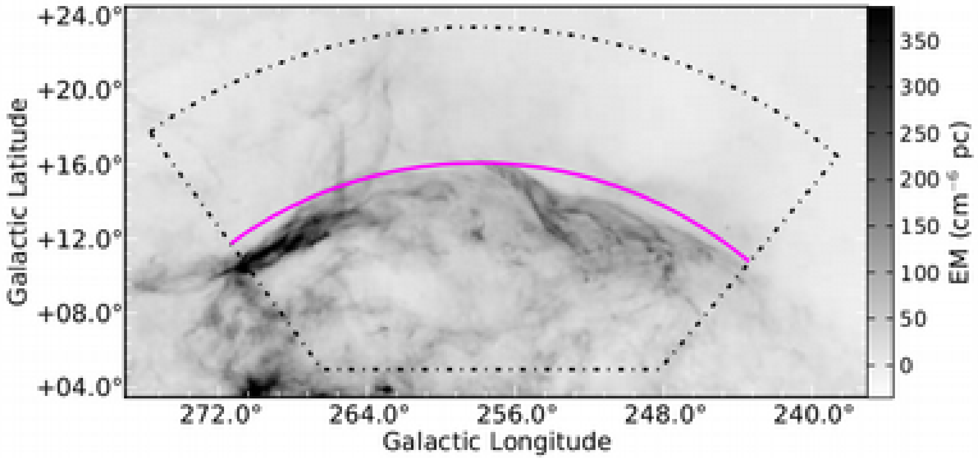

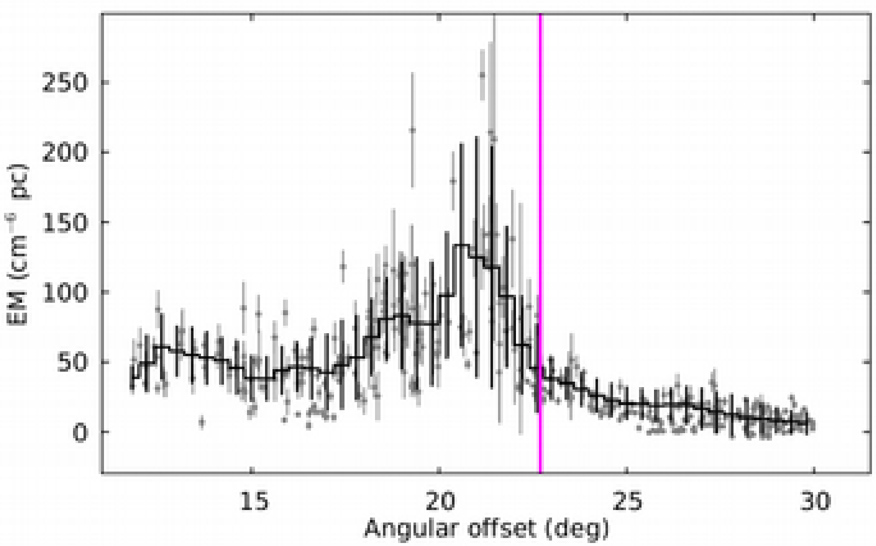

- B and n_e are degenerate, so must constrain n_e using other data

$$\mathrm{RM} = 0.81 \int_{obs}^{src} n_e \, B_{||} \, dl \quad \mathrm{rad\, m^{-2}}.$$

- Estimate electron-density from Hα

$$\mathrm{EM} = \int_0^{\infty} n_e^2 \, dl \quad \mathrm{cm^{-6}}.$$

$$\mathrm{EM} = 2.75 \left(\frac{T_e}{10^4\,\mathrm{K}} \right)^{0.9} \left(\frac{I_{\mathrm{H}_\alpha}}{\mathrm{R}} \right) e^{\tau} \quad \mathrm{cm^{-6}\,pc}.$$

Aside: electron density

Extinction corrected Hα map:

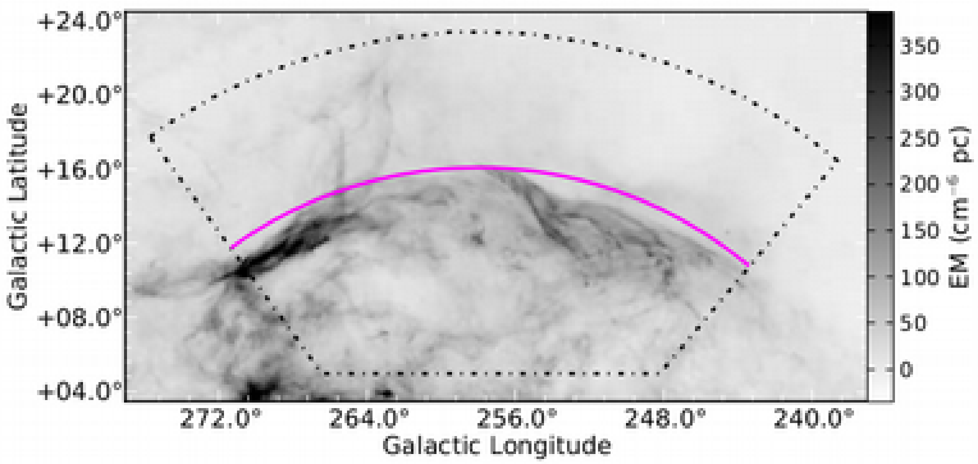

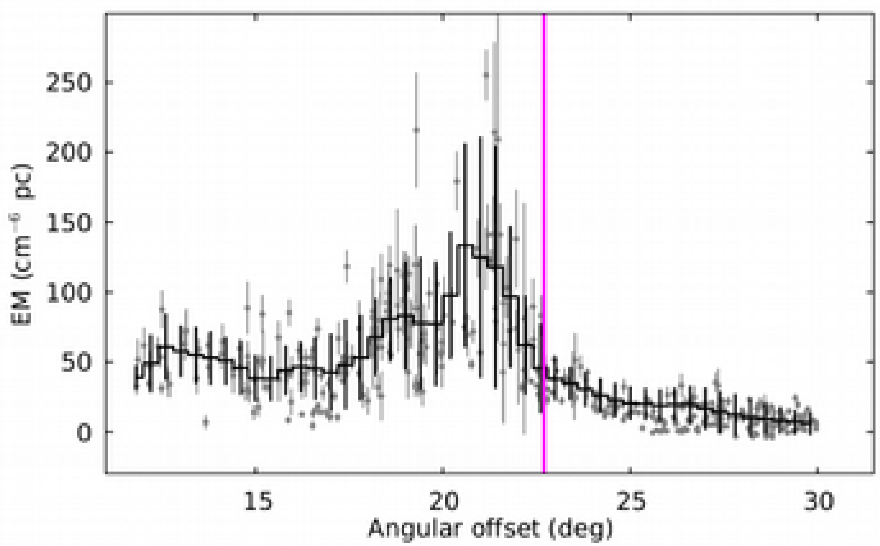

- B and n_e are degenerate, so must constrain n_e using other data

$$\mathrm{RM} = 0.81 \int_{obs}^{src} n_e B_{||} \, dl \quad \mathrm{rad\,m^{-2}}.$$

- Estimate electron-density from Hα

$$\mathrm{EM} = \int_0^{\infty} n_e^2 \, dl \quad \mathrm{cm^{-6}}.$$

$$\mathrm{EM} = 2.75 \left(\frac{T_e}{10^4\,\mathrm{K}} \right)^{0.9} \left(\frac{I_{\mathrm{H}_\alpha}}{\mathrm{R}} \right) e^{\tau} \quad \mathrm{cm^{-6}\,pc}.$$

$$n_0 = \sqrt{\frac{\mathrm{EM}}{fL}} \quad \mathrm{cm^{-3}},$$

Aside: electron density

Electron density map:

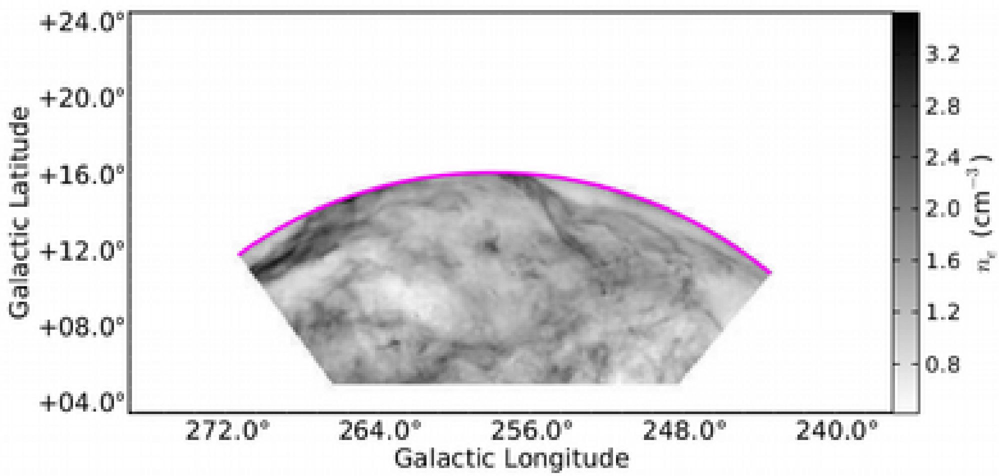

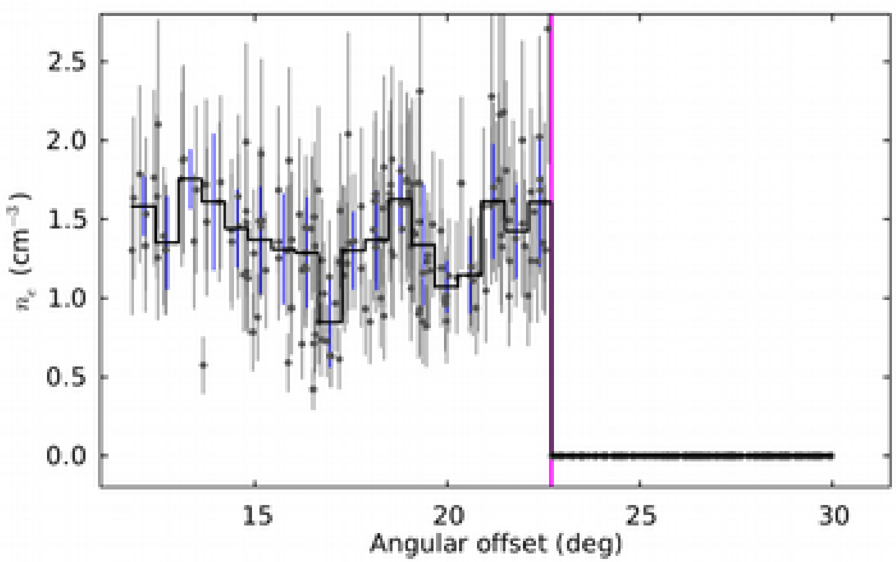

- B and n_e are degenerate, so must constrain n_e using other data

$$\mathrm{RM} = 0.81 \int_{obs}^{src} n_e \, B_{||} \, dl \quad \mathrm{rad\,m^{-2}}.$$

- Estimate electron-density from Hα

$$\mathrm{EM} = \int_0^{\infty} n_e^2 \, dl \quad \mathrm{cm^{-6}}.$$

$$\mathrm{EM} = 2.75 \left(\frac{T_e}{10^4\,\mathrm{K}}\right)^{0.9} \left(\frac{I_{\mathrm{H}_\alpha}}{\mathrm{R}}\right) e^{\tau} \quad \mathrm{cm^{-6}\,pc}.$$

$$n_0 = \sqrt{\frac{\mathrm{EM}}{fL}} \quad \mathrm{cm^{-3}},$$

- **n_e = 1.4 +/- 0.4 cm^{-3}**
- Set as prior in the fitting procedure

Fitting the model

- Fit the model to the RM data using a maximum likelihood method
- Explore the posterior distribution using the MCMC sampler EMCEE

emcee
The MCMC Hammer

http://dan.iel.fm/emcee/current/

Fitting the model

- Fit the model to the RM data using a maximum likelihood method
- Explore the posterior distribution using the MCMC sampler EMCEE
- Error bars on Taylor RM catalogue are underestimated for Galactic RMs.
- Used a hyperparameter to scale the errorbars to be consistent with the scatter in the data (see Lahav et al. 2000, Hobson et al. 2002)
- Hyperparameter also encodes small scale structure not in the model

emcee The MCMC Hammer

http://dan.iel.fm/emcee/current/

$$\chi^2 = \sum_{\mathrm{i}} \left[\frac{(\mathrm{RM_i} - \mathrm{RM_{mod}})^2}{\sigma(\mathrm{RM})^2_{\mathrm{tot,i}}} + \ln(2\,\pi\,\sigma(\mathrm{RM})^2_{\mathrm{tot,i}}) \right]$$

$$\sigma(\mathrm{RM})^2_{\mathrm{tot,i}} = \sigma(\mathrm{RM})^2 + \exp[\,2\ln(\delta(\mathrm{RM})\,)\,]$$

Results

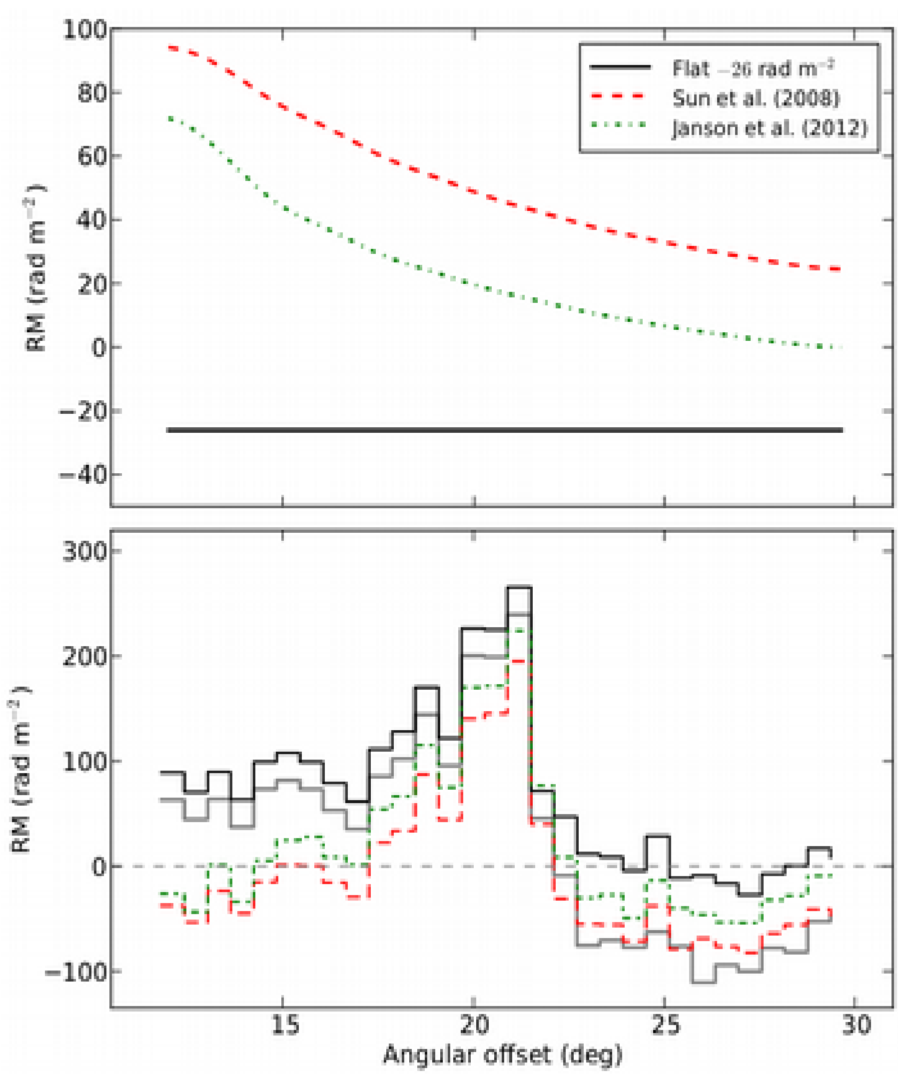

- Fit the data three times assuming three guesses for RM-background of the Galaxy
  - Flat median background
  - Jansson & Farrah 2012 model
  - Sun et al 2008 model

Results

Confidence Plots:

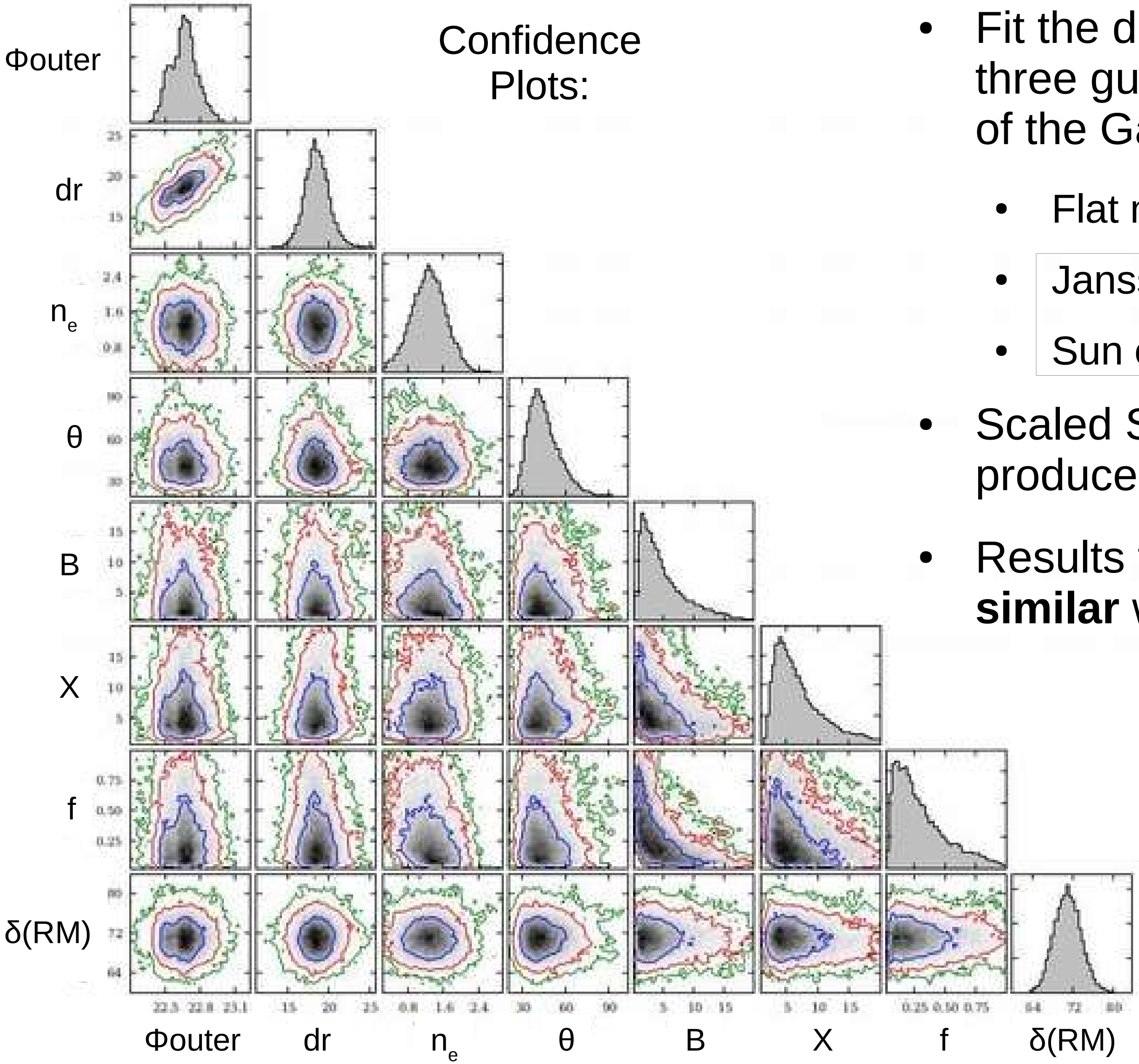

- Fit the data three times assuming three guesses for RM-background of the Galaxy
  - Flat median background
  - Jansson & Farrah 2012 model
  - Sun et al 2008 model
- Scaled Sun and Jannson models produced almost identical results.
- Results for all three backgrounds **similar** within errors

Results

Best fitting model:

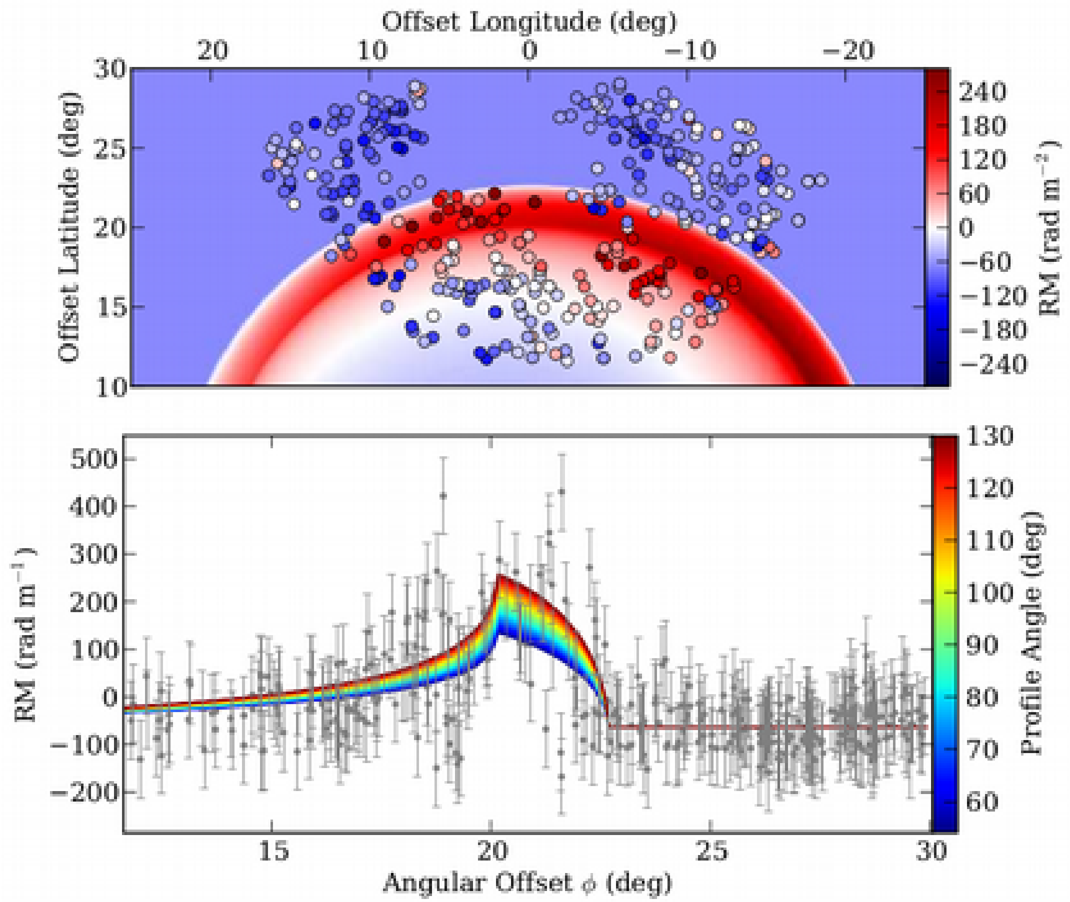

- Fit the data three times assuming three guesses for RM-background of the Galaxy
  - Flat median background
  - Jansson & Farrah 2012 model
  - Sun et al 2008 model
- Scaled Sun and Jannson models produced almost identical results.
- Results for all three backgrounds **similar** within errors

Results

Best fitting model:

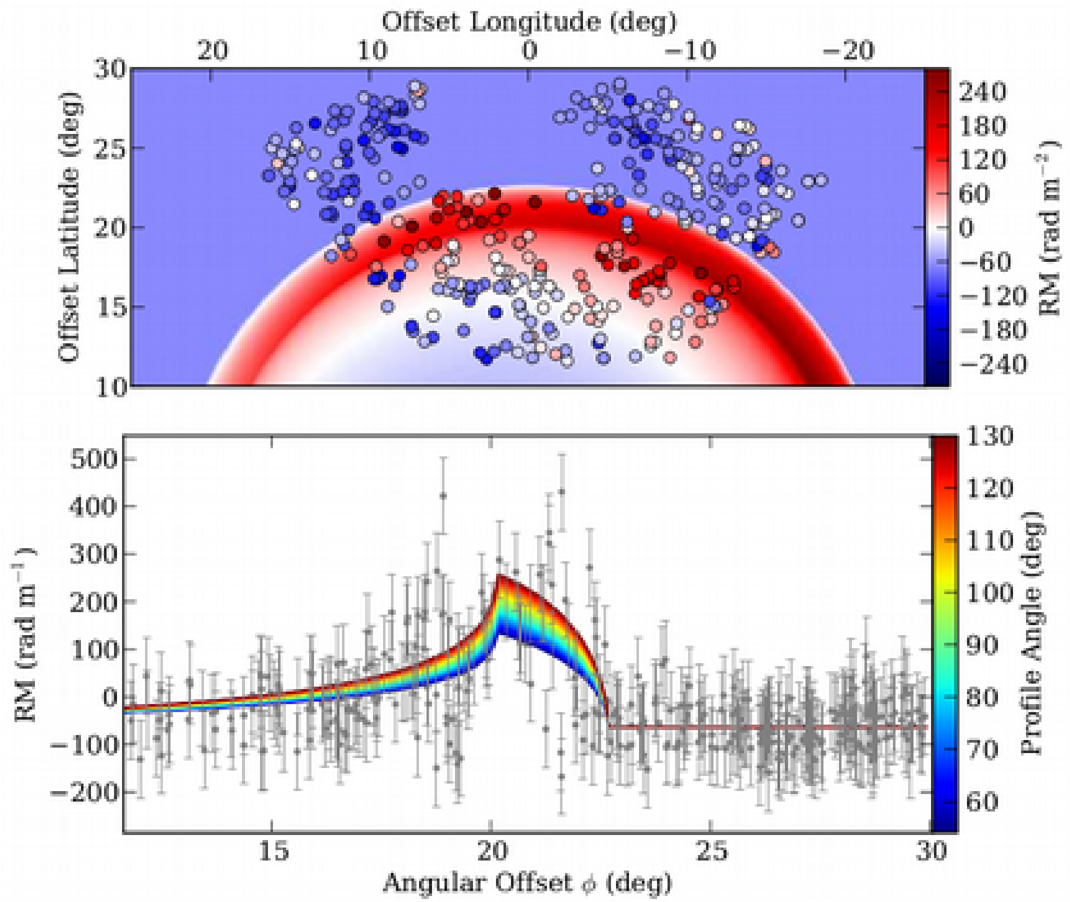

- Fit the data three times assuming three guesses for RM-background of the Galaxy
  - Flat median background
  - Jansson & Farrah 2012 model
  - Sun et al 2008 model
- Scaled Sun and Jannson models produced almost identical results.
- Results for all three backgrounds **similar** within errors
- OK, so what can we tell from the results?

Results

Table 2: Results of fitting the ionised shell model to the RM catalogue.

(1) Parameter	(2) Symbol	(3) Unit	(4) Notes	(5) Assumed Background Level: Flat	(6) Assumed Background Level: Sun et al. (2008)	(7) Assumed Background Level: Jansson & Farrar (2012)
Distance	D	pc	Fixed	450	450	450
Background RM	$\mathrm{RM}_{\mathrm{bg}}$	$\mathrm{rad\,m^{-2}}$	Fixed	−26.4	−64.0	−36.6
Filling factor	f	–	Free	$0.4^{+0.3}_{-0.2}$	$0.3^{+0.3}_{-0.1}$	$0.2^{+0.2}_{-0.1}$
Angular radius	ϕ_{outer}	deg.	Free	$22.7^{+0.2}_{-0.1}$	$22.7^{+0.1}_{-0.1}$	$22.7^{+0.1}_{-0.1}$
Shell thickness	dr	pc	Free	$20.2^{+1.8}_{-1.6}$	$18.5^{+1.5}_{-1.4}$	$18.5^{+1.3}_{-1.3}$
Field angle	Θ	deg.	Free	55^{+15}_{-12}	43^{+13}_{-9}	55^{+16}_{-12}
Field strength	B_0	μG	Free	$8.8^{+6.1}_{-4.0}$	$3.9^{+4.9}_{-2.2}$	$3.9^{+4.2}_{-2.1}$
Compression factor	X	–	Free	$1.1^{+0.5}_{-0.3}$	$6.0^{+5.1}_{-2.5}$	$6.8^{+5.3}_{-2.8}$
Electron density	n_e	$\mathrm{cm^{-3}}$	Prior	$1.4^{+0.4}_{-0.4}$	$1.3^{+0.4}_{-0.4}$	$1.2^{+0.4}_{-0.4}$
Additional RM Scatter	$\delta(\mathrm{RM})$	$\mathrm{rad\,m^{-2}}$	Free	$75.1^{+2.9}_{-2.7}$	$71.0^{+2.7}_{-2.7}$	$70.0^{+2.9}_{-2.6}$

Results

Table 2: Results of fitting the ionised shell model to the RM catalogue.

(1) Parameter	(2) Symbol	(3) Unit	(4) Notes	(5) Assumed Background Level: Flat	(6) Assumed Background Level: Sun et al. (2008)	(7) Assumed Background Level: Jansson & Farrar (2012)
Distance	D	pc	Fixed	450	450	450
Background RM	$\mathrm{RM_{bg}}$	$\mathrm{rad\,m^{-2}}$	Fixed	−26.4	−64.0	−36.6
Filling factor	f	–	Free	$0.4^{+0.3}_{-0.2}$	$0.3^{+0.3}_{-0.1}$	$0.2^{+0.2}_{-0.1}$
Angular radius	ϕ_{outer}	deg.	Free	$22.7^{+0.2}_{-0.1}$	$22.7^{+0.1}_{-0.1}$	$22.7^{+0.1}_{-0.1}$
Shell thickness	dr	pc	Free	$20.2^{+1.8}_{-1.6}$	$18.5^{+1.5}_{-1.4}$	$18.5^{+1.3}_{-1.3}$
Field angle	Θ	deg.	Free	55^{+15}_{-12}	43^{+13}_{-9}	55^{+16}_{-12}
Field strength	B_0	μG	Free	$8.8^{+6.1}_{-4.0}$	$3.9^{+4.9}_{-2.2}$	$3.9^{+4.2}_{-2.1}$
Compression factor	X	–	Free	$1.1^{+0.5}_{-0.3}$	$6.0^{+5.1}_{-2.5}$	$6.8^{+5.3}_{-2.8}$
Electron density	n_e	$\mathrm{cm^{-3}}$	Prior	$1.4^{+0.4}_{-0.4}$	$1.3^{+0.4}_{-0.4}$	$1.2^{+0.4}_{-0.4}$
Additional RM Scatter	$\delta(\mathrm{RM})$	$\mathrm{rad\,m^{-2}}$	Free	$75.1^{+2.9}_{-2.7}$	$71.0^{+2.7}_{-2.7}$	$70.0^{+2.9}_{-2.6}$

- Two results of significant interest:
  - The compression factor at the edge of the nebula
  - The angle of the magnetic field (equivalent to spiral arm pitch angle)

Results: compression factor

- We fit a compression factor at the edge of the shell to be

  ~1 assuming a flat RM background

  ~6 assuming a model gradient

- This relatively low compression suggests that the supernova theory of origin is less likely. We would expect a X>100 for such a large old SNR (currently modelling this for confirmation)

- X is approximately unity for a HII region and so is consistent, however, a classical HII region model cannot explain the shell-structure

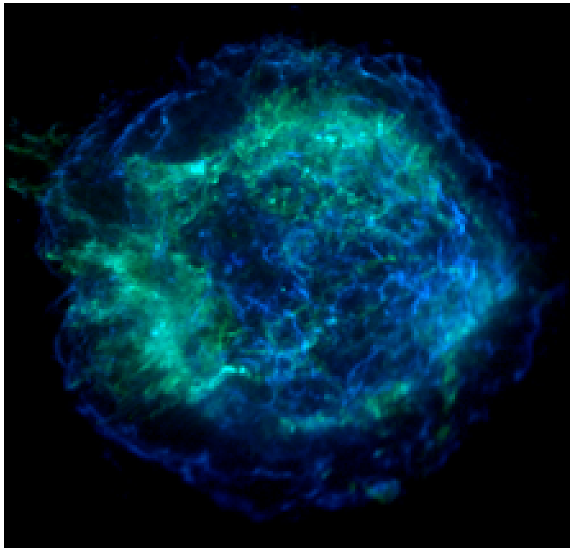

SNR Evolution:

1) Free expansion

2) Adiabatic expansion

3) Radiative expansion

4) Slowing & dissipation

Results: compression factor

- We fit a compression factor at the edge of the shell to be

  ~1 assuming a flat RM background

  ~6 assuming a model gradient

- This relatively low compression suggests that the supernova theory of origin is less likely. We would expect a X>100 for such a large old SNR (currently modelling this for confirmation)
- X is approximately unity for a HII region and so is consistent, however, a classical HII region model cannot explain the shell-structure
- Weaver et al (1977) model of a wind-blown-bubble matches the data very well and seems most likely.

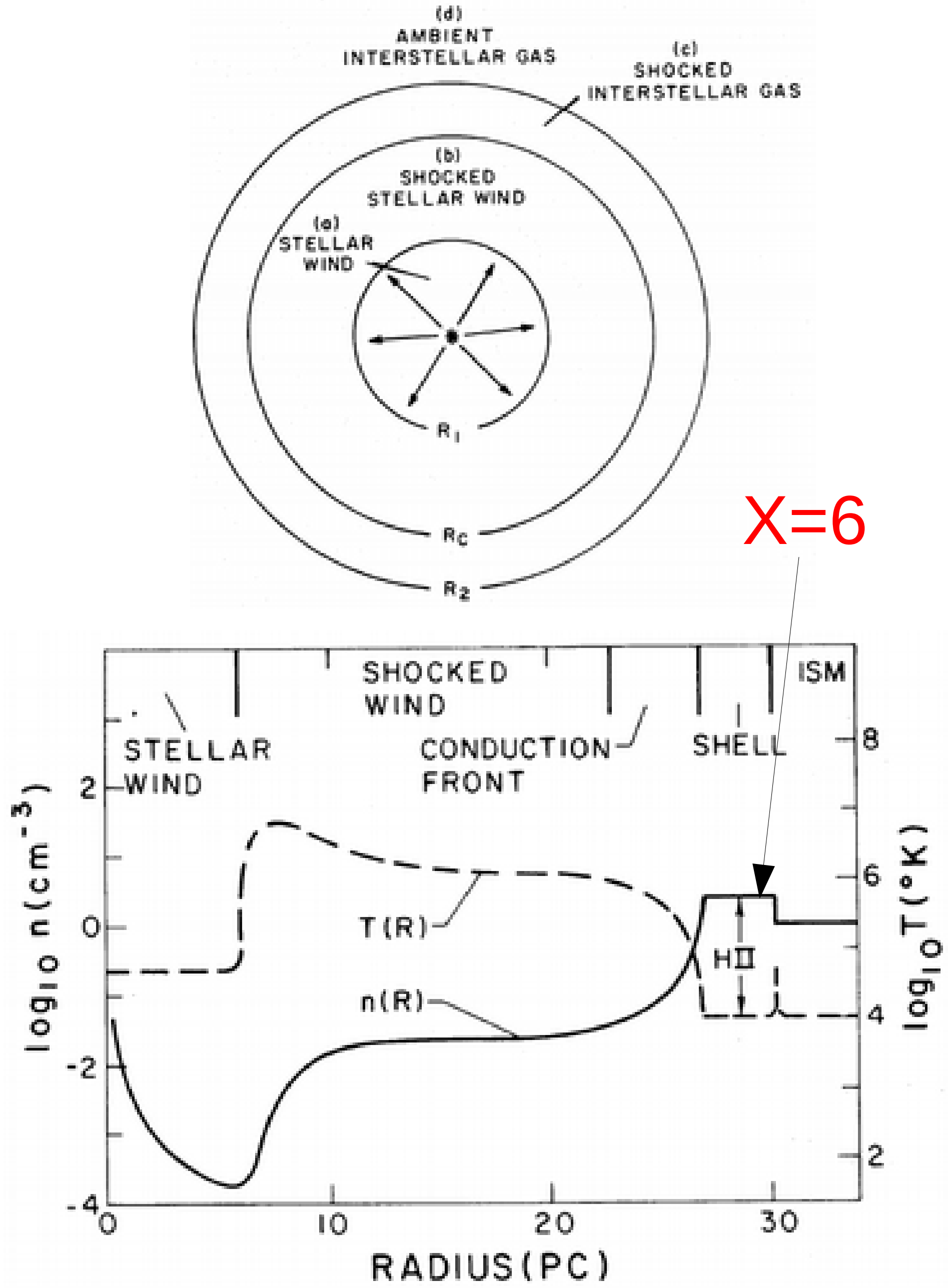

Results: compression factor, depolarisation

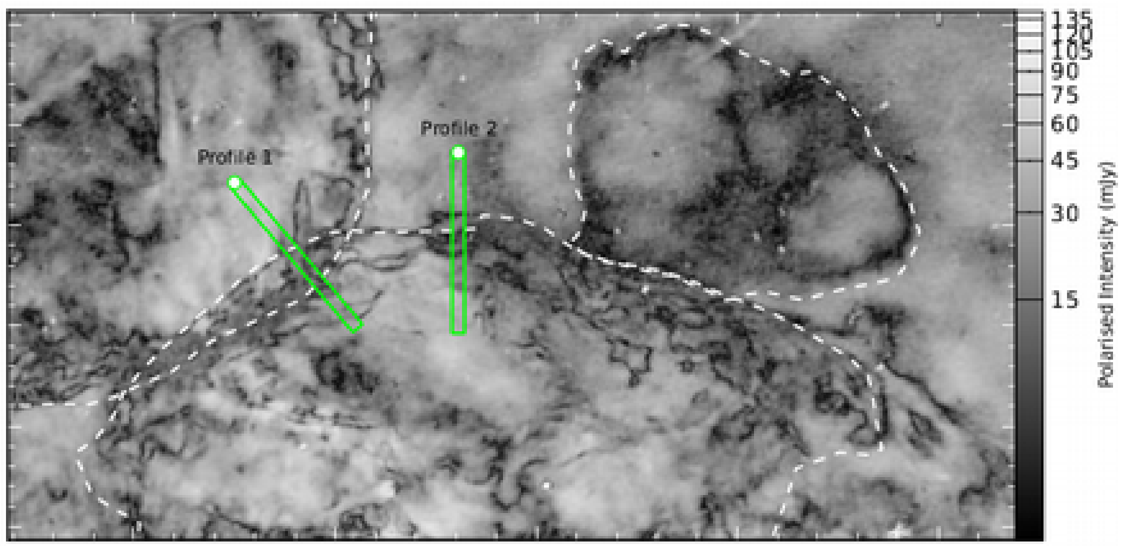

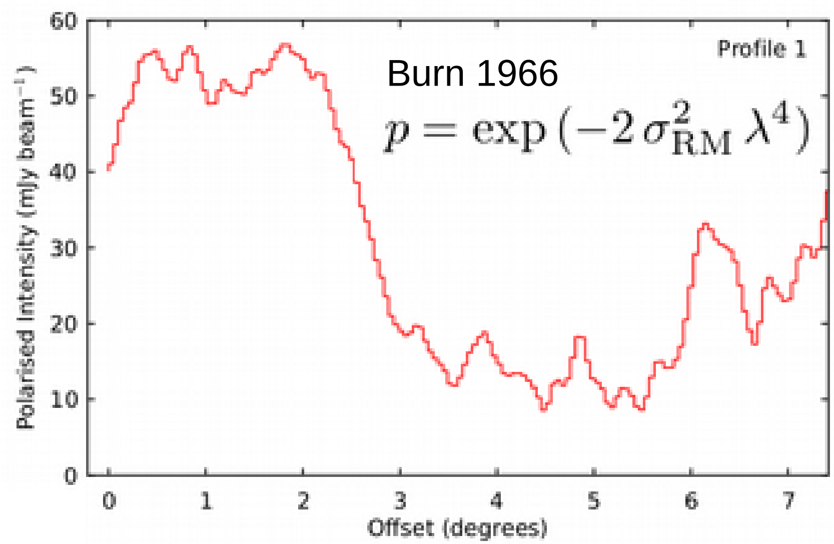

Results: compression factor, depolarisation

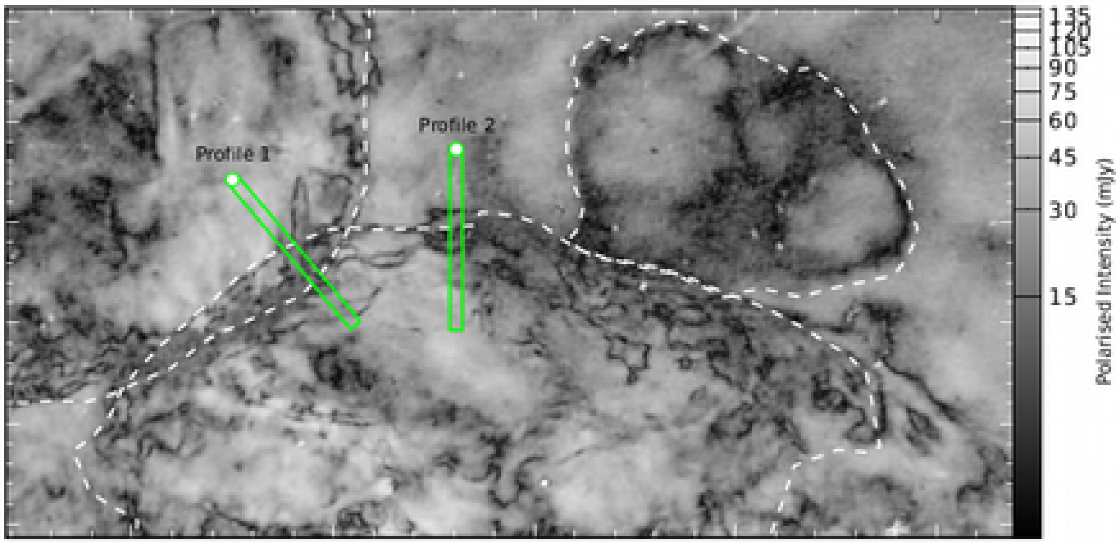

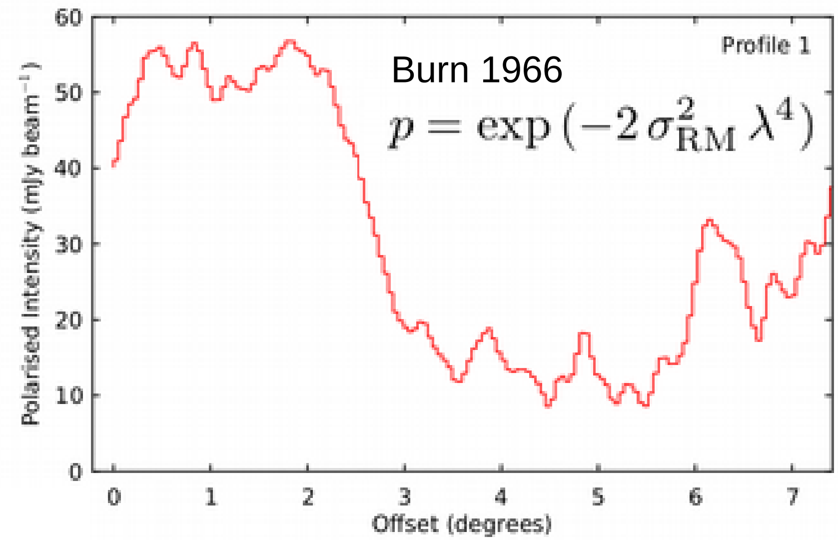

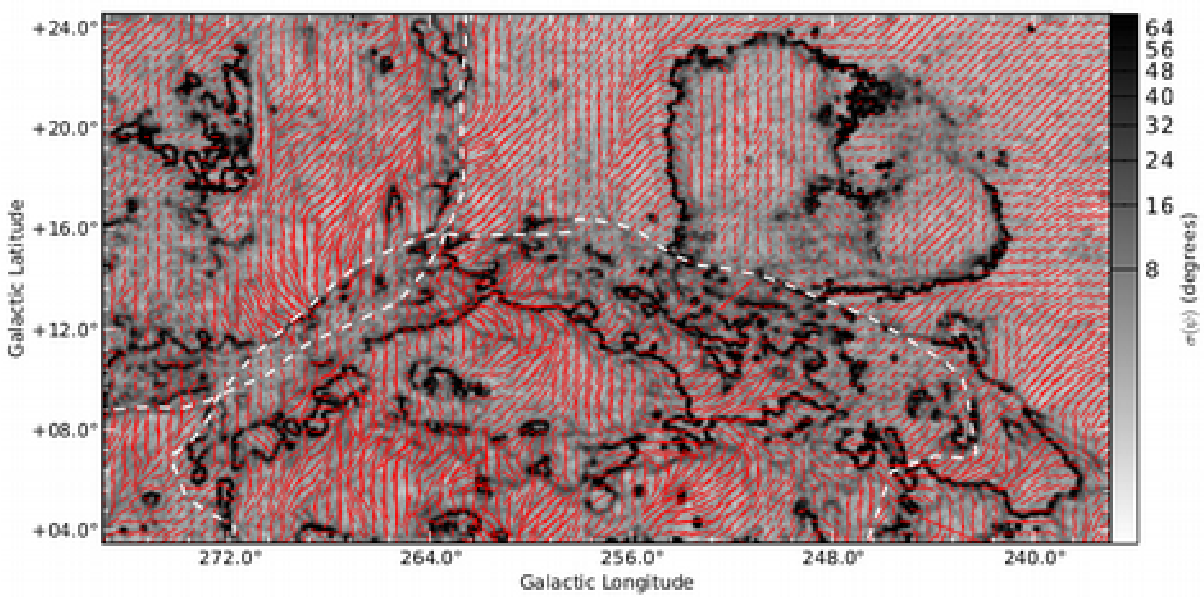

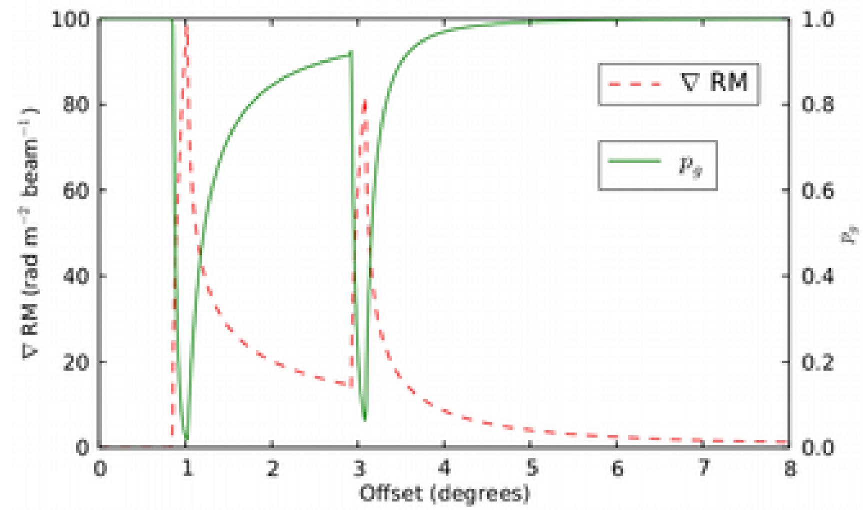

$$p_g = exp\left[-\frac{1}{ln\,2}\left(\frac{d\mathrm{RM}}{dr}\right)^2\lambda^4\right]$$

Results: spectral index

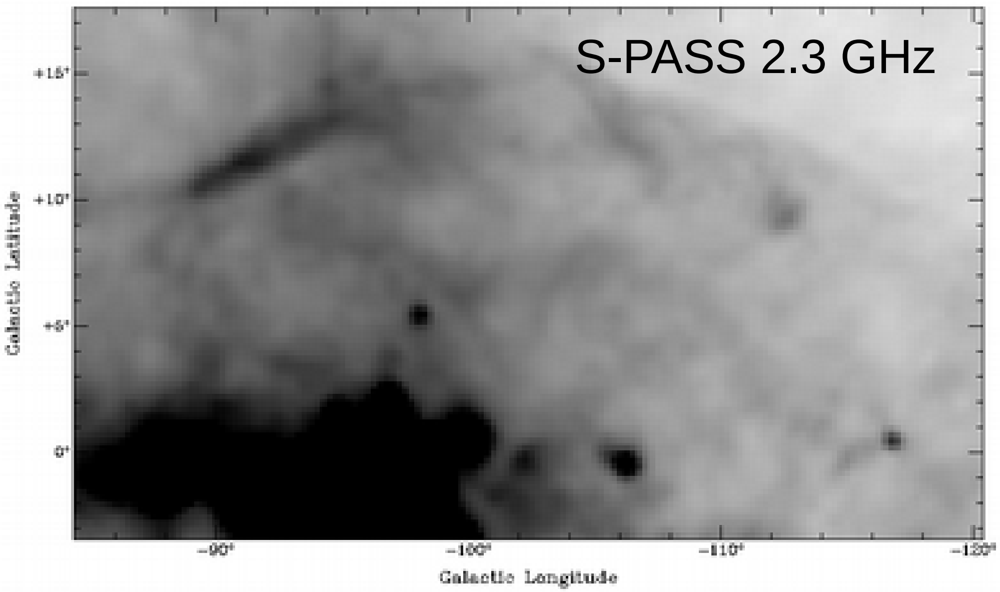

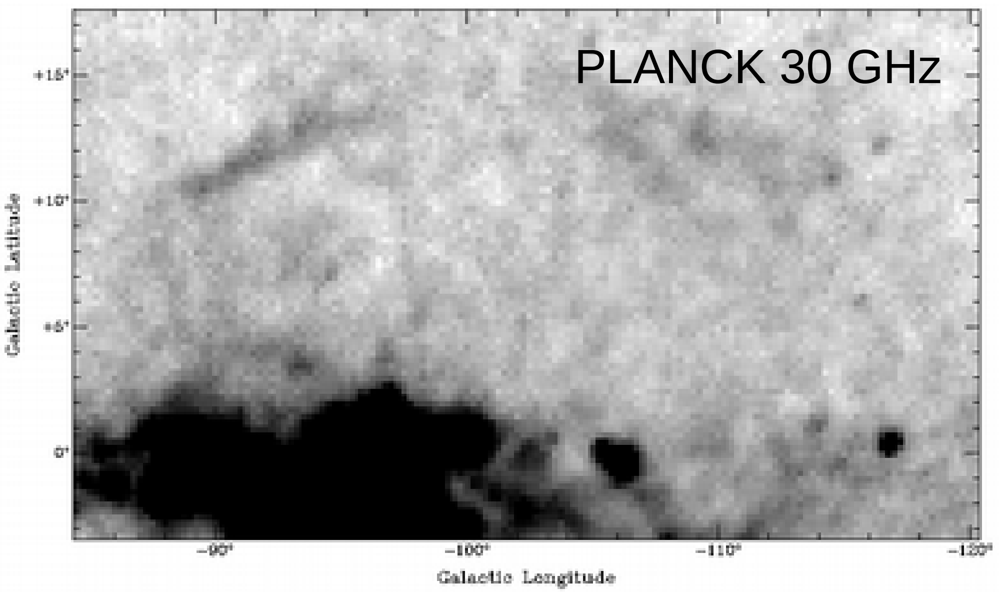

Results: spectral index

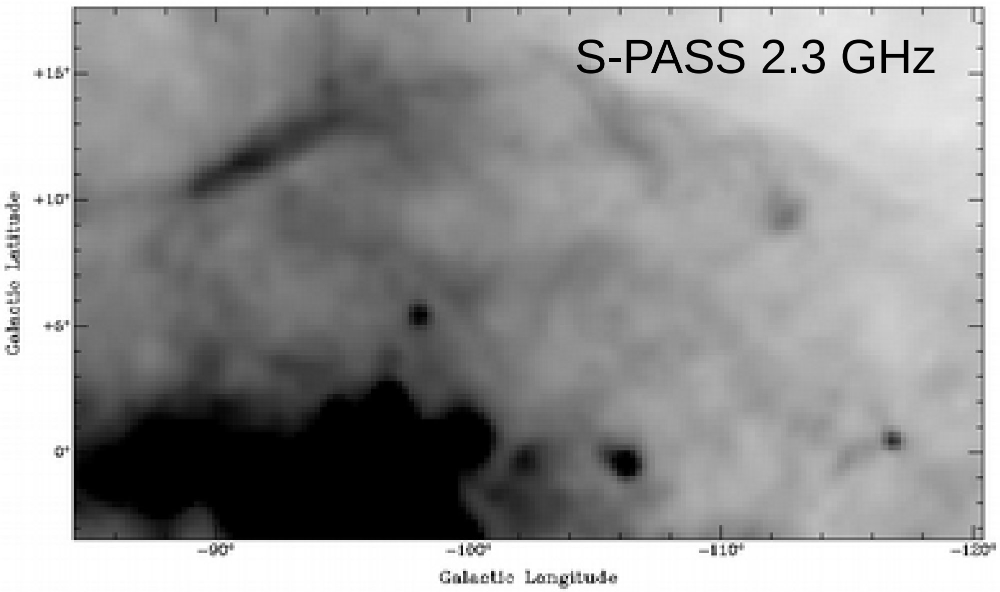

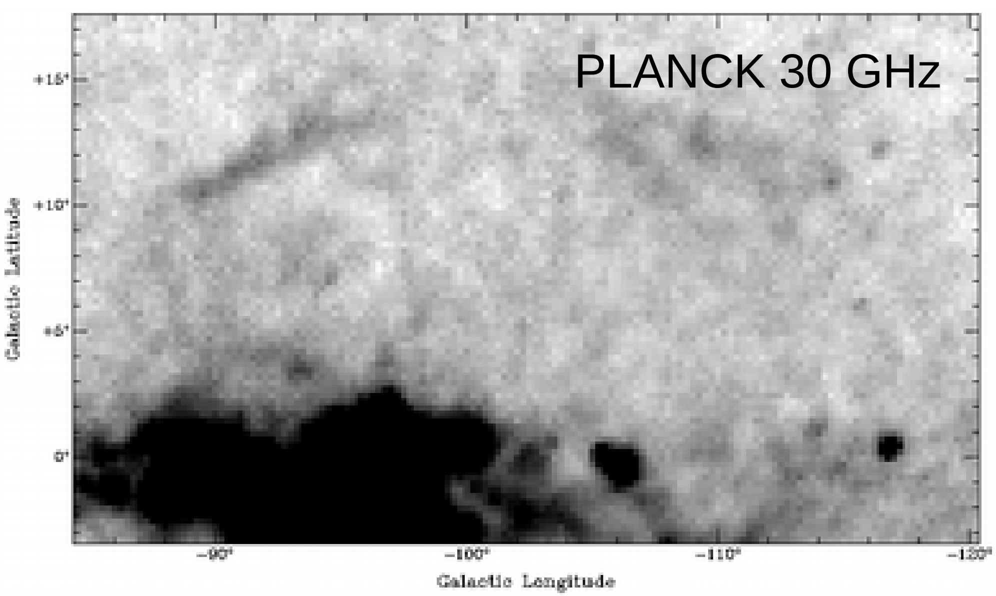

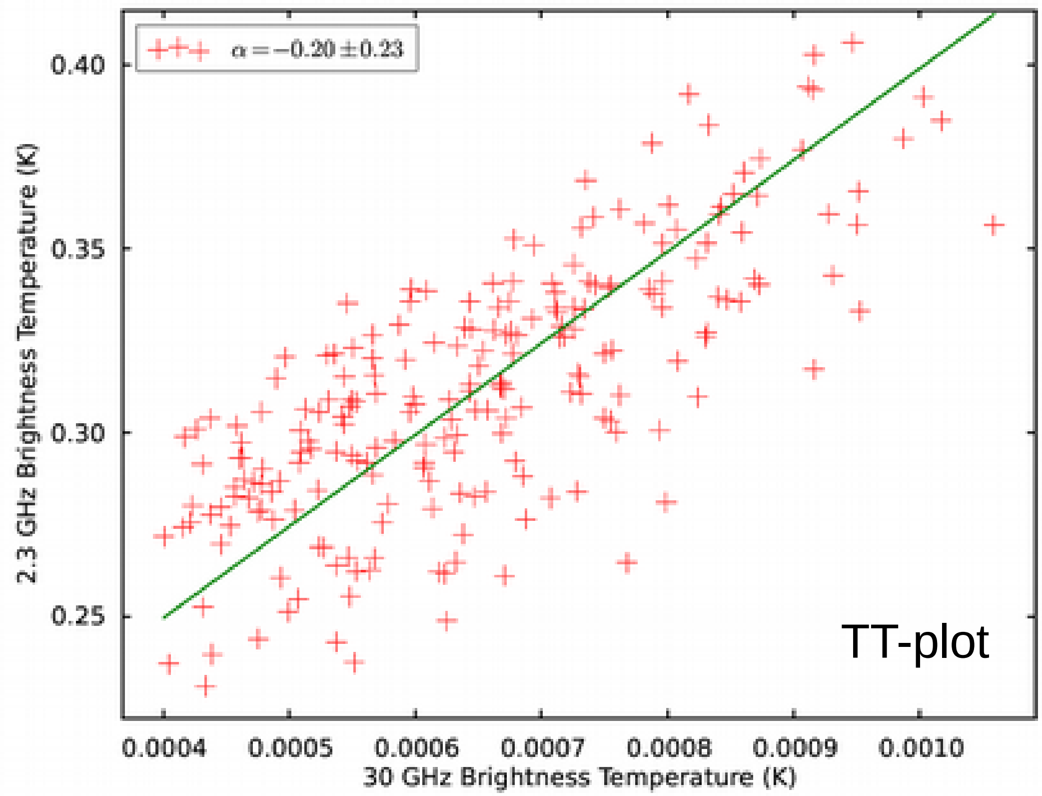

- Spectral index over the shell is consistent with thermal emission
  - More detailed analysis planned for future papers

Results: magnetic field angle

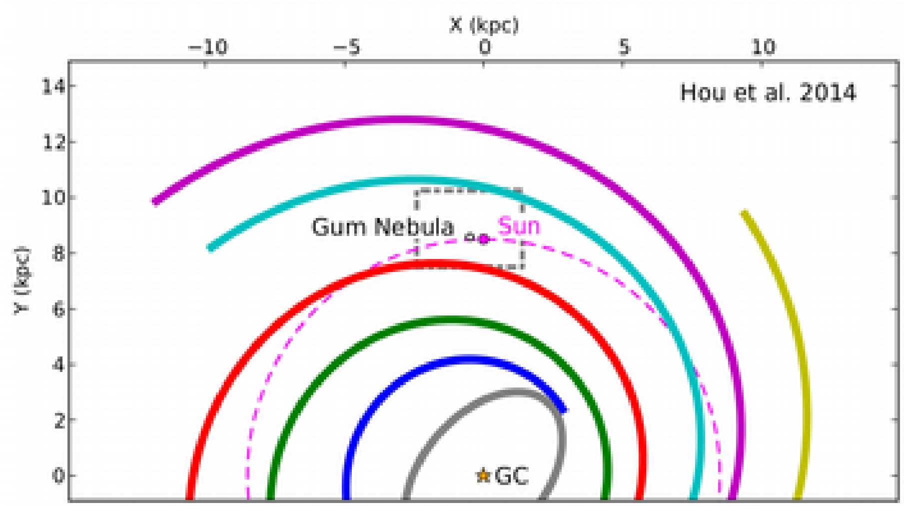

- Prior pitch angle measurements:
  - -6 to -11.5 degrees
  - Large volumes or large area covered

Inoue & Tabara (1981)
Vallee (1988)
Han & Qiao (1994)
Han et al. (1999)
Heiles (1996)
Van Eck et al. (2011)
Pavel et al. (2012)

Results: magnetic field angle

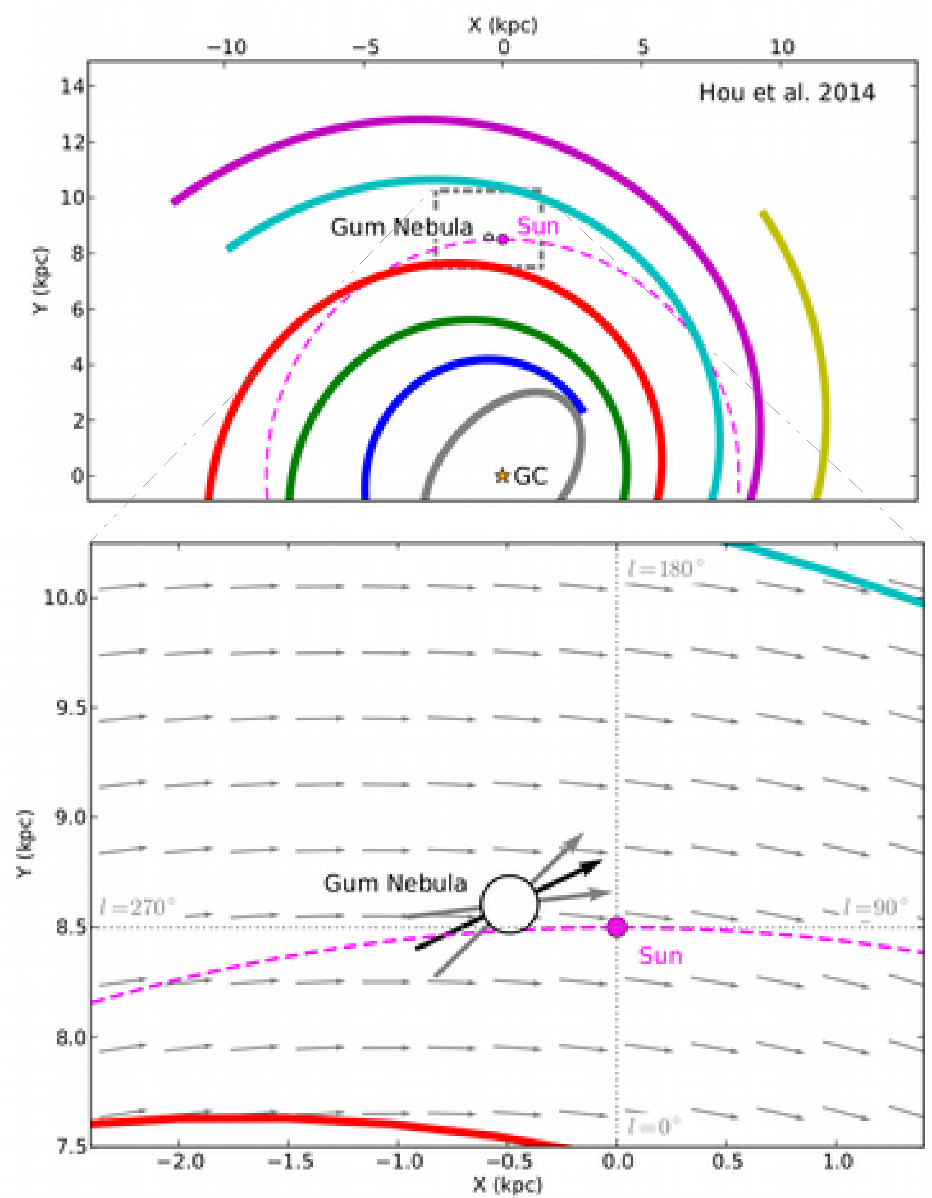

- Prior pitch angle measurements:
  - -6 to -11.5 degrees
  - Large volumes or large area covered

Inoue & Tabara (1981)
Vallee (1988)
Han & Qiao (1994)
Han et al. (1999)
Heiles (1996)
Van Eck et al. (2011)
Pavel et al. (2012)

- Our measurements localised to a region of space ~350pc in scale
- We find $+7^\circ \lesssim p \lesssim +44^\circ$

Results: magnetic field angle

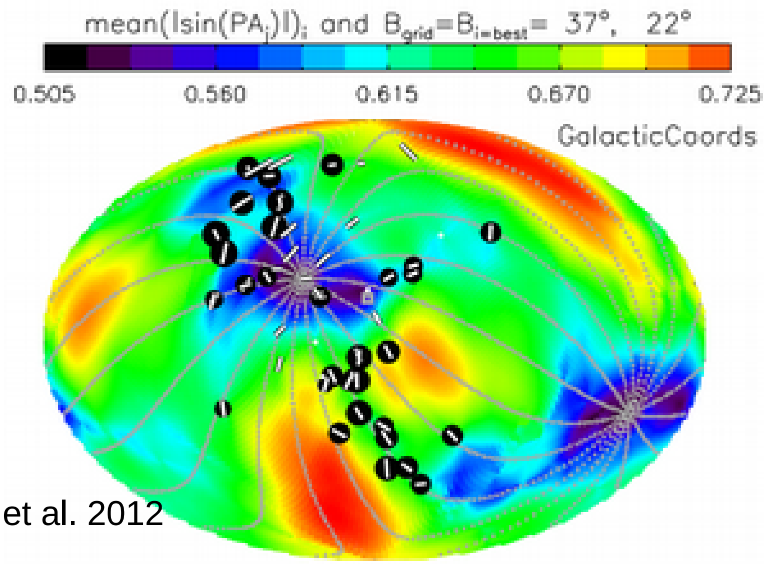

Frisch et al. 2012

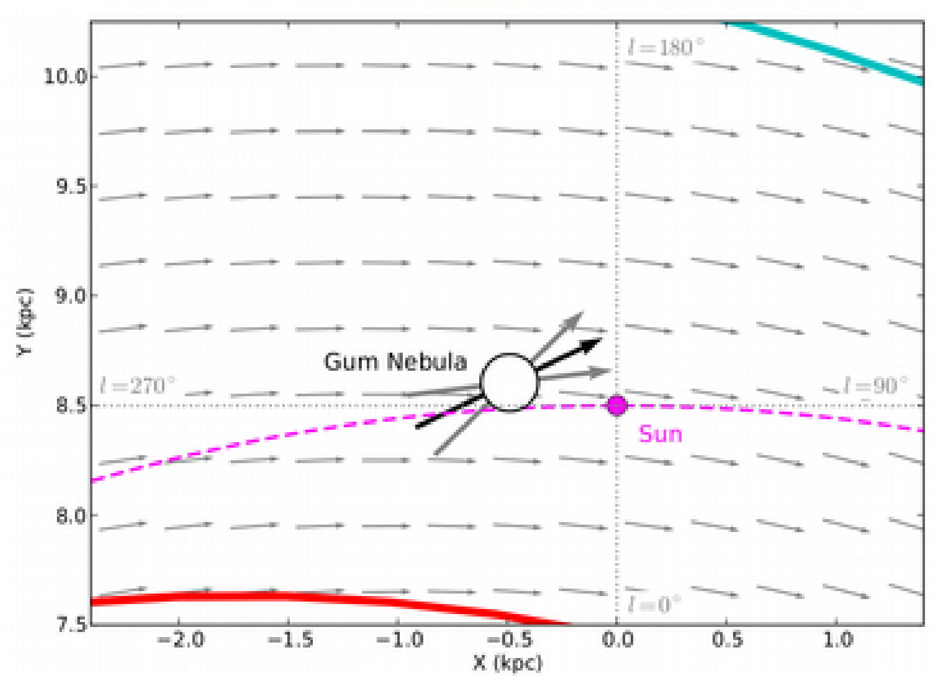

- Prior pitch angle measurements:
  - -6 to -11.5 degrees
  - Large volumes or large area covered

Inoue & Tabara (1981)
Vallee (1988)
Han & Qiao (1994)
Han et al. (1999)
Heiles (1996)
Van Eck et al. (2011)
Pavel et al. (2012)

- Our measurements localised to a region of space ~350pc in scale
- We find $+7^\circ \lesssim p \lesssim +44^\circ$
- Starlight polarisation measurements within 40pc of the Sun suggest even more extreme local deviations (Frisch et al. 2012)

Results: magnetic field angle

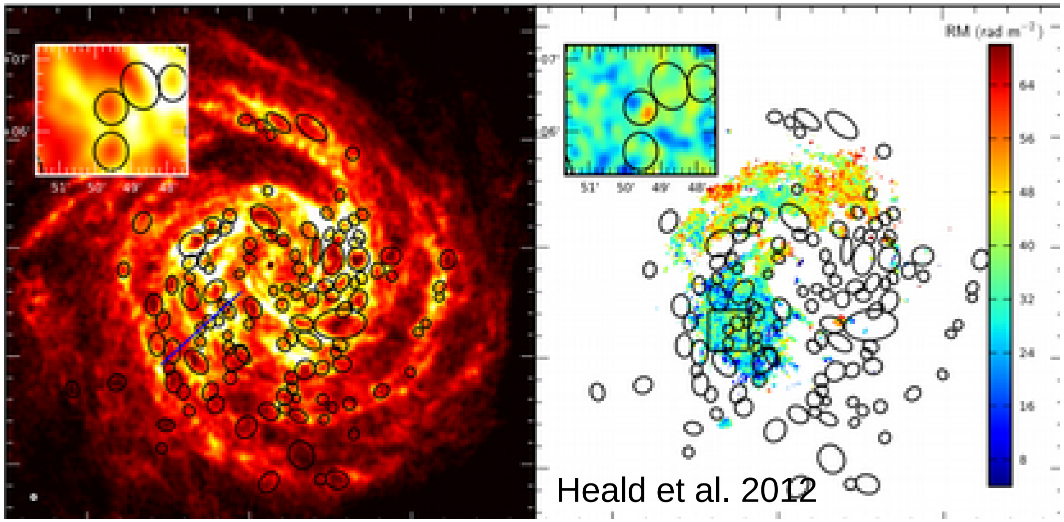

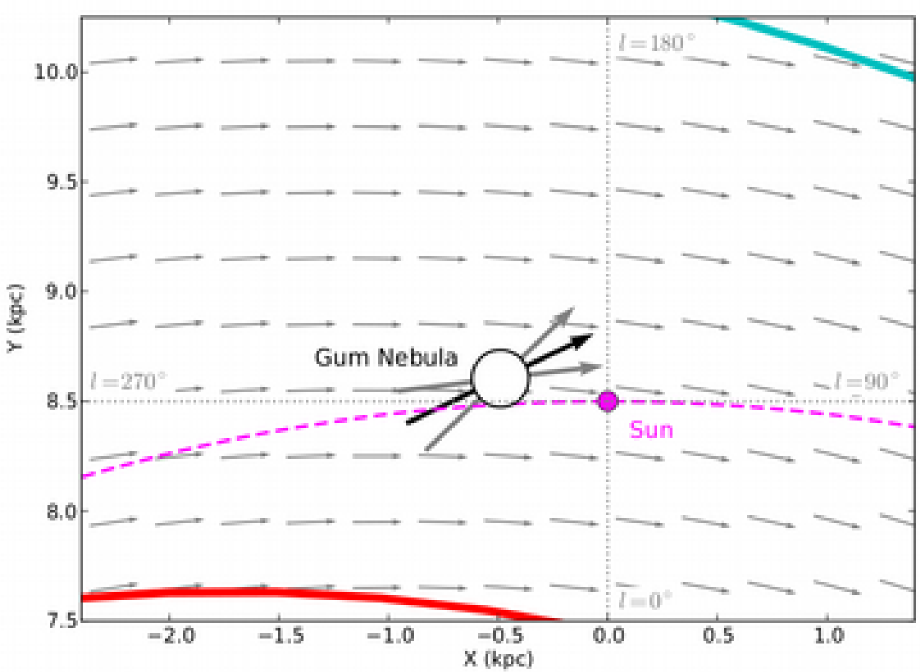

- Prior pitch angle measurements:
  - -6 to -11.5 degrees
  - Large volumes or large area covered

Inoue & Tabara (1981)
Vallee (1988)
Han & Qiao (1994)
Han et al. (1999)
Heiles (1996)
Van Eck et al. (2011)
Pavel et al. (2012)

- Our measurements localised to a region of space ~350pc in scale
- We find $+7^\circ \lesssim p \lesssim +44^\circ$
- Starlight polarisation measurements within 40pc of the Sun suggest even more extreme local deviations (Frisch et al. 2012)
- A vertical deviation has been seen in one external Galaxy, e.g., Heald (2012)
- Such deviations likely common to star-forming galaxies

Summary and conclusions

- RMs for the Gum nebula well fitted by a simple ionised shell model
- Origin of nebula is unlikely to be a SNR as previously claimed
- Best fitting model is consistent with the Weaver (1977) model of a wind-blown -bubble

- We constrain the pitch angle of the ordered field to $+7^\circ \lesssim p \lesssim +44^\circ$ significantly different to measurements on larger scales
- Such deviations likely a common feature of the star-formation processes in galaxies

- This work illustrates how challenging the analysis of RM data will be in the age of the SKA and precursors.

Thanks for listening!